THE GOLGI ARF-GEF SEC7 INTEGRATES MULTIPLE SIGNALING PATHWAYS

A Dissertation

Presented to the Faculty of the Graduate School

of Cornell University

In Partial Fulfillment of the Requirements for the Degree of

Doctor of Philosophy

By

Caitlin Marie McDonold

August 2014

THE GOLGI ARF-GEF SEC7 INTEGRATES MULTIPLE SIGNALING PATHWAYS

Caitlin Marie McDonold, Ph.D.

Cornell University 2014

Arf family GTPases are important molecular switches that regulate vesicular trafficking and membrane dynamics in eukaryotic cells. Arf-GDP, the inactive form of Arf, is soluble and only transiently associates with membranes; however, nucleotide exchange catalyzed by an Arf-GEF (guanine nucleotide exchange factor) induces a conformational change that allows Arf to tightly interact with membranes through an exposed N-myristoylated α-helix. Arf-GTP then recruits effectors such as coat proteins and lipid modifying enzymes. The basic mechanisms of GEF activation of Arf are understood, but the mechanisms regulating Arf recruitment to specific membrane compartments have not been investigated in detail.

Arf is activated at the Golgi complex by Arf-GEFs of the BIG and GBF families, which are large (180-200 kDa) proteins that share multiple homology domains of unknown function. In *Saccharomyces cerevisiae,* the BIG/GBF Arf-GEFs include Sec7, Gea1, and Gea2. Sec7 activates Arf1 at the trans-Golgi, but it is largely unknown how Sec7 itself is recruited and regulated. We first determined that the HDS1 domain of Sec7 interacts with Arf1-GTP to stably recruit Sec7 to membranes via positive feedback. I subsequently determined that Sec7 is an effector of two Rab GTPases, Ypt1 (Rab1) and Ypt31/32 (Rab11), which interact with the HDS2-3 region of Sec7. I established that Arf1, Arl1, and Ypt1 primarily affect the membrane localization of Sec7, whereas Ypt31/32 exerts a dramatic stimulatory effect on the nucleotide exchange activity of Sec7. Direct regulation by Arf1, Arl1, and Ypt1 suggests that Sec7 provides a mechanistic link between incoming and outgoing vesicle traffic. Subsequent interactions with

Ypt31/32 then further stimulates the activity of Sec7 and drives Sec7-dependent cargo sorting events, providing a mechanistic explanation for Ypt31/32 function in vesicle biogenesis. Taken together, my data suggest that multiple signaling pathways integrate to control both Sec7 recruitment to membranes and Sec7 GEF activity.

BIOGRAPHICAL SKETCH

Born in Seattle, Washington in the summer of 1987, Caitlin Marie McDonold was soon relocated to Camillus, NY for her first several years. In 1995, she moved with her family to Woodbury, CT, where she spent most of her childhood running through the woods, occasionally accompanied by her younger sister Siobhan. In 2001, Caitlin enrolled at Westover School, an all-girls high school in Middlebury, CT, where she was carefully molded into a grammar fanatic with a passion for biology and photography. She was also accepted into the Women In Science and Engineering (WISE) program, through which she was introduced to computer science and independent research. She graduated in 2005, earning High Honors with Distinction.

Caitlin then attended Skidmore College in Saratoga Springs, NY. She was a recipient of the Porter Presidential Scholarship in Science and Mathematics, a merit-based, four-year scholarship awarded for superior accomplishment and exceptional promise in science and mathematics. At Skidmore, Caitlin majored in Biology with a concentration in Molecular Biology, Cell Biology, and Genetics and also completed a minor in Mathematics. During the summer after her freshman year, Caitlin joined the laboratory of Dr. Patricia J. Hilleren, where she studied mRNA processing in the budding yeast *Saccharomyces cerevisiae*; she continued working in the lab throughout college, including two additional summers. Additionally, she participated in a Research Experience for Undergraduates (REU) at Duke University in the summer of 2007, during which she worked in the laboratory of Dr. Greg Crawford and characterized potential DNA enhancer elements as part of the ENCODE project. Caitlin earned her Bachelor of Arts from Skidmore College in May 2009 and graduated *cum laude* with Honor in Biology.

From Skidmore, Caitlin moved to Ithaca, NY and began her doctoral studies in Biochemistry, Molecular & Cell Biology at Cornell University in the fall of 2009. Switching from her undergraduate focus in molecular biology to biochemistry and cell biology, she began her dissertation research on vesicle trafficking at the *trans*-Golgi network under the direction of Dr. Chris Fromme. Her favorite model organism is *S. cerevisiae*, and when not in the lab, Caitlin can often be found either baking bread and other treats for her friends and lab mates or drinking some yeast-produced refreshments at one of Ithaca's local bars.

ACKNOWLEDGEMENTS

My graduate career would have been short-lived if not for the support and guidance of my advisor Chris Fromme. He has been very patient and encouraged me when I became frustrated and discouraged by experimental science. I would also like to thank my lab mates for providing advice, entertainment, and assistance throughout my time at Cornell. Brian Richardson has worked with me on the Sec7 project since I first joined the lab, and he taught me various biochemical techniques and procedures. In addition to his contributions to my first paper, he has been as a source of advice and troubleshooting assistance. Maggie Gustafson joined the Arf-GEF group in 2012 and took up the Gea1/2 project, and was a helpful sounding board and co-conspirator. And although they didn't work on the Arf-GEFs, Jon Paczkowski and Amanda Strassner were always helpful and, having joined the lab a year before me, were an excellent source of grad school advice. I also want to thank my other committee members, Scott Emr and Rick Cerione, for providing useful advice and suggestions.

I'm also grateful to have been a part of the Weill Institute for Cell and Molecular Biology. I'd like to thank both the Emr and Bretscher labs for innumerable advice, reagents, and equipment used throughout my graduate research. Thank you in particular to Kirk Donovan for his assistance with the *sec7-1* screen, to Felipe Santiago for plasmids and protocols, and to Chris Stefan for microscopy assistance. I also owe a huge debt to the Bretscher lab for letting me us their fluorometer, which I used for all of my GEF activity assays and which was eventually moved to the Fromme lab as a result.

Going back even further, I'd like to acknowledge the people who helped to inspire me and encourage me to pursue a career in science. Many of my teachers at Westover were

instrumental in encouraging my academic interests and were among the first to show me that women do belong in math and science: my biology and chemistry teachers Alice Hallaran, Melinda Burbank, and Heather Nuzzo; Sonja Mitchell, my academic advisor and math teacher, and Ann Pollina, the head of school and my BC Calculus teacher. At Skidmore, Michelle Frey first sparked my interest in biochemistry, and nearly convinced me to switch majors. Pat Hilleren gave me my first chance at real experimental research, and I'll be forever grateful and slightly bemused by how she called out to my from her office as I was walking down the hall one day, asked me what I was doing for the summer, and invited me to come work in her lab. I also owe a lot to my family, especially my mother, who encouraged me and took me to science museums, homeschooled me for several years when it became clear that I wasn't being challenged enough, and made a special effort to ensure I had access to the necessary resources and activities to nurture my budding passion.

Finally, I want to thank all my friends in Ithaca for helping me survive the grad school experience by commiserating with me when things weren't going so well, celebrating with me when they were, and keeping me sane when thing got hectic (which was most of the time). To my BMCB friends Erin, Amy, Nick, Carolyn, Elliot, Tony, Greg: thanks for getting me through the first two years and beyond. Thanks as well to my extended physicist and physics-adjacent family, Yariv, Katie, Veronica, Matt, Ben, Brian, C, Lauren, Sam(s), etc. – you made my last three years in Ithaca memorable and worthwhile; thanks for making me an honorary physicist. Lastly, I'd like to give a shout-out to my college friends in the GDNN for our yearly reunions and the friendships that have thus far held up against distance and time.

This work was partially funded by an NIH Cellular & Molecular Biology Training Grant and by NIH grant 5R01GM098621-03.

TABLE OF CONTENTS

LIST OF FIGURES

LIST OF TABLES

LIST OF ABBREVIATIONS

AP:	Adaptor protein
ARF:	ADP-ribosylation factor
ARFRP1:	ARF-related protein 1
ARL:	ARF-like
ASAP:	ArfGAP with SH3 domain, ankyrin repeat, and PH domain
BAR:	Bin-amphysin-Rvs
BFA:	Brefeldin A
BIG1/2:	Brefeldin A-inhibited GEF 1/2
CERT:	Ceramide transfer
COG:	Conserved oligomeric Golgi
COPI/II:	Coat protein complex I/II
DCB:	Dimerization and cyclophilin binding
E. coli:	*Escherichia coli*
ER:	Endoplasmic reticulum
ERGIC:	ER-Golgi intermediate complex
FAPP1/2:	Four-phosphate-adaptor protein 1 and 2
GAP:	GTPase-activating protein
GARP:	Golgi-associated retrograde protein
GBF:	Golgi-specific Brefeldin A-resistance factor
GDF:	GDI displacement factor
GDI:	GDP dissociation inhibitor
GDP:	Guanosine diphosphate
GEF:	Guanine nucleotide exchange factor
GFP:	Green fluorescent protein
GGA:	Golgi-localized, γ-ear containing ADP-ribosylation factor binding proteins
GGT:	Geranylgeranyl transferase
GPI:	Glycosylphosphatidylinositol
GRIP:	golgin-97, RabBP2α, Imh1p, and p230
GST:	Glutathione S-transferase
GTP:	Guanosine-5'-triphosphate
GYP:	GAP for Ypt proteins
HA:	Hemagglutinin
HDS:	Homology downstream of Sec7
HEPES:	4-(2-hydroxyethyl)-1-piperazineethanesulfonic acid
HUS:	Homology upstream of Sec7
PC:	Phosphatidylcholine
PH:	Pleckstrin homology
PI4P:	Phosphatidylinositol 4-phosphate
PI4,5P:	Phosphatidylinositol 4,5-bisphosphate
PKD:	Protein kinase D
PLD:	Phospholipase D
PM:	Plasma membrane
RAB:	Ras-like protein in brain
RAS:	Rat sarcoma

RE:	Recycling endosome
REP:	Rab escort protein
S. cerevisiae:	*Saccharomyces cerevisiae*
SNARE:	Soluble N-ethylmaleimide-sensitive factor attachment protein receptor protein
TEV:	Tobacco etch virus
TGN:	*trans*-Golgi network
TRAPP:	Transport protein particle
YIP:	Ypt-interacting protein

CHAPTER 1

INTRODUCTION

Eukaryotic cells are subdivided into numerous membrane-bound compartments called organelles that have specialized functions, including protein translation, folding, and modification, lipid synthesis, storage, and the breakdown of cellular waste products. These membrane-bound organelles together comprise the endomembrane system, a network that is highly conserved throughout eukaryotes (Figure 1.1). The different organelles perform distinct tasks and can be distinguished by their specific lipid composition and membrane proteins. Lipids, proteins, and carbohydrates must be transported between the organelles of the endomembrane system while still maintaining the proper lipid and protein identity of each organelle (Behnia and Munro, 2005; Bonifacino and Lippincott-Schwartz, 2003). Therefore, eukaryotic cells have evolved an elaborate and highly regulated trafficking system to sort, package, and deliver cargo through the endomembrane system via small membrane-bound transporters called vesicles (Palade, 1975).

The first genetic insights into intracellular membrane trafficking were discovered using the budding yeast *Saccharomyces cerevisiae*. Highly organized trafficking pathways were discovered using electron micrographs of temperature-sensitive gene mutations (called the "sec" mutants) that disrupted the transport of cargo (Novick et al., 1980; Novick and Schekman, 1979). Newly synthesized secretory proteins were observed to move from the endoplasmic reticulum (ER), the site of synthesis, to the Golgi apparatus, where protein modifications occurred, and finally out to the plasma membrane (PM). Each step of this pathway was associated with multiple gene mutations that interrupted the flow of cargo; mutations in genes that acted early in the pathway accumulated ER membranes, those that acted in the middle accumulated Golgi

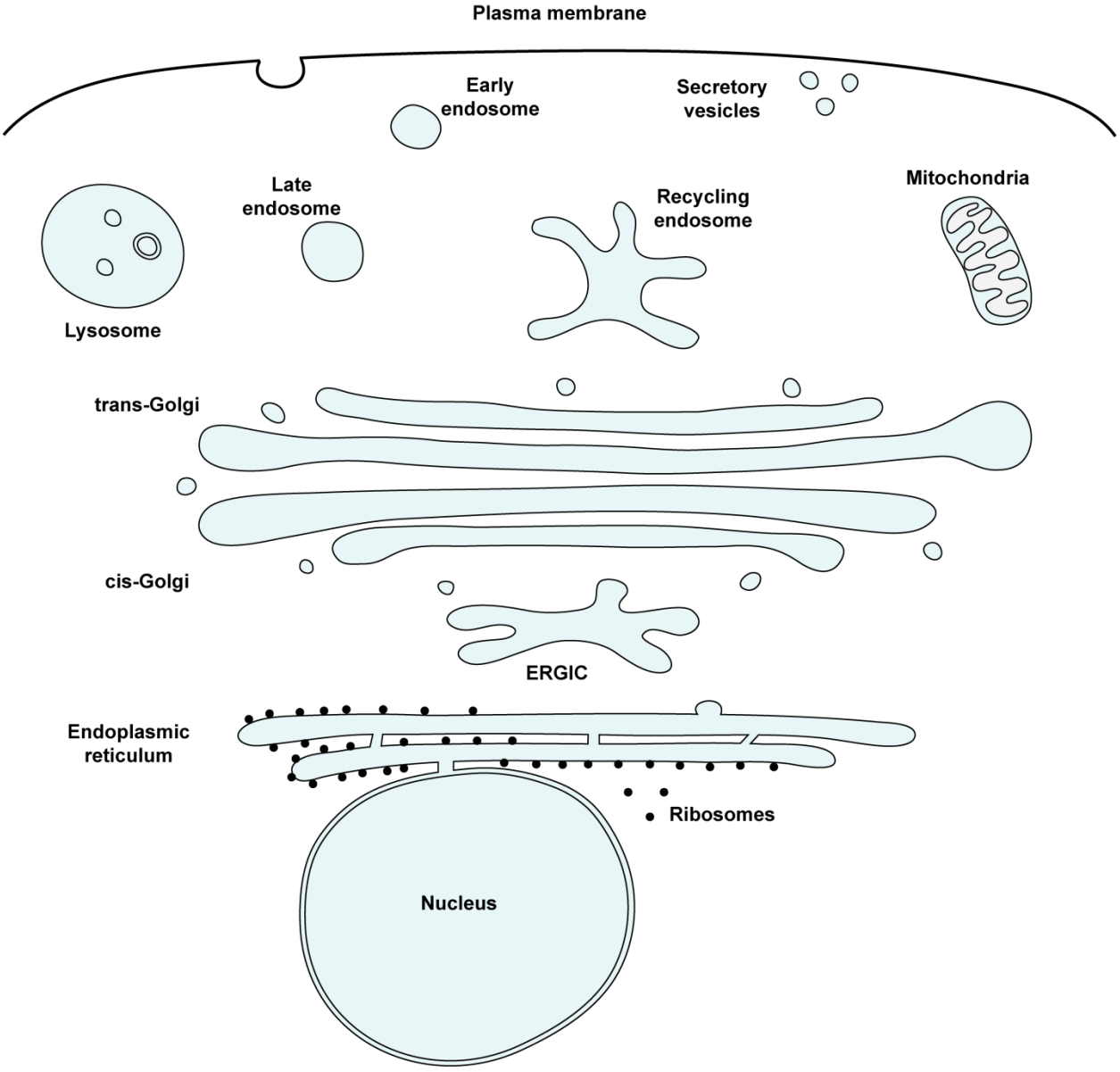

Figure 1.1: The eukaryotic endomembrane system. Eukaryotic cells contain a number of specialized membrane-bound organelles that carry out processes such as protein synthesis, protein modification, storage, lipid synthesis, metabolism, and degradation. Each organelle has a distinct membrane and protein composition to establish organelle identity. With the exception of the mitochondria, all of the organelles shown are connected through elaborate membrane trafficking pathways.

membranes, and those involved in the final step accumulated small secretory vesicles (Novick et al., 1981). A cell-free system using isolated mammalian Golgi cisternae confirmed the intra-Golgi transport of a radiolabeled protein (Balch et al., 1984a; Balch et al., 1984b). Two of the proteins responsible for this transport were later found to be homologous to two of the sec mutants identified in yeast, confirming that trafficking machinery is highly conserved (Griff et al., 1992; Wilson et al., 1989).

Many of these trafficking pathways have been extensively studied, and our understanding of the mechanisms of vesicle formation and trafficking has increased greatly. Most vesicle trafficking is mediated by small GTPases, cargo adaptors, and coat proteins that act to sequester cargo proteins and deform membranes (Figure 1.2). At the ER, newly synthesized proteins are packaged into vesicles via coat protein complex II (COPII) for transport to the ER-Golgi intermediate complex (ERGIC) or the Golgi complex (Bonifacino and Glick, 2004). At the *cis*-Golgi, COPI captures resident ER proteins for recycling back to the ER and also controls the retrograde transport of proteins within the Golgi complex (Hsu et al., 2009). At the *trans*-Golgi network, clathrin and a variety of clathrin adaptors act together to transport cargo from the Golgi complex to the PM via endosomes or to lysosomes, with each pathway involving specific adaptor protein (AP) complexes (De Matteis and Luini, 2008; Kirchhausen, 2000). Clathrin and clathrin adaptors also control the endocytosis and recycling of proteins from the PM to endosomes and the *trans*-Golgi network (TGN). Several important pathways have not been associated with coat proteins or cargo adaptors thus far, most notably the direct transport of secretory vesicles from the Golgi to the apical PM (Bard and Malhotra, 2006; De Matteis and Luini, 2008). Complicating matters further, some trafficking events seem to be mediated by long tubules rather than discrete vesicle carriers (De Matteis and Luini, 2008).

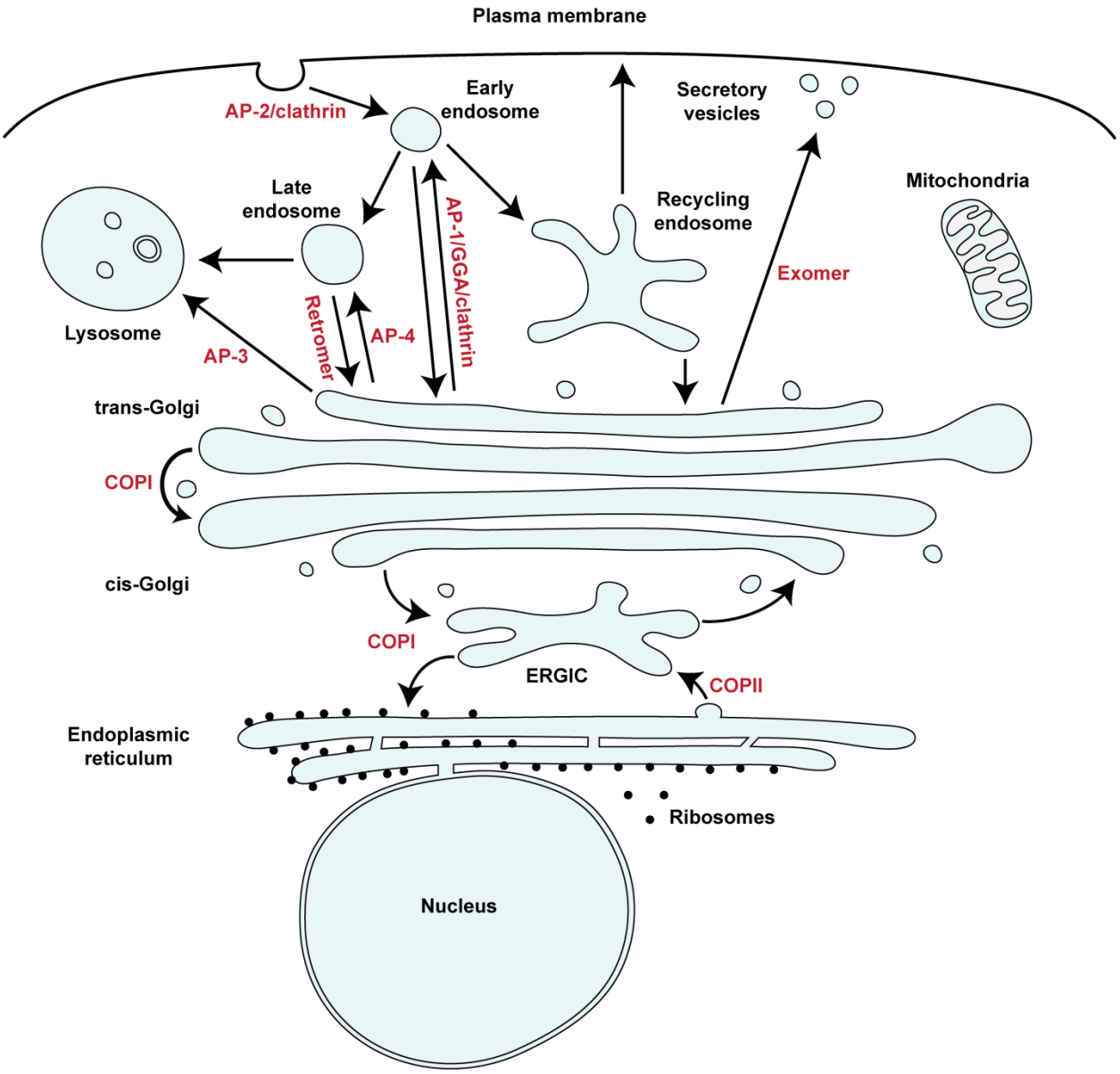

Figure 1.2: Eukaryotic trafficking pathways. Proteins synthesized by ribosomes at the ER must be transported to the Golgi complex for processing and modification before being sent to their target compartment or membrane within the cell. Cargo adaptors and coat proteins package proteins into vesicles and drive vesicle formation. COPII-coated vesicles carry proteins from the ER to the Golgi, while COPI-coated vesicles recycle proteins from the late to early Golgi and from the Golgi back to the ER. At the *trans*-Golgi network, clathrin and adaptor protein complexes sort and deliver cargo to the plasma membrane, endosomes, and lysosomes.

Vesicle transport can be divided into four main steps: 1) cargo recruitment and vesicle budding, 2) transport, 3) tethering to the target membrane and 4) vesicle fusion (Figure 1.3). While each organelle recruits a distinct set of membrane trafficking proteins for cargo recruitment and vesicle formation, they primarily follow the same basic set of steps. First, small GTPases are recruited to membranes and activated by guanine nucleotide exchange factors (GEFs), which catalyze the exchange of GDP for GTP. The GTP- and membrane-bound GTPases then recruit cargo adaptors, which capture cargo molecules and sequester them into the forming bud. Coat proteins are recruited to the membrane surface by both the small GTPases and adaptors, inducing membrane curvature and further cargo recruitment (Kirchhausen, 2000). The vesicle buds as coat assembly drives membrane deformation, and the bud neck constricts, eventually leading to vesicle scission. While the mechanisms of membrane fission are not well understood, members of the Arf family of small GTPases and the Bin-amphysin-Rvs-domain (BAR-domain) containing proteins, which sense and generate membrane curvature, dynamins, which assemble at the bud neck, and protein kinase D (PKD) have all been implicated in the process (Campelo and Malhotra, 2012).

The formation of COPII-coated vesicles for the transport of proteins from the ER to the Golgi complex is well understood and provides a good example of vesicle budding, cargo recruitment, and coat formation (Figure 1.4). The process is initiated by the GEF Sec12, which stimulates nucleotide exchange of the small GTPase Sar1, allowing it to adopt its active GTP-bound form (Barlowe and Schekman, 1993; Nakano and Muramatsu, 1989). Sar1-GTP then associates with the ER membrane via an N-terminal myristoylated amphipathic helix, and the membrane-bound Sar1 recruits the Sec23-Sec24 cargo adaptor complex through a direct interaction with Sec23 (Barlowe et al., 1994; Bi et al., 2002). The Sec23/24 complex captures

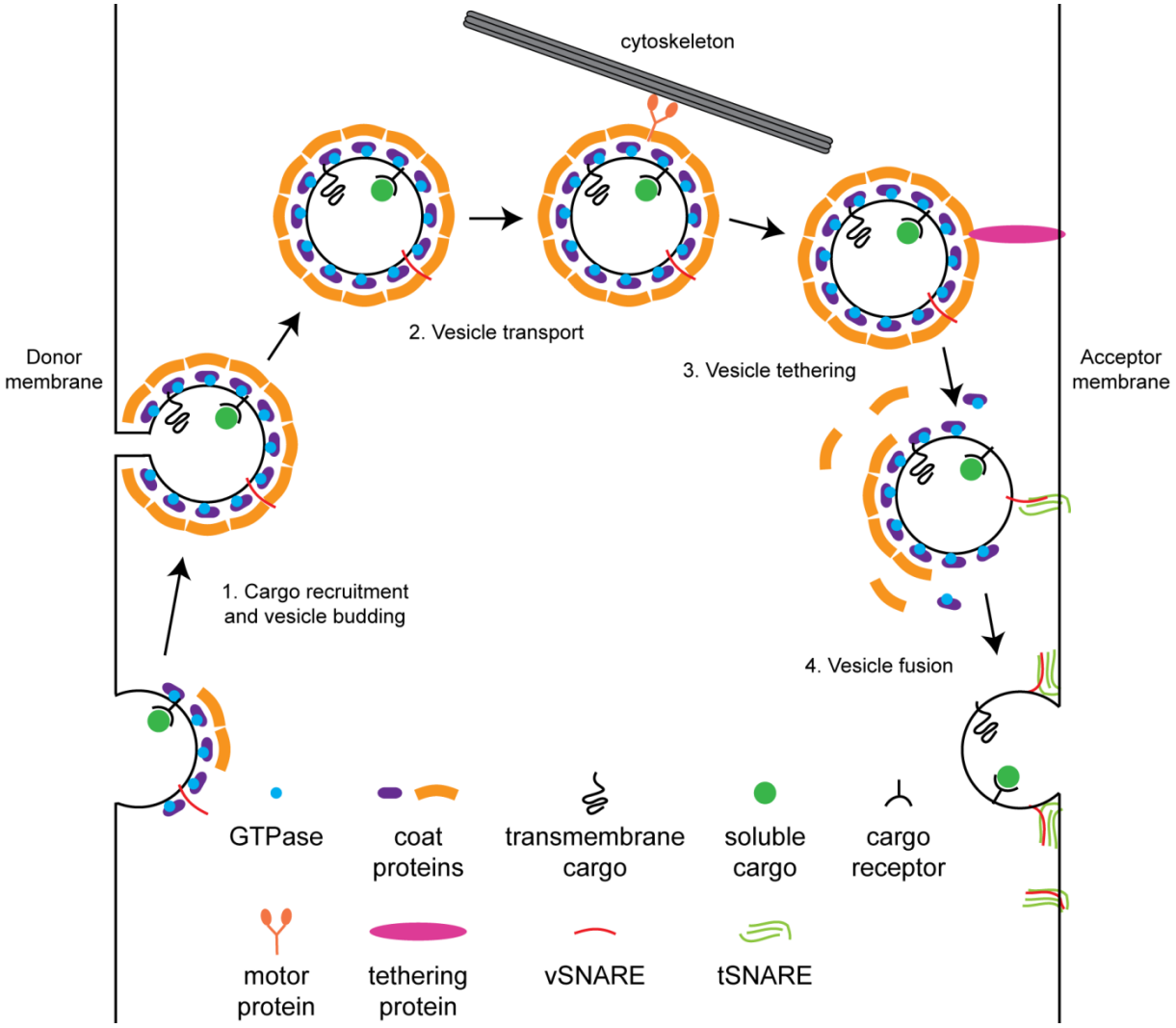

Figure 1.3: Steps of vesicle transport. (1) Small GTPases recruit cargo adaptors to capture cargo and SNARES and coat proteins to induce vesicle budding. (2) The vesicle either moves by diffusion or is transported along the cytoskeleton to the target membrane. (3) Proteins on the vesicle (often Rab GTPases) recognize and bind to specific tethering proteins on the target membrane. (4) The vesicle coat is shed and the vSNAREs and tSNAREs assemble into a tight complex, bringing the two membranes together and driving fusion. (Adapted from Bonifacino and Glick, 2004; Cai et al., 2007a).

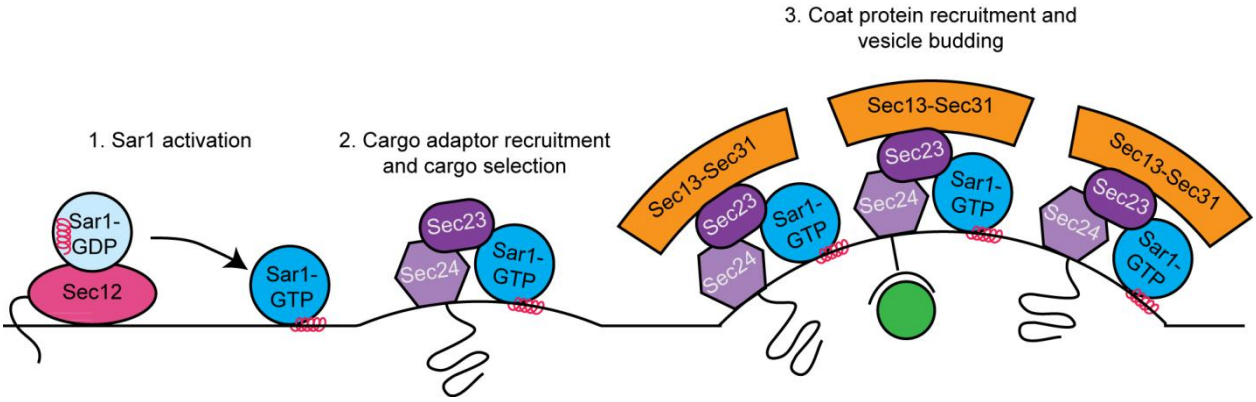

Figure 1.4: The formation of COPII-coated vesicles. (1) The guanine nucleotide exchange factor (GEF) Sec12 catalyzes nucleotide exchange of the small GTPase Sar1, recruiting it to the membrane surface. (2) GTP-bound Sar1 interacts with Sec23 and recruits the Sec23/24 cargo adaptor complex. Sec24 recognizes and binds to cargo proteins. (3) Sec23/24 bring in the Sec13/31 coat complex, which polymerize to form a cage, increasing membrane curvature and driving vesicle budding. . (Adapted from Bonifacino and Glick, 2004).

cargo through direct interactions of Sec24 with the cytosolic tails of cargo proteins, including the v-SNARE Bet1 and the Golgi protein Sys1 (Aridor et al., 1998; Kuehn et al., 1998; Miller et al., 2002; Miller et al., 2003). The Sar1/Sec23 complex also recruits the Sec13/31 coat complex, which polymerizes to form a cage that induces membrane deformation and drives vesicle budding (Bhattacharya et al., 2012; Fath et al., 2007; Salama et al., 1993; Stagg et al., 2006). No proteins specifically involved in vesicle fission have been identified, but the induction of membrane curvature by Sar1 and the polymerization of the Sec13/31 cage may together drive budding and fission (Bonifacino and Glick, 2004).

After budding from the donor membrane, the vesicles must then be transported to the target (acceptor) membrane. Vesicles reach their target membranes either by diffusion or by associating with motor proteins such as myosin, kinesin, and dynein for transport along the cytoskeleton. The vesicle must then recognize and associate with the target membrane. Membrane recognition and docking is mediated both by interactions between small GTPases on the vesicle and specific tethering proteins on the target membrane and by interactions between soluble N-ethylmaleimide-sensitive factor attachment protein receptor proteins (SNAREs) (Cai et al., 2007a). Much of the specificity of vesicle docking comes from interactions between vesicle-bound proteins with specific tethering proteins on the target membrane (Cai et al., 2007b; Cao et al., 1998; Sacher et al., 2001; Whyte and Munro, 2002; Yu and Hughson, 2010). The vesicle coat must also be shed before the vesicle can fuse to the target membrane: the GTP-bound initiating small GTPase is hydrolyzed by a GTPase-activating proteins (GAP), enabling the GTPases to dissociate from the vesicle surface along with the associated coat proteins (Cai et al., 2007b). After vesicle tethering and coat disassembly, SNARE complexes form between two populations of SNAREs: v-SNAREs, which are specific to trafficking vesicles, and t-SNAREs,

which are specific to the target membranes (Rothman, 1994). Different v-SNARE and t-SNARE complexes form for distinct vesicle/target pairs in membrane trafficking (McNew et al., 2000). The paired SNAREs then form a tight four-helix bundle (one from the vSNARE and three from the tSNARE complex), bringing the vesicle and target membrane close enough to drive fusion (Bonifacino and Glick, 2004).

The small GTPases of the Rab and ADP-ribosylation factor (Arf) families regulate nearly every step of intracellular membrane trafficking. They act as molecular switches that cycle between a cytosolic, GDP-bound "off" state and a membrane-associated, GTP-bound "on" state. Members of the Arf family are primarily involved in vesicle formation and cargo recruitment via its effector proteins, while the Rab GTPases control vesicle transport and the recognition, tethering, and fusion of vesicle to the target membrane (Barr, 2009; D'Souza-Schorey and Chavrier, 2006; Mizuno-Yamasaki et al., 2012). Small GTPases are activated by guanine nucleotide exchange factors (GEFs) and inactivated by GTPase-activating proteins (GAPs); the specific mechanisms of Arf and Rab regulation and recruitment to membranes will be discussed in detail later. Many of these small GTPases act at multiple membranes and at multiple stages of the trafficking pathways, but are activated at each location by a membrane-specific GEF. Therefore, understanding how these small GTPases and their GEFs are recruited to membranes and activated is vital to understanding the regulation of membrane trafficking.

Trafficking out of the Golgi complex and the *trans*-Golgi network

The Golgi complex is the primary processing and sorting station for newly synthesized transmembrane and soluble cargo proteins in the secretory and endosomal pathways, and thus is maintained by a complex vesicle trafficking system. The Golgi complex receives proteins from

the ER, directs the processing of these proteins, and targets them to their final destinations (Glick and Nakano, 2009; Wilson et al., 2011). In addition, various lipids are synthesized or modified at the Golgi for delivery to their target membranes (De Matteis and Luini, 2008). The Golgi complex is composed of disk-shaped structures called cisternae that are arranged in an ordered stack from the *cis* face to the *trans* face in most organisms. However, the Golgi cisternae in *S. cerevisiae* exist as separate compartments that can be divided into *cis*, *medial*, *trans*, and TGN cisternae (Brigance et al., 2000; Papanikou and Glick, 2009). The cisternae mature over time, and once cargo molecules have traversed the Golgi complex, they must be sorted into carrier vesicles and targeted to different destinations (De Matteis and Luini, 2008). The TGN is the central sorting hub for protein and lipid cargos leaving the Golgi. Most vesicles leaving the Golgi and TGN are coat-dependent, but some pathways do not require coat proteins, such as secretory vesicles in yeast (Bard and Malhotra, 2006; De Matteis and Luini, 2008).

In addition to its role in sorting proteins in the biosynthetic pathway, the TGN in yeast is also responsible for sorting and recycling endocytosed proteins. In contrast, mammalian cells have separate organelles called recycling endosomes (REs) that serve as a sorting hub for endocytic cargo (Santiago-Tirado and Bretscher, 2011). The TGN and endosomes are closely linked; BFA (Brefeldin A) treatment, which fuses the Golgi complex to the ER, causes the TGN to fuse instead with endosomes (Lippincott-Schwartz et al., 1991; Wood et al., 1991). The localization of several proteins also highlights this connection: yeast Sec7, a GEF for Arf1/2, is used as a marker for the *trans*-Golgi and TGN, but its mammalian homologs BIG1/2 are found on both the TGN and endosomes (Franzusoff et al., 1991; Shin et al., 2004). Similarly, the Rab GTPases Ypt31/32 primarily localize to the TGN in yeast, whereas their mammalian homolog Rab11 localizes to REs (Benli et al., 1996; Jedd et al., 1997; Ullrich et al., 1996). Incoming and

outgoing pathways at the TGN and endosomes must be carefully regulated to maintain the proper morphology and function of these compartments, though it remains unclear how these pathways might be linked.

Cargo from the TGN needs to be sorted and delivered to a variety of destinations, including early and late endosomes, the PM, and lysosomes. Polarized cells need to sort proteins even further to target cargos to the appropriate domains of particular organelles. For example, the PM is divided into the basolateral and apical domains in mammalian epithelial cells. Even relatively simple organisms such as *S. cerevisiae* display polarized growth and have developed mechanisms to deliver cargo to the bud tips and bud neck (Brennwald and Rossi, 2007). A variety of cargo adaptors are therefore utilized at the TGN to provide specificity for the different trafficking destinations. The AP-1 complex and GGA (Golgi-localized, gamma-ear containing, ARF-binding) proteins package cargos destined for endosomes into clathrin-coated vesicles, and AP-1/clathrin are also involved in targeting cargo to the basolateral domain in polarized cells (Bonifacino, 2014; Park and Guo, 2014). In yeast, a recent study has identified two distinct waves of clathrin-dependent cargo sorting at the TGN: Gga2 assembles first, followed by the AP-1 complex as Gga2 is trafficked away (Daboussi et al., 2012). The AP-3 complex also localizes to the TGN in yeast and to tubular endosomal compartments in mammals and targets cargos to the vacuole (yeast) or lysosome (mammals) (Park and Guo, 2014; Santiago-Tirado and Bretscher, 2011).

It remains unclear how cargo is sorted into secretory vesicles in yeast and into vesicles destined for the apical PM in mammalian cells (De Matteis and Luini, 2008). The only known cargo adaptor involved in transport directly from the TGN to the PM in yeast is the exomer complex, and no cargo adaptors have yet been identified that transport cargos to the apical PM in

mammals (Barfield et al., 2009; Wang et al., 2006; Zanolari et al., 2011). In addition, these pathways appear to be independent of clathrin or other known coat proteins (Mellman and Nelson, 2008; Payne and Schekman, 1985). The transport and delivery of yeast secretory vesicles, on the other hand, has been well-studied: the Rab GTPase Sec4 forms a complex with the motor protein Myo2 to direct secretory vesicles to the PM, and Sec2, the GEF for Sec4, interacts with the exocyst tethering complex at the PM (Santiago-Tirado and Bretscher, 2011).

The Arf family of small GTPases, specifically Arf1/2 in yeast, control nearly all traffic leaving the Golgi complex (Figure 1.5) (D'Souza-Schorey and Chavrier, 2006). Activated Arf1 recruits the COPI coat complex for retrograde transport between Golgi cisternae and from the *cis*-Golgi to the ER (Donaldson and Jackson, 2011). In addition, Arf1 at the TGN initiates the formation of transport vesicles in both the clathrin-dependent and coat-independent exit pathways, and Arf1 and phosphatidylinositol 4-phosphate (PI4P) participate in cargo sorting by recruiting cargo adaptors and proteins that modulate Golgi morphology (Santiago-Tirado and Bretscher, 2011). The AP-1 and AP-3 complexes and the GGAs are all Arf effectors, as are several proteins that are required for coat-independent trafficking, such as phospholipase D (PLD), four-phosphate-adaptor protein 1 and 2 (FAPP1/2), and exomer (Brown et al., 1993; Cockcroft et al., 1994; Godi et al., 2004; Santiago-Tirado and Bretscher, 2011). However, the regulation of Arf1 activation at the Golgi complex is not well understood. Arf1 is recruited and activated by Arf-GEFs, and while the biochemical mechanism of activation has been characterized, little is known about how the Golgi Arf-GEFs are recruited or how their GEF activity is regulated. The Golgi Arf-GEFs are very large proteins (180-200 kDa) that contain multiple conserved domains of unknown function and thus have the potential to interact with multiple proteins to integrate trafficking signals and coordinate distinct cargo sorting events.

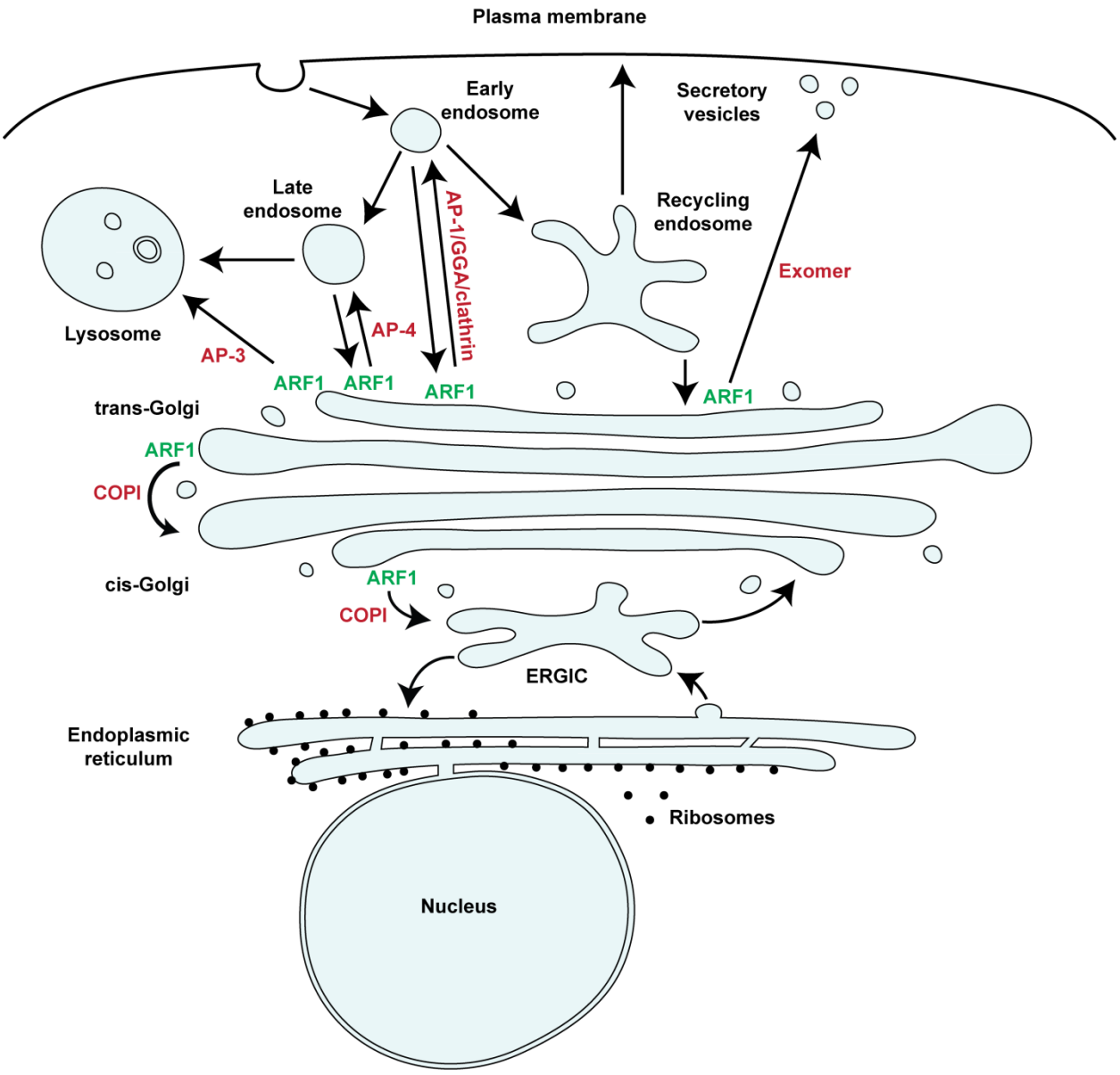

Figure 1.5: The Arf-mediated Golgi trafficking pathways. Arf1 controls nearly all protein trafficking out of the Golgi complex. It recruits clathrin and the adaptor complexes, the GGAs, exomer, and COPI to generate transport vesicles with diverse destinations, including endosomes, the plasma membrane, and retrograde transport to the endoplasmic reticulum.

Determining the factors that regulate Arf-GEF recruitment and activity should provide insights into the regulation of Arf-dependent membrane trafficking at the Golgi.

The Ras superfamily of small GTPases

Ras superfamily GTPases function as molecular switches that alternate between two conformational states, GTP-bound ("on") and GDP-bound ("off"), to regulate diverse cellular functions such as gene expression, cell proliferation and survival, differentiation, cytoskeletal organization, cell polarity and movement, cell-cell interactions, and membrane trafficking (Rojas et al., 2012; Wennerberg et al., 2005). The Ras superfamily is divided into five branches based on sequence and functional similarities: the Ras (Rat sarcoma), Rab (Ras-like proteins in brain), Rho (Ras homologous), Ran (Ras-like nuclear), and Arf (ADP-ribosylation factor) GTPases (Rojas et al., 2012; Wennerberg et al., 2005). While the specific roles of these GTPases vary, they all share the ability to recruit specific effectors when in their GTP-bound conformation. The nucleotide-bound state of these GTPases is regulated by GEFs, which exchange GDP for GTP, and GAPs, which stimulate GTP hydrolysis. Upon GTP binding, all Ras superfamily GTPases undergo conformational changes in the switch 1 and switch 2 regions; most Ras effector proteins bind to the switch regions when they are in the GTP-bound conformation (Wennerberg et al., 2005). The small GTPases of the Rab and Arf families regulate nearly every step of intracellular membrane trafficking and will be discussed in greater detail.

The Arf family of GTPases

Members of the Arf protein family play important roles in the trafficking events of the secretory and endocytic pathways. The Arf proteins are divided into three classes based on

sequence homology: the Class I Arfs (Arf1-3) are found in all eukaryotes and regulate cargo adaptor and coat recruitment to budding vesicles in the secretory pathway; the Class II Arfs (Arf4-5) localize to the Golgi, but are only found in higher eukaryotes and appear to play specialized roles in Golgi trafficking; the sole member of the Class III Arfs, Arf6, localizes to the plasma membrane and endosomes, where it regulates endocytic trafficking and actin remodeling (D'Souza-Schorey and Chavrier, 2006; Donaldson and Jackson, 2011; Gillingham and Munro, 2007b). In addition to the main Arf proteins, the Arf family also includes over 20 Arf-like proteins (Arls), which share structural features with the main Arfs but do not have ADP-ribosylation activity. The Arl proteins play a wide variety of roles, though only a handful are conserved throughout eukaryotes. Sar1 is also grouped with the Arf family because of its structural and functional similarities (Gillingham and Munro, 2007b).

The budding yeast *S. cerevisiae* contains seven Arf family GTPases: Arf1 and Arf2, which are functionally redundant Class I Arfs; Arf3, the Class III ARF6 homologue; the Arf-like proteins Arl1, Arl3, and Cin4; and Sar1 (Gillingham and Munro, 2007b). The Class I Arfs in yeast, Arf1 and Arf2, are of particular interest, as they control nearly all vesicle trafficking out of the Golgi complex. For simplicity, I will refer to Arf1/2 only as Arf1. Arf1 recruits COPI to vesicles for Golgi-to-ER and intra-Golgi retrograde trafficking, and it also initiates the formation of clathrin-coated vesicles at the TGN and endosomes by recruiting clathrin adaptors (Donaldson and Jackson, 2011). Arf3, which only shares 66% sequence identity with Arf1, is involved in endocytosis, membrane lipid modification, and endocytic recycling (D'Souza-Schorey and Chavrier, 2006; Donaldson and Jackson, 2011). Recruitment of Arf3 to the PM increases the levels of PI4,5P2 in the PM (Smaczynska-de et al., 2008). There are no Class II Arfs in yeast, as they evolved later, possibly with the emergence of metazoans. The yeast Arls, Arl1 and Arl3,

both localize to the TGN. Arl1 recruits the only GRIP (golgin-97, RabBP2α, Imh1p, and p230)-domain golgin in yeast, Imh1, to the TGN, while Arl3, a homologue of Arf-related protein 1 (ARFRP1), controls the pathway leading to Arl1 recruitment (Panic et al., 2003; Setty et al., 2003). Cin4, an Arl2 homologue, participates in β-tubulin folding through interactions with homologues of cofactors D (Cin1) and E (Pac2), though this pathway is nonessential (Bhamidipati et al., 2000; Hoyt et al., 1997). As discussed earlier, Sar1 recruits the COPII coat to vesicles for ER-Golgi trafficking (Fath et al., 2007; Oka and Nakano, 1994).

All Arf family proteins have a myristoylated N-terminal amphipathic helix that inserts into the lipid bilayer to mediate membrane interaction (Randazzo et al., 1995). This helix is masked in the GDP-bound form, preventing untargeted membrane association; however, Arf GTPases undergo an additional conformational change in the interswitch region upon GTP binding that displaces the helix from a hydrophobic pocket, exposing the helix and promoting its insertion into the lipid bilayer (Figure 1.6) (Beraud-Dufour et al., 1998; Gillingham and Munro, 2007b; Goldberg, 1998; Randazzo et al., 1995). Activation by a GEF therefore brings Arfs into close contact with the target membrane, whereas small GTPases of the Rab and Rho families have long, flexible carboxy-terminal linkers separating the GTPase from its membrane anchor (Donaldson and Jackson, 2011). Unlike Rab family members, Arf GTPases do not require other factors beyond GEFs and GAPs to regulate membrane recruitment and activation (Donaldson and Jackson, 2011; Wennerberg et al., 2005). Therefore, the Arf-GEFs are directly responsible for the recruitment of Arf GTPases to membranes, making the understanding of GEF recruitment and localization an important element in understanding Arf-directed membrane trafficking.

The Arf-GEFs are divided into seven families, six of which contain a conserved, 200-residue GEF domain, called the Sec7 domain, that catalyzes nucleotide exchange. The Arf

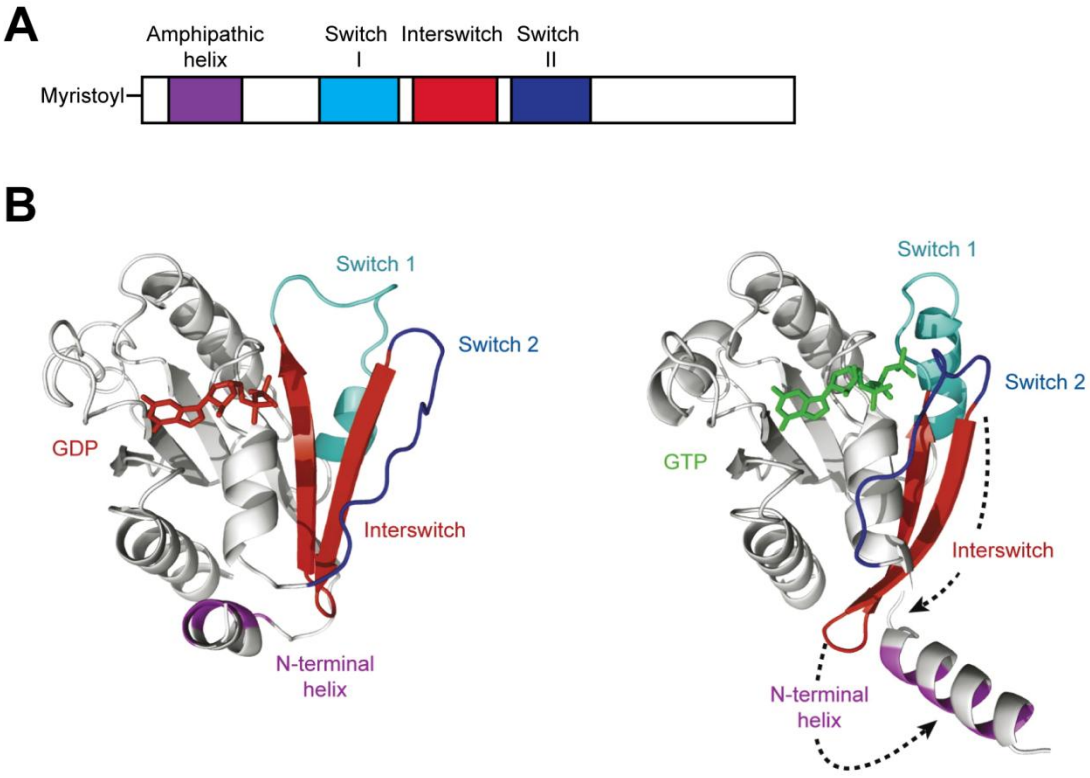

Figure 1.6: The small GTPase Arf1. (A) Schematic representation of Arf family GTPases. **(B)** The structure of Arf1 in its GDP-bound state (Amor et al., 1994) and GTP-bound state (Shiba et al., 2003). Upon activation by a GEF, Arf1 undergoes a conformational change in which the interswitch region displaces the N-terminal amphipathic helix, allowing it to interact instead with the membrane surface. (Part B from Gillingham and Munro, 2007b).

switch I and switch II regions insert into a hydrophobic groove in the Sec7 domain; Arf rotates around this surface, bringing the catalytic glutamate residue of the Sec7 domain close to the GDP binding site and destabilizing the interaction with GDP. A GTP molecule can then diffuse into the empty binding pocket (Gillingham and Munro, 2007b). The known yeast Arf-GEFs are Sec7, Gea1, Gea2, Yel1, Syt1, and Sec12. Sec7 recruits Arf1 to the *trans*-Golgi and TGN, while Gea1 and Gea2 activate Arf1 at the *cis*-Golgi (Chantalat et al., 2003; Franzusoff et al., 1991; Zhao et al., 2002). The Arf-GEF Yel1, an EAF6 ortholog, activates Arf3 at the plasma membrane, while Syt1 activates Arl1 at the late Golgi (Chen et al., 2010; Gillingham and Munro, 2007a; Smaczynska-de et al., 2008). Sec12 is the Arf-GEF for Sar1, and is the only Arf-GEF that does not contain a Sec7 domain (Gillingham and Munro, 2007b). As the Arf-GEFs play such a pivotal role in regulating the spatial and temporal recruitment of Arf1 to membranes, they will be explored in greater detail later.

The Arf-GAPs catalyze nucleotide hydrolysis of GTP-bound Arfs, as most Arfs have negligible intrinsic GTP hydrolysis activity. There are 10 families of Arf-GAPs, though most are not represented in yeast (Kahn et al., 2008). All Arf-GAPs contain a conserved GAP domain of ~130 residues that contains a zinc finger motif consisting of four cysteines and conserved arginine, $CX_2CX_{16}CX_2CX_4R$, that is required for activity (Kahn et al., 2008). The zinc finger is thought to serve an architectural role, while the arginine serves as a catalytic "arginine finger". The only structure of a GTP-bound Arf with an Arf-GAP is that of ASAP3 (ArfGAP with SH3 domain, ankyrin repeat, and PH domain 3) with Arf6 (Arf3 in yeast); this structure reveals that the Arf-GAP interacts with switches 1 and 2 of Arf6 and that the arginine finger inserts into the catalytic pocket of Arf6 (Ismail et al., 2010). The yeast Arf-GAPs identified thus far include Gcs1, Glo3, Gts1, Age1 and Age2. None of the yeast GAPs are essential on their own, as they

share overlapping functions (Poon et al., 1999; Poon et al., 2001; Zhang et al., 2003). Gcs1, Glo3, Age1, and Age2 all act on Arf1, and Gcs1 also displays GAP activity on Arl1 (Liu et al., 2005; Poon et al., 1999; Poon et al., 2001; Poon et al., 1996; Zhang et al., 2003). On its own, Gcs1 can compensate for the *glo3*Δ*/age1*Δ*/age2*Δ triple deletion (Zhang et al., 2003). Gcs1, Age1, and Age2, orthologs of mammalian ArfGAP1, are all involved in trafficking out of the *trans*-Golgi. However, Gcs1 and Age2 seem to be more important, as cells missing both Gcs1 and Age2 are inviable, though overexpression of Age1 can compensate for the double deletion (Benjamin et al., 2011b; Poon et al., 2001; Zhang et al., 2003). Glo3, an ortholog of mammalian ArfGAP2/3, is the main GAP involved in Golgi-ER retrograde trafficking, and is a component of COPI-coated vesicles (Lewis et al., 2004; Poon et al., 1999). Gts1 is the Arf-GAP for Arf3 at the PM, and loss of Gts1 increases the level of Arf3 and the level of PtdIns(4,5)P2 at the PM (Smaczynska-de et al., 2008).

The primary function of all small GTPases is to interact with and recruit effectors while in their GTP-bound states. At the Golgi complex, Arf1 recruits the COPI coat for recycling of ER resident proteins back to the ER and for retrograde intra-Golgi trafficking. Arf1 effectors at the TGN include the cargo adaptors AP-1, AP-3, and AP-4, GGA1-3, and exomer, all of which recruit cargo proteins to budding vesicles at the TGN and endosomes (Donaldson and Jackson, 2011; Park and Guo, 2014). Arf1 also recruits lipid-modifying enzymes such as PLD, FAPP1/2, and CERT (ceramide transfer) to the Golgi (Donaldson and Jackson, 2011). Arl1 effectors at the TGN include the GRIP-domain protein Imh1 and the GARP (Golgi-associated retrograde protein) complex, which are both involved in tethering endosomal vesicles to the TGN, while Arl3 controls the recruitment of Arl1 to the TGN (Chen et al., 2010; Panic et al., 2003; Setty et al., 2003).

Arf1, Arf6 and Sar1 have all been shown to induce membrane deformation and participate in vesicle formation through insertion of their N-terminal amphipathic helices into the lipid bilayer (Krauss et al., 2008; Lee et al., 2005; Lundmark et al., 2008). Both Arf1 and Sar1 have also been show to generate membrane tubules (Aridor et al., 2001; Krauss et al., 2008; Lee et al., 2005). Arf1 tubulation is dependent on Arf1 dimerization, and an Arf1 mutant incapable of dimerization was unable to induce membrane deformation (Beck et al., 2008). In mammalian cells, this mutant was able to recruit the COPI coat, but could not form vesicles, and the mutation was lethal when introduced into yeast (Beck et al., 2008). Further studies revealed that the dimerization mutant was able to induce the formation of small buds, but these vesicles could not undergo scission from the donor membrane; however, cross-linking the mutant Arf1 restored scission, strongly indicating that Arf1 dimerization not only leads to membrane deformation but may also play an important role in membrane fission (Beck et al., 2011). Additionally, both Arf1 and Arf6 act as sensors of membrane curvature, leading to a model in which GEFs generate local concentrations of Arf1-GTP, which induces positive membrane curvature that acts to further recruit Arf1-GTP in a positive-feedback loop (Lundmark et al., 2008).

The Rab family of GTPases

The Rab GTPases comprise the largest family of small GTPases; humans express over 60 Rab proteins, many of which have specialized roles, though only 11 Rabs are expressed in yeast. Rab GTPases are also important regulators of intracellular trafficking and typically direct vesicle transport, target membrane recognition and tethering, and fusion to the target membrane (Kelly et al., 2012; Stenmark, 2009). The Rab GTPases differ from Arf GTPases in several key ways: 1) instead of an N-terminal amphipathic helix, Rab GTPases interact with membranes via 1-2

geranylgeranylated Cys residues at the C-terminus, and Rab escort proteins (REPs) are responsible for chaperoning newly-synthesized Rabs to geranylgeranyl transferases (GGTs); 2) Rabs contain a long flexible linker between the lipid anchor and the rest of the GTPase, allowing them to extend much further from the membrane surface; 3) Rab GTPase cycling is controlled by GDP dissociation inhibitors (GDIs), which associate with GDP-bound Rabs to stabilize the inactive form, and by GDI displacement factors (GDFs), which displace GDIs at target membranes and allow Rabs to associate with the membrane. However, very few GDFs have been discovered, and recent studies suggest that the GEF will often act as the GDF (Figure 1.7) (Gillingham and Munro, 2007b; Kelly et al., 2012; Stenmark, 2009).

The Rab GTPases found in yeast include Ypt1 (Rab1 ortholog), Vps21 and Ypt52/53 (Rab5 orthologs), Ypt6 (Rab6 ortholog), Ypt7 (Rab7 ortholog), Sec4 (Rab8 ortholog), Ypt31/32 (Rab11 orthologs), Ypt10 and Ypt11. Ypt1, Ypt6, and Ypt31/32 are involved in membrane trafficking steps at the Golgi complex and will be discussed in detail (Figure 1.8). Sec4 is required for the transport of secretory vesicles to the PM by interacting with the Myo2 motor protein (Wagner et al., 2002; Walch-Solimena et al., 1997). Vps21, Ypt52, and Ypt53 are involved in endocytosis and help mediate fusion to early endosomes, while Ypt7 acts on late endosomes to mediate recycling and fusion with the vacuole (Balderhaar et al., 2010; Horazdovsky et al., 1994; Singer-Kruger et al., 1994; Singer-Kruger et al., 1995). The role of Ypt10 has not been well studied, though an endocytic function has been proposed, and Ypt11 is involved in ER and mitochondria inheritance (Buvelot Frei et al., 2006; Lewandowska et al., 2013).

The regulators of Rab function at the Golgi include the GDI ortholog Gdi1 (also known as Sec19), the Gyp (GAP for Ypt proteins) family of GAPs, and the GEF complexes

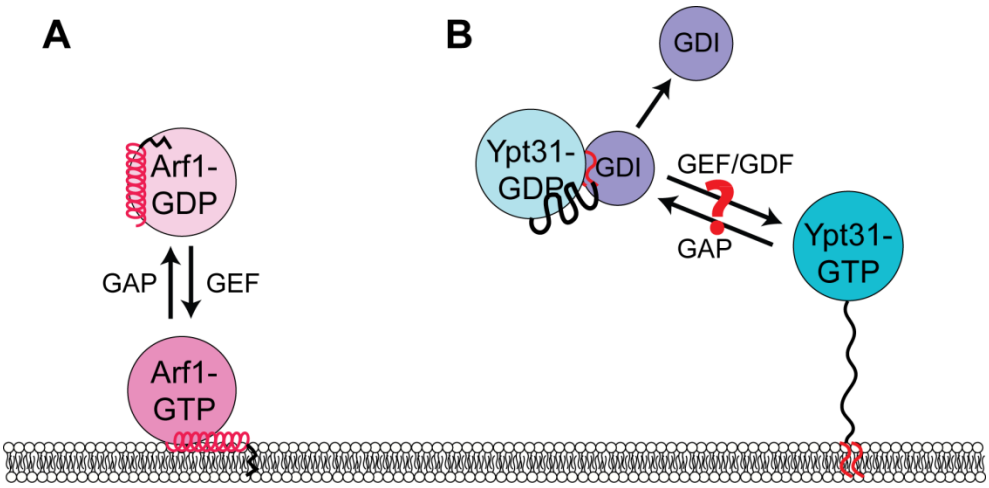

Figure 1.7: The Rab family of GTPases
(A) Activation of Arf GTPases by a GEF causes a conformational change that exposes a short myristoylated N-terminal helix, coupling activation with membrane recruitment.
(B) In contrast, cytosolic Rab GTPases are bound to GEF dissociation inhibitors (GDIs), and a GDI displacement factor (GDF) is needed to recruit Rabs to membrane. Additionally, Rab GTPases interact with membranes via a long, geranylgeranylated C-terminal linker and are not held as closely to the membrane surface.

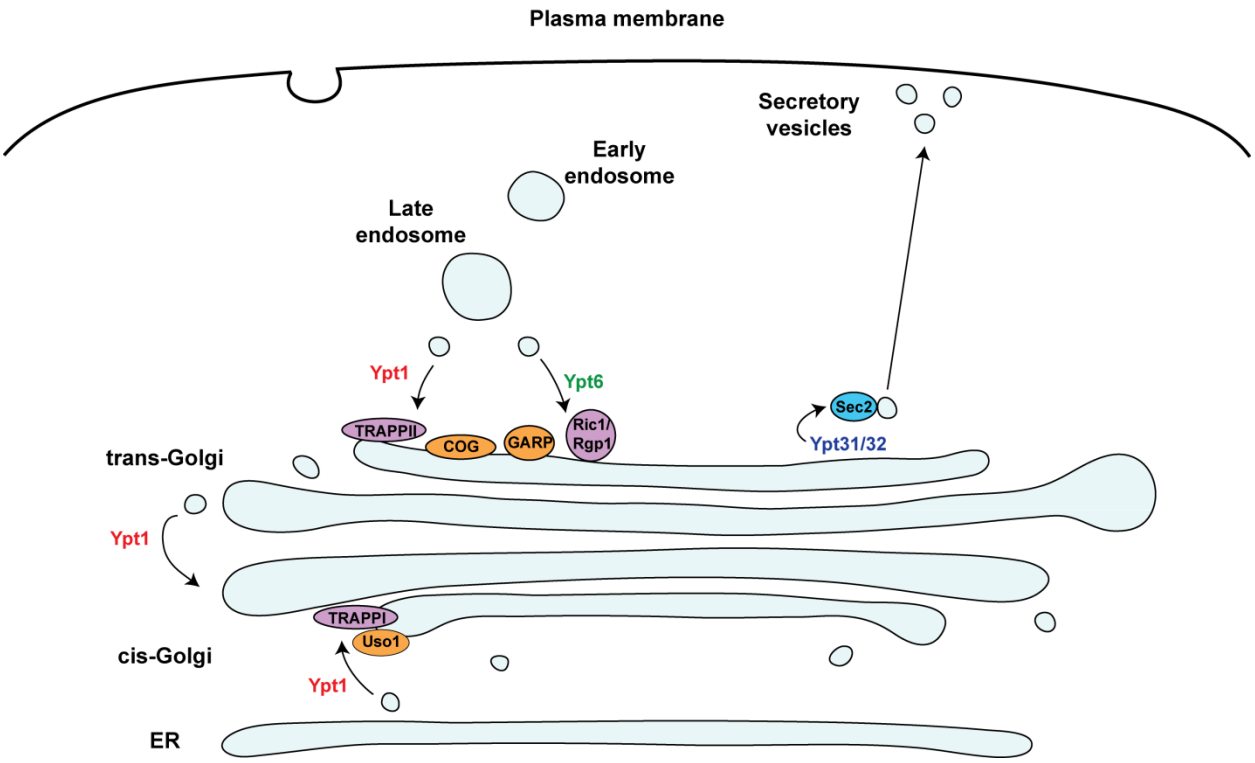

Figure 1.8: Roles of the Golgi-localized Rab GTPases. Ypt1, Ypt6, and Ypt31/32 all act in membrane trafficking pathways at the Golgi complex. Ypt1 is required for ER-Golgi transport; it is activated by the GEF TRAPPI at the *cis*-Golgi and interacts with Uso1 to tether incoming vesicles. Ypt1 also interacts with the GEF TRAPPII and the GARP and COG tethering complexes for endosome-Golgi and retrograde Golgi trafficking. Ypt6 is activated by the Ric1/Rgp1 GEF complex and tethers endosomal vesicles to the Golgi via the GARP and COG complexes. Ypt31/32 recruit the GEF Sec2 to secretory vesicles, which enables recruitment of the Myo2 motor protein via the small GTPase Sec4. Ypt31/32 also appear to play a direct role in vesicle biogenesis from the TGN, though this has not yet been confirmed. GEFs are shown in purple and tethers are shown in orange.

TRAPPI/II/III and Ric1/Rgp1 (Buvelot Frei et al., 2006). Gdi1 regulates the yeast Rabs by binding to the GDP-bound forms of Rabs on target membranes, extracting them from the lipid bilayer, and recycling them back to the appropriate donor membrane (Ignatev et al., 2008; Pylypenko et al., 2006; Rak et al., 2003). The GDFs responsible for recruiting Rabs to membranes and displacing Gdi1 has not yet been identified in yeast, though the Yip (Ypt-interacting protein) family of proteins may play a role (Barrowman et al., 2003; Geng et al., 2005; Sivars et al., 2003). It has also been suggested that the GEFs themselves act as GDFs. The relevant Rab GAPs in yeast include Gyp1, Gyp2, Gyp5, Gyp6, Gyp7, and Gyp8 (Albert and Gallwitz, 1999; De Antoni et al., 2002; Du and Novick, 2001; Strom et al., 1993; Vollmer et al., 1999; Will and Gallwitz, 2001). Like the Arf GAPS, the Rab GAPs have overlapping functions, and nearly all identified Rab GAPs have been shown to catalyze exchange on multiple Rabs *in vitro* (Albert and Gallwitz, 1999; Du et al., 1998). However, only a handful of Rab-GAP pairings have been shown to have *in vivo* relevance thus far, including Gyp1 with Ypt1 at the *cis*-Golgi, Msb3/4 with Sec4 during exocytosis, and Msb3 with both Vps21 and Ypt7 in the endocytic pathway (Du and Novick, 2001; Gao et al., 2003; Lachmann et al., 2012).

The three TRAPP complexes all localize to the Golgi, but each play a distinct role in the membrane trafficking. TRAPPI is the core TRAPP complex and is composed of six subunits, Bet3, Bet5, Trs20, Trs23, Trs31, and Trs33 (Barrowman et al., 2010). TRAPPI is a GEF for Ypt1 and is involved in targeting COPII-coated vesicles from the ER to the *cis*-Golgi (Sacher et al., 2001; Sacher et al., 1998). TRAPPII contains Trs65, Trs120, and Trs130 in addition to the core complex and may play a similar role as TRAPPI in enabling COPI-coated vesicle tethering during intro-Golgi trafficking (Cai et al., 2005; Yip et al., 2010). However, it remains controversial whether TRAPPII is a GEF for Ypt1, Ypt31/32, or both. While several studies have

shown that TRAPPII stimulates GEF exchange of Ypt31/32 and not Ypt1 (Morozova et al., 2006), both structural studies and biochemical assays with highly purified TRAPPI and TRAPPII complexes suggest that both GEFs act only on Ypt1 (Cai et al., 2008; Wang and Ferro-Novick, 2002; Yip et al., 2010). The most likely explanation for the conflicting data is that the Ypt31/32 GEF is an effector of either Ypt1 or TRAPPII, though this putative GEF has not yet been isolated (Wang and Ferro-Novick, 2002). TRAPPIII, the final TRAPP complex, contains the core complex plus Trs85; it is a GEF for Ypt1 and is required for autophagy (Lynch-Day et al., 2010).

Ypt1 is most known for its role in the early secretory pathway, where it is required for ER to Golgi and intra-Golgi transport (Bacon et al., 1989; Jedd et al., 1995; Segev et al., 1988). Ypt1 targets COPII-coated vesicles to the *cis*-Golgi and is required for tethering incoming vesicles via Uso1 and the TRAPPI complex (Cao et al., 1998; Rexach and Schekman, 1991; Sacher et al., 2001; Segev, 1991). The interesting aspect of this is that TRAPPI is located on the acceptor membrane rather than the donor membrane, indicating that Ypt1 is loaded onto COPII-coated vesicles in its GDP-bound form and is not activated until the vesicle reaches the Golgi complex (Jones et al., 1998; Sacher et al., 2001). The localization of GEFs and GAPs for several other Rabs involved in vesicle transport follow a similar pattern, suggesting that activation by GEFs at the target membrane and deactivation by GAPs at the donor membrane may be a general regulation mechanism of Rabs involved in vesicle targeting and fusion. In addition, many of these GEFs interact with other factors present on the incoming vesicles. TRAPPI directly interacts with the Sec23 component of the COPII coat, providing an additional level of specificity to vesicle docking (Cai et al., 2007b; Yu et al., 2006). Besides mediating ER-to-Golgi traffic, Ypt1 also mediates the retrograde trafficking of intra-Golgi COPI-coated vesicles by interacting with the COG (conserved oligomeric Golgi) tethering complex (containing Cog1-8),

which binds to both SNAREs and the COPI vesicle coat to tether vesicles to the Golgi (Suvorova et al., 2002). The TRAPPII complex likely also plays a role in this pathway by activating Ypt1 from the incoming intra-Golgi vesicles and interacting with the COPI coat (Chen et al., 2011).

In addition to its role in the early Golgi, Ypt1 also localizes to the *trans*-Golgi, and mutants that specifically effect fusion of endosomal vesicles to the late Golgi, but do not effect earlier stages of the secretory pathway, have been recently described (Sclafani et al., 2010). Rather than accumulating ER or Golgi membranes, these mutants amass small vesicles and are defective in recycling Snc1 (Sclafani et al., 2010). Finally, Ypt1, together with the recently discovered TRAPPIII complex, have been shown to play a role in autophagy, possibly by tethering together the necessary membranes for autophagosome formation (Lynch-Day et al., 2010). In summary, Ypt1 is a master regulator of vesicle traffic at the Golgi, controlling the flow of vesicles into both the *cis* and *trans* faces, and it may also play a role in membrane expansion during autophagy.

Ypt31 and Ypt32, which are functionally redundant, act at the *trans*-Golgi downstream of Ypt1 (Benli et al., 1996). The regulation of Ypt31/32 remains unclear, as the identity of the Ypt31/32 GEF remains controversial. While some believe that the TRAPPII-specific components switch the GEF specificity of TRAPP from Ypt1 to Ypt31/32, others have proposed that the Ypt31/32 GEF is an unidentified effector of Ypt1 that is distinct from the TRAPPII complex (Morozova et al., 2006; Wang and Ferro-Novick, 2002). Gyp2 has been suggested to be a Ypt31/32 GAP *in vivo*, as deleting Gyp2 from the *ypt1-101/ypt32*Δ strain rescues both the growth and trafficking defects (Sciorra et al., 2005). Ypt31/32 plays a role in secretory vesicle transport by recruiting the GEF Sec2 to secretory vesicles, which activates the Rab GTPase Sec4 (Ortiz et al., 2002). Activated Sec4 then forms a complex with Myo2 to direct polarized vesicle

secretion (Bielli et al., 2006; Lipatova et al., 2008; Wagner et al., 2002). However, genetic interactions between Ypt31/32 and both Syt1 and Sec7 at the *trans*-Golgi have also been demonstrated: overexpression of Syt1, an Arl1 GEF, rescues the growth phenotype of a *ypt31Δ/ypt32* mutant, while overexpression of Ypt31/32 rescues the growth of a *sec7* mutant (Jones et al., 1999). Additionally, mutations in Ypt31/32, similar to those in Sec7, result in enlarged Golgi morphology (Benli et al., 1996; Jedd et al., 1997; Novick et al., 1980). Taken together, these data indicate that Ypt31/32 play a direct role in vesicle biogenesis from the TGN prior to Sec2 recruitment, though the exact nature of that role has not yet been determined.

Ypt6 is involved in recycling from endosomes to the Golgi and is required for the fusion of endosome-derived vesicles with the Golgi (Siniossoglou et al., 2000; Siniossoglou and Pelham, 2001). Ypt6-GDP is recruited to endosomes and is activated by the Ric1/Rgp1 GEF complex upon reaching the *trans*-Golgi (Bensen et al., 2001; Siniossoglou et al., 2000). Activated Ypt6 then recruits the GARP (Golgi-associated retrograde protein) complex to tether vesicles to the Golgi. The GARP complex is composed of Vps51, Vps52, Vps53, and Vps54 and interacts with both Ypt6 and the SNARE Tlg1 at the TGN, leading to vesicle fusion (Conibear et al., 2003; Siniossoglou and Pelham, 2001). Endosome-to-Golgi traffic mediated by Ypt6 is at least partly regulated by a Rab-GAP cascade initiated by Ypt31/32: activation of Ypt31/32 at the TGN leads to the recruitment of Gyp6, a Ypt31/32 effector and GAP for Ypt6, which in turn hydrolyzes Ypt6 and prevents the fusion of early endosomes with the Golgi complex (Suda et al., 2013; Will and Gallwitz, 2001).

Interplay between the Rab and Arf pathways

Given the importance of the Arf and Rab GTPases at the Golgi, one would expect to find crosstalk between the Arf and Rab pathways to help coordinate the various trafficking events at the Golgi. At the *cis*-Golgi in mammals, the Arf-GEF GBF1 (Gea1/2) is an effector of Rab1 (Ypt1) and interacts directly with Rab1-GTP via its N-terminus (Monetta et al., 2007). In addition, the TRAPPII component Trs65 directly binds to the C-terminus of Gea2 in yeast, and this interaction appears to be important in stabilizing the TRAPPII complex on the membrane (Chen et al., 2011). At the *trans*-Golgi, deletion of Ypt6 leads to the mislocalization of Sys1 and subsequent proteins in the Arl1 pathway, including Arl1 itself and its effector Imh1 (Benjamin et al., 2011a). Genetic interactions between the Rabs Ypt1 and Ypt31/32 and the Golgi Arf-GEFs also hint at crosstalk between the Arf and Rab pathways. As mentioned previously, overexpression of Ypt32 rescues the growth defect of the *sec7-4* allele. The same study also found that overexpression of Ypt1 rescued the growth of both the *sec7-1* and the *gea1-6* temperature-sensitive strains (Jones et al., 1999). While these studies provide tantalizing clues to interactions between the Rab and Arf pathways at the Golgi, and specifically the TGN, the mechanisms of these interactions has not been determined.

The BIG/GBF family of Arf-GEFs

As mentioned earlier, Arf1 controls nearly all protein trafficking out of the Golgi complex, and the Arf-GEFs control where and when Arf1 is activated. Therefore, understanding how the Arf-GEFs are regulated and recruited to membranes is vital to understanding how vesicle trafficking in the Golgi is regulated and balanced. At the *cis*-Golgi, Arf1 is activated by Gea1/2 in yeast and by GBF1 (Golgi-specific Brefeldin A-resistance factor) in mammalian cells,

and at the *trans*-Golgi and TGN it is activated by Sec7 in yeast and BIG (Brefeldin A-inhibited GEF) 1/2 in mammalian cells (Figure 1.5). However, it is not known how the recruitment and activity of the Golgi Arf-GEFs is regulated (Franzusoff et al., 1991; Zhao et al., 2002).

The Arf-GEFs determine both the spatial and temporal activation of Arf proteins. The majority of the Arf-GEFs share a common 200-amino acid Sec7 domain, named after the protein in which it was discovered, which binds to Arfs and causes GDP dissociation, allowing GTP to bind (Figure 1.9). The only Arf-GEF that does not contain a Sec7 domain is Sec12, which activates Sar1 (Barlowe and Schekman, 1993; Futai and Schekman, 2005; Nakano and Muramatsu, 1989). The remaining Sec7 domain-containing GEFs are divided into six families based on evolutionary conservation: the GBF, BIG, cytohesin, EAF6, BRAG, and FBOX families (Gillingham and Munro, 2007b). However, only the BIG, GBF, and EAF6 families are represented in yeast. The cytohesins are the smallest Arf-GEFs and function in plasma membrane-endosomal trafficking pathways. While the mechanisms controlling the spatial regulation of cytohesins are mostly understood, no cytohesins are found in yeast (Donaldson and Jackson, 2011). Yeast contain two members of the EAF6 family: Yel1 activates Arf3 at the plasma membrane, and Syt1 activates Arl1p at the late Golgi (Chen et al., 2010; Donaldson and Jackson, 2011; Smaczynska-de et al., 2008). The BIG and GBF families contain the largest Arf-GEFs, ranging in size from 180-200 kDa, and are closely related; Sec7 is a BIG family GEF, while Gea1 and Gea2 belong to the GBF family.

The BIG and GBF GEFs share five conserved homology domains outside of the Sec7 domain: the DCB (dimerization and cyclophilin binding) domain, the HUS (homology upstream of Sec7) domain, and the HDS1-3 (homology downstream of Sec7) domains (Figure 1.9) (Bui et al., 2009; Mouratou et al., 2005). BIG GEFs also contain one extra HDS domain, HDS4, that

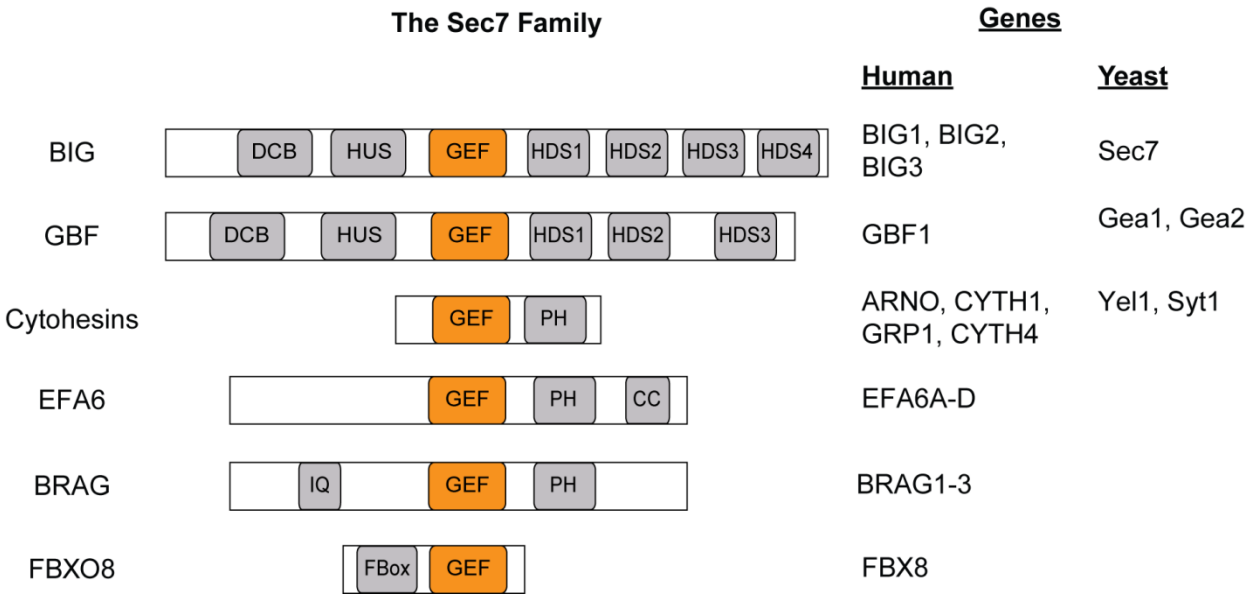

Figure 1.9: The Sec7 family of Arf-GEFs. The domain architecture of the Sec7 family of Arf-GEFs. While the majority of the families contain domains with known functions, such as the Pleckstrin homology (PH) domain, the BIG and GBF Arf-GEFs contain 5-6 conserved domains with mostly unknown functions.

is not found in the GBF GEFs. While many of the smaller Arf-GEFs contain common domains with known functions, such as PH (pleckstrin homology) domains, the function of most of the BIG/GBF domains remains unknown (Gillingham and Munro, 2007b). The central Sec7 domain splits the BIG and GBF GEFs into two halves: the N-terminal half contains the DCB and HUS domains, while the C-terminal half contains the HDS domains. The DCB has been shown to mediate homodimerization of the BIG and GBF GEFs and also interacts with the HUS domain, specifically with the highly conserved HUS box region (Ramaen et al., 2007). The functions of the remaining domains are unknown, but their conservation suggests that they play important regulatory functions. The DCB and HUS domains are the most highly conserved domains outside of the Sec7 domain, particularly among the GBF members; a stretch of seven amino acids in the HUS domain is especially conserved and has been termed the HUS box. The HDS2 and HDS3 domains are the least conserved domains, and all the HDS domains are less conserved in the GBF GEFs than in the BIG GEFs. The second half of HDS2 is especially conserved among BIG GEFs, while this region in this region in the GBF GEFs has very few conserved residues (Bui et al., 2009).

The size of the BIG/GBF Arf-GEFs makes them difficult to purify and crystallize; only the structure of the Sec7 domain has been determined thus far (Figure 1.10). The Sec7 domain is composed of 10 α-helices and induces a conformational change in Arf1-GDP that forces the dissociation of GDP (Goldberg, 1998; Mossessova et al., 1998). Secondary structure prediction indicates that the BIG/GBF Arf-GEFs are likely to be elongated proteins composed primarily of alpha helices (Bui et al., 2009; Mouratou et al., 2005). The BIG/GBF GEFs are inhibited by the fungal metabolite Brefeldin A (BFA), which binds to the Arf-GDP/GEF complex and prevents the conformational changes needed to release GDP, locking the GEF into an unproductive

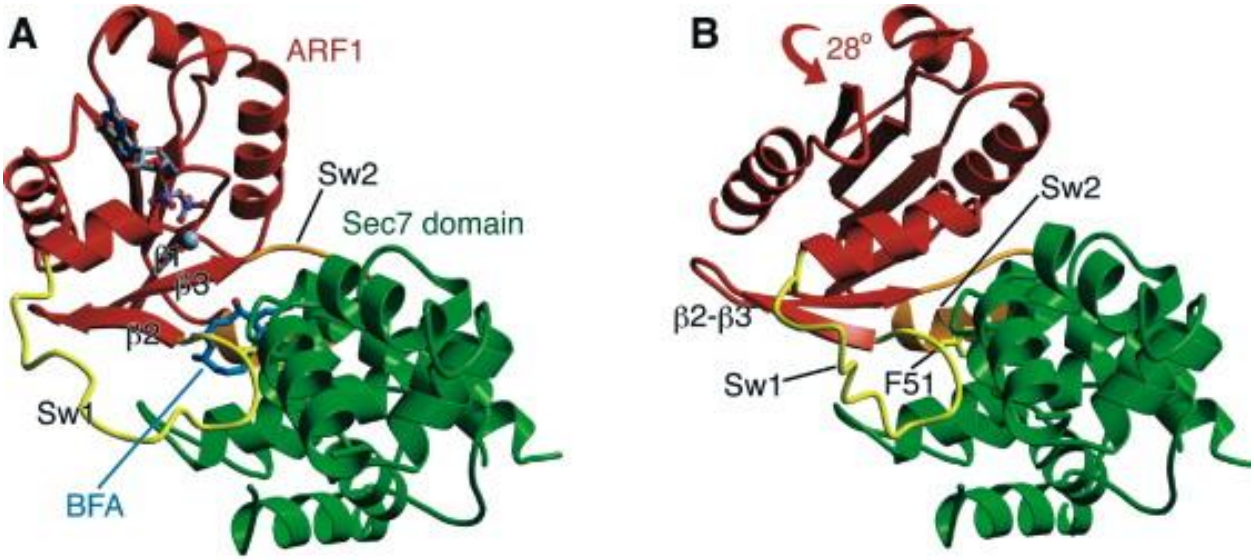

Figure 1.10: The Sec7 GEF domain. (A) The structure of an Arf1-GDP/GEF domain complex trapped using BFA, an inhibitor of the BIG and BGF Arf-GEFs. BFA blocks a necessary conformational change in Arf1. **(B)** The structure of the nucleotide-free Arf1/GEF domain complex. Arf1 has rotated around the GEF domain, forcing the displacement of GDP. (From Mossessova et al., 2003).

complex; however, BFA does not effect other Arf-GEFs, with the possible exception of Syt1 (Cox et al., 2004; Mossessova et al., 2003; Peyroche et al., 1999; Sata et al., 1998).

Only a handful of proteins have been shown to interact directly with the BIG/GBF GEFs. As mentioned previously, human GBF1 has been shown to bind Rab1 via its N-terminus, and TRAPPII binds to Gea2 in yeast (Chen et al., 2011; Monetta et al., 2007). In addition, GBF1/Gea1 interact directly with the γCOP/Sec21 subunit of the COPI coat in humans and yeast (Deng et al., 2009). Both Gea1 and Gea2 interact with Gmh1, a conserved integral membrane protein of unknown function located at the *cis*-Golgi; however, this interaction is not necessary for recruitment of Gea1/2 to the Golgi (Chantalat et al., 2003). Gea1 and Gea2 in yeast are 50% identical, and while they have overlapping functions and complement for the loss of the other, they are not completely redundant and do not fully colocalize (Peyroche et al., 1996; Spang et al., 2001). In addition, some Gea2 can be found in later Golgi compartments along with Kex2 and Drs2, which are late Golgi proteins (Chantalat et al., 2004). Yeast Gea2 has also been shown to interact with Drs2, a *trans*-Golgi flippase that maintains membrane lipid asymmetry in secretory vesicles, and both Gea2 and PI4P are needed to activate Drs2 (Chantalat et al., 2004; Natarajan et al., 2009).

Even fewer direct interactions have been demonstrated with the BIG family members. Mammalian BIG1 and BIG2 are 74% identical and have overlapping but not redundant roles; BIG1 appears to play a larger role in maintaining Golgi morphology, whereas BIG2 is needed to maintain endosomal integrity (Boal and Stephens, 2010; Ishizaki et al., 2008; Shin et al., 2004). Additionally, several genetic diseases in humans have been linked with mutations in BIG2, highlighting the importance of the BIG2-specific functions. Mammalian BIG1 interacts with myosin IXb, and BIG2 interacts with the Exo70 complex of the exocyst, a tethering complex that

is important for cytokinesis (Saeki et al., 2005; Xu et al., 2005). Yeast Sec7 has been shown to directly interact with Rsp5, an E3 essential ubiquitin ligase, and deletion of the Rsp5 binding region from the C-terminus of Sec7 partially mislocalizes Sec7 to the cytoplasm (Dehring et al., 2008). While the protein interactions identified for the BIG/GBF GEFs so far present important clues to the function of these GEFs, none of these interactions are necessary for the Golgi localization of the GEFs or have been shown to regulate the activity of the GEFs.

Project Overview

Despite their importance in regulating Arf recruitment to the Golgi complex, little is known about the function of the domains outside of the GEF domain or about how these proteins are regulated (Anders and Jurgens, 2008; Bui et al., 2009). In particular, it is not known how the BIG/GBF Arf-GEFs are recruited to their specific sites within the Golgi or how their GEF activity is regulated. The importance of the BIG/GBF Arf-GEFs in regulating the activation of Arf1/2 at the Golgi demands further investigation into the mechanisms regulating their localization and regulation. In particular, determining the function of the conserved homology domains outside of the GEF domain and identifying interacting proteins involved in the recruitment and GEF activation is crucial to our understanding of the Arf-dependent trafficking pathways. In the following chapters, I will present evidence of Sec7 regulation by both autoinhibition and positive feedback. In addition, I will discuss recently identified interactions between Sec7 and multiple small GTPases of the Arf and Rab families and the implications of these interactions for membrane trafficking at the Golgi. Based on my data, I propose that Sec7 links the Arf and Rab pathways and is a master regulator involved in balancing incoming and outgoing traffic at the Golgi.

REFERENCES

Albert, S., and Gallwitz, D. (1999). Two new members of a family of Ypt/Rab GTPase activating proteins. Promiscuity of substrate recognition. The Journal of biological chemistry *274*, 33186-33189.

Amor, J.C., Harrison, D.H., Kahn, R.A., and Ringe, D. (1994). Structure of the human ADP-ribosylation factor 1 complexed with GDP. Nature *372*, 704-708.

Anders, N., and Jurgens, G. (2008). Large ARF guanine nucleotide exchange factors in membrane trafficking. Cellular and molecular life sciences : CMLS *65*, 3433-3445.

Aridor, M., Fish, K.N., Bannykh, S., Weissman, J., Roberts, T.H., Lippincott-Schwartz, J., and Balch, W.E. (2001). The Sar1 GTPase coordinates biosynthetic cargo selection with endoplasmic reticulum export site assembly. J Cell Biol *152*, 213-229.

Aridor, M., Weissman, J., Bannykh, S., Nuoffer, C., and Balch, W.E. (1998). Cargo selection by the COPII budding machinery during export from the ER. J Cell Biol *141*, 61-70.

Bacon, R.A., Salminen, A., Ruohola, H., Novick, P., and Ferro-Novick, S. (1989). The GTP-binding protein Ypt1 is required for transport in vitro: the Golgi apparatus is defective in ypt1 mutants. J Cell Biol *109*, 1015-1022.

Balch, W.E., Dunphy, W.G., Braell, W.A., and Rothman, J.E. (1984a). Reconstitution of the transport of protein between successive compartments of the Golgi measured by the coupled incorporation of N-acetylglucosamine. Cell *39*, 405-416.

Balch, W.E., Glick, B.S., and Rothman, J.E. (1984b). Sequential intermediates in the pathway of intercompartmental transport in a cell-free system. Cell *39*, 525-536.

Balderhaar, H.J., Arlt, H., Ostrowicz, C., Brocker, C., Sundermann, F., Brandt, R., Babst, M., and Ungermann, C. (2010). The Rab GTPase Ypt7 is linked to retromer-mediated receptor recycling and fusion at the yeast late endosome. J Cell Sci *123*, 4085-4094.

Bard, F., and Malhotra, V. (2006). The formation of TGN-to-plasma-membrane transport carriers. Annu Rev Cell Dev Biol *22*, 439-455.

Barfield, R.M., Fromme, J.C., and Schekman, R. (2009). The exomer coat complex transports Fus1p to the plasma membrane via a novel plasma membrane sorting signal in yeast. Mol Biol Cell *20*, 4985-4996.

Barlowe, C., Orci, L., Yeung, T., Hosobuchi, M., Hamamoto, S., Salama, N., Rexach, M.F., Ravazzola, M., Amherdt, M., and Schekman, R. (1994). COPII: a membrane coat formed by Sec proteins that drive vesicle budding from the endoplasmic reticulum. Cell *77*, 895-907.

Barlowe, C., and Schekman, R. (1993). SEC12 encodes a guanine-nucleotide-exchange factor essential for transport vesicle budding from the ER. Nature *365*, 347-349.

Barr, F.A. (2009). Rab GTPase function in Golgi trafficking. Semin Cell Dev Biol *20*, 780-783.

Barrowman, J., Bhandari, D., Reinisch, K., and Ferro-Novick, S. (2010). TRAPP complexes in membrane traffic: convergence through a common Rab. Nature reviews Molecular cell biology *11*, 759-763.

Barrowman, J., Wang, W., Zhang, Y., and Ferro-Novick, S. (2003). The Yip1p.Yif1p complex is required for the fusion competence of endoplasmic reticulum-derived vesicles. The Journal of biological chemistry *278*, 19878-19884.

Beck, R., Prinz, S., Diestelkotter-Bachert, P., Rohling, S., Adolf, F., Hoehner, K., Welsch, S., Ronchi, P., Brugger, B., Briggs, J.A., *et al.* (2011). Coatomer and dimeric ADP ribosylation factor 1 promote distinct steps in membrane scission. J Cell Biol *194*, 765-777.

Beck, R., Sun, Z., Adolf, F., Rutz, C., Bassler, J., Wild, K., Sinning, I., Hurt, E., Brugger, B., Bethune, J., *et al.* (2008). Membrane curvature induced by Arf1-GTP is essential for vesicle formation. Proc Natl Acad Sci USA *105*, 11731-11736.

Behnia, R., and Munro, S. (2005). Organelle identity and the signposts for membrane traffic. Nature *438*, 597-604.

Benjamin, J.J., Poon, P.P., Drysdale, J.D., Wang, X., Singer, R.A., and Johnston, G.C. (2011a). Dysregulated Arl1, a regulator of post-Golgi vesicle tethering, can inhibit endosomal transport and cell proliferation in yeast. Molecular biology of the cell *22*, 2337-2347.

Benjamin, J.J., Poon, P.P., Lewis, S.M., Auger, A., Wong, T.A., Singer, R.A., and Johnston, G.C. (2011b). The yeast Arf GTPase-activating protein Age1 is regulated by phospholipase D for post-Golgi vesicular transport. The Journal of biological chemistry *286*, 5187-5196.

Benli, M., Doring, F., Robinson, D.G., Yang, X., and Gallwitz, D. (1996). Two GTPase isoforms, Ypt31p and Ypt32p, are essential for Golgi function in yeast. EMBO J *15*, 6460-6475.

Bensen, E.S., Yeung, B.G., and Payne, G.S. (2001). Ric1p and the Ypt6p GTPase function in a common pathway required for localization of trans-Golgi network membrane proteins. Mol Biol Cell *12*, 13-26.

Beraud-Dufour, S., Robineau, S., Chardin, P., Paris, S., Chabre, M., Cherfils, J., and Antonny, B. (1998). A glutamic finger in the guanine nucleotide exchange factor ARNO displaces Mg2+ and the beta-phosphate to destabilize GDP on ARF1. EMBO J *17*, 3651-3659.

Bhamidipati, A., Lewis, S.A., and Cowan, N.J. (2000). Adp Ribosylation Factor-like Protein 2 (Arl2) Regulates the Interaction of Tubulin-Folding Cofactor D with Native Tubulin. The Journal of cell biology *149*, 1087-1096.

Bhattacharya, N., J, O.D., and Stagg, S.M. (2012). The structure of the Sec13/31 COPII cage bound to Sec23. Journal of molecular biology *420*, 324-334.

Bi, X., Corpina, R.A., and Goldberg, J. (2002). Structure of the Sec23/24-Sar1 pre-budding complex of the COPII vesicle coat. Nature *419*, 271-277.

Bielli, P., Casavola, E.C., Biroccio, A., Urbani, A., and Ragnini-Wilson, A. (2006). GTP drives myosin light chain 1 interaction with the class V myosin Myo2 IQ motifs via a Sec2 RabGEF-mediated pathway. Molecular microbiology *59*, 1576-1590.

Boal, F., and Stephens, D.J. (2010). Specific functions of BIG1 and BIG2 in endomembrane organization. PloS one *5*, e9898.

Bonifacino, J.S. (2014). Adaptor proteins involved in polarized sorting. The Journal of cell biology *204*, 7-17.

Bonifacino, J.S., and Glick, B.S. (2004). The mechanisms of vesicle budding and fusion. Cell *116*, 153-166.

Bonifacino, J.S., and Lippincott-Schwartz, J. (2003). Coat proteins: shaping membrane transport. Nature reviews Molecular cell biology *4*, 409-414.

Brennwald, P., and Rossi, G. (2007). Spatial regulation of exocytosis and cell polarity: yeast as a model for animal cells. FEBS Lett *581*, 2119-2124.

Brigance, W.T., Barlowe, C., and Graham, T.R. (2000). Organization of the yeast Golgi complex into at least four functionally distinct compartments. Molecular biology of the cell *11*, 171-182.

Brown, H.A., Gutowski, S., Moomaw, C.R., Slaughter, C., and Sternweis, P.C. (1993). ADP-ribosylation factor, a small GTP-dependent regulatory protein, stimulates phospholipase D activity. Cell *75*, 1137-1144.

Bui, Q.T., Golinelli-Cohen, M.P., and Jackson, C.L. (2009). Large Arf1 guanine nucleotide exchange factors: evolution, domain structure, and roles in membrane trafficking and human disease. Molecular genetics and genomics : MGG *282*, 329-350.

Buvelot Frei, S., Rahl, P.B., Nussbaum, M., Briggs, B.J., Calero, M., Janeczko, S., Regan, A.D., Chen, C.Z., Barral, Y., Whittaker, G.R., *et al.* (2006). Bioinformatic and comparative localization of Rab proteins reveals functional insights into the uncharacterized GTPases Ypt10p and Ypt11p. Molecular and cellular biology *26*, 7299-7317.

Cai, H., Reinisch, K., and Ferro-Novick, S. (2007a). Coats, tethers, Rabs, and SNAREs work together to mediate the intracellular destination of a transport vesicle. Dev Cell *12*, 671-682.

Cai, H., Yu, S., Menon, S., Cai, Y., Lazarova, D., Fu, C., Reinisch, K., Hay, J.C., and Ferro-Novick, S. (2007b). TRAPPI tethers COPII vesicles by binding the coat subunit Sec23. Nature *445*, 941-944.

Cai, H., Zhang, Y., Pypaert, M., Walker, L., and Ferro-Novick, S. (2005). Mutants in trs120 disrupt traffic from the early endosome to the late Golgi. The Journal of cell biology *171*, 823-833.

Cai, Y., Chin, H.F., Lazarova, D., Menon, S., Fu, C., Cai, H., Sclafani, A., Rodgers, D.W., De La Cruz, E.M., Ferro-Novick, S., *et al.* (2008). The structural basis for activation of the Rab Ypt1p by the TRAPP membrane-tethering complexes. Cell *133*, 1202-1213.

Campelo, F., and Malhotra, V. (2012). Membrane fission: the biogenesis of transport carriers. Annual review of biochemistry *81*, 407-427.

Cao, X., Ballew, N., and Barlowe, C. (1998). Initial docking of ER-derived vesicles requires Uso1p and Ypt1p but is independent of SNARE proteins. EMBO J *17*, 2156-2165.

Chantalat, S., Courbeyrette, R., Senic-Matuglia, F., Jackson, C.L., Goud, B., and Peyroche, A. (2003). A novel Golgi membrane protein is a partner of the ARF exchange factors Gea1p and Gea2p. Mol Biol Cell *14*, 2357-2371.

Chantalat, S., Park, S.K., Hua, Z., Liu, K., Gobin, R., Peyroche, A., Rambourg, A., Graham, T.R., and Jackson, C.L. (2004). The Arf activator Gea2p and the P-type ATPase Drs2p interact at the Golgi in Saccharomyces cerevisiae. J Cell Sci *117*, 711-722.

Chen, K.Y., Tsai, P.C., Hsu, J.W., Hsu, H.C., Fang, C.Y., Chang, L.C., Tsai, Y.T., Yu, C.J., and Lee, F.J. (2010). Syt1p promotes activation of Arl1p at the late Golgi to recruit Imh1p. J Cell Sci *123*, 3478-3489.

Chen, S., Cai, H., Park, S.K., Menon, S., Jackson, C.L., and Ferro-Novick, S. (2011). Trs65p, a subunit of the Ypt1p GEF TRAPPII, interacts with the Arf1p exchange factor Gea2p to facilitate COPI-mediated vesicle traffic. Mol Biol Cell *22*, 3634-3644.

Cockcroft, S., Thomas, G.M., Fensome, A., Geny, B., Cunningham, E., Gout, I., Hiles, I., Totty, N.F., Truong, O., and Hsuan, J.J. (1994). Phospholipase D: a downstream effector of ARF in granulocytes. Science *263*, 523-526.

Conibear, E., Cleck, J.N., and Stevens, T.H. (2003). Vps51p mediates the association of the GARP (Vps52/53/54) complex with the late Golgi t-SNARE Tlg1p. Molecular biology of the cell *14*, 1610-1623.

Cox, R., Mason-Gamer, R.J., Jackson, C.L., and Segev, N. (2004). Phylogenetic analysis of Sec7-domain-containing Arf nucleotide exchangers. Molecular biology of the cell *15*, 1487-1505.

D'Souza-Schorey, C., and Chavrier, P. (2006). ARF proteins: roles in membrane traffic and beyond. Nature reviews Molecular cell biology *7*, 347-358.

Daboussi, L., Costaguta, G., and Payne, G.S. (2012). Phosphoinositide-mediated clathrin adaptor progression at the trans-Golgi network. Nat Cell Biol *14*, 239-248.

De Antoni, A., Schmitzova, J., Trepte, H.H., Gallwitz, D., and Albert, S. (2002). Significance of GTP hydrolysis in Ypt1p-regulated endoplasmic reticulum to Golgi transport revealed by the analysis of two novel Ypt1-GAPs. The Journal of biological chemistry *277*, 41023-41031.

De Matteis, M.A., and Luini, A. (2008). Exiting the Golgi complex. Nature reviews Molecular cell biology *9*, 273-284.

Dehring, D.A., Adler, A.S., Hosseini, A., and Hicke, L. (2008). A C-terminal sequence in the guanine nucleotide exchange factor Sec7 mediates Golgi association and interaction with the Rsp5 ubiquitin ligase. The Journal of biological chemistry *283*, 34188-34196.

Deng, Y., Golinelli-Cohen, M.P., Smirnova, E., and Jackson, C.L. (2009). A COPI coat subunit interacts directly with an early-Golgi localized Arf exchange factor. EMBO reports *10*, 58-64.

Donaldson, J.G., and Jackson, C.L. (2011). ARF family G proteins and their regulators: roles in membrane transport, development and disease. Nature reviews Molecular cell biology *12*, 362-375.

Du, L.L., Collins, R.N., and Novick, P.J. (1998). Identification of a Sec4p GTPase-activating protein (GAP) as a novel member of a Rab GAP family. The Journal of biological chemistry *273*, 3253-3256.

Du, L.L., and Novick, P. (2001). Yeast rab GTPase-activating protein Gyp1p localizes to the Golgi apparatus and is a negative regulator of Ypt1p. Molecular biology of the cell *12*, 1215-1226.

Fath, S., Mancias, J.D., Bi, X., and Goldberg, J. (2007). Structure and organization of coat proteins in the COPII cage. Cell *129*, 1325-1336.

Franzusoff, A., Redding, K., Crosby, J., Fuller, R.S., and Schekman, R. (1991). Localization of components involved in protein transport and processing through the yeast Golgi apparatus. J Cell Biol *112*, 27-37.

Futai, E., and Schekman, R. (2005). Purification and functional properties of yeast Sec12 GEF. Methods Enzymol *404*, 74-82.

Gao, X.D., Albert, S., Tcheperegine, S.E., Burd, C.G., Gallwitz, D., and Bi, E. (2003). The GAP activity of Msb3p and Msb4p for the Rab GTPase Sec4p is required for efficient exocytosis and actin organization. The Journal of cell biology *162*, 635-646.

Geng, J., Shin, M.E., Gilbert, P.M., Collins, R.N., and Burd, C.G. (2005). Saccharomyces cerevisiae Rab-GDI displacement factor ortholog Yip3p forms distinct complexes with the Ypt1 Rab GTPase and the reticulon Rtn1p. Eukaryotic cell *4*, 1166-1174.

Gillingham, A.K., and Munro, S. (2007a). Identification of a guanine nucleotide exchange factor for Arf3, the yeast orthologue of mammalian Arf6. PloS one *2*, e842.

Gillingham, A.K., and Munro, S. (2007b). The small G proteins of the Arf family and their regulators. Annual review of cell and developmental biology *23*, 579-611.

Glick, B.S., and Nakano, A. (2009). Membrane traffic within the Golgi apparatus. Annual review of cell and developmental biology *25*, 113-132.

Godi, A., Di Campli, A., Konstantakopoulos, A., Di Tullio, G., Alessi, D.R., Kular, G.S., Daniele, T., Marra, P., Lucocq, J.M., and De Matteis, M.A. (2004). FAPPs control Golgi-to-cell-surface membrane traffic by binding to ARF and PtdIns(4)P. Nat Cell Biol *6*, 393-404.

Goldberg, J. (1998). Structural basis for activation of ARF GTPase: mechanisms of guanine nucleotide exchange and GTP-myristoyl switching. Cell *95*, 237-248.

Griff, I.C., Schekman, R., Rothman, J.E., and Kaiser, C.A. (1992). The yeast SEC17 gene product is functionally equivalent to mammalian alpha-SNAP protein. The Journal of biological chemistry *267*, 12106-12115.

Horazdovsky, B.F., Busch, G.R., and Emr, S.D. (1994). VPS21 encodes a rab5-like GTP binding protein that is required for the sorting of yeast vacuolar proteins. Embo j *13*, 1297-1309.

Hoyt, M.A., Macke, J.P., Roberts, B.T., and Geiser, J.R. (1997). Saccharomyces cerevisiae PAC2 functions with CIN1, 2 and 4 in a pathway leading to normal microtubule stability. Genetics *146*, 849-857.

Hsu, V.W., Lee, S.Y., and Yang, J.S. (2009). The evolving understanding of COPI vesicle formation. Nat Rev Mol Cell Biol *10*, 360-364.

Ignatev, A., Kravchenko, S., Rak, A., Goody, R.S., and Pylypenko, O. (2008). A structural model of the GDP dissociation inhibitor rab membrane extraction mechanism. J Biol Chem *283*, 18377-18384.

Ishizaki, R., Shin, H.W., Mitsuhashi, H., and Nakayama, K. (2008). Redundant roles of BIG2 and BIG1, guanine-nucleotide exchange factors for ADP-ribosylation factors in membrane traffic between the trans-Golgi network and endosomes. Molecular biology of the cell *19*, 2650-2660.

Ismail, S.A., Vetter, I.R., Sot, B., and Wittinghofer, A. (2010). The structure of an Arf-ArfGAP complex reveals a Ca2+ regulatory mechanism. Cell *141*, 812-821.

Jedd, G., Mulholland, J., and Segev, N. (1997). Two new Ypt GTPases are required for exit from the yeast trans-Golgi compartment. J Cell Biol *137*, 563-580.

Jedd, G., Richardson, C., Litt, R., and Segev, N. (1995). The Ypt1 GTPase is essential for the first two steps of the yeast secretory pathway. The Journal of cell biology *131*, 583-590.

Jones, S., Jedd, G., Kahn, R.A., Franzusoff, A., Bartolini, F., and Segev, N. (1999). Genetic interactions in yeast between Ypt GTPases and Arf guanine nucleotide exchangers. Genetics *152*, 1543-1556.

Jones, S., Richardson, C.J., Litt, R.J., and Segev, N. (1998). Identification of regulators for Ypt1 GTPase nucleotide cycling. Molecular biology of the cell *9*, 2819-2837.

Kahn, R.A., Bruford, E., Inoue, H., Logsdon, J.M., Jr., Nie, Z., Premont, R.T., Randazzo, P.A., Satake, M., Theibert, A.B., Zapp, M.L., *et al.* (2008). Consensus nomenclature for the human ArfGAP domain-containing proteins. The Journal of cell biology *182*, 1039-1044.

Kelly, E.E., Horgan, C.P., Goud, B., and McCaffrey, M.W. (2012). The Rab family of proteins: 25 years on. Biochemical Society transactions *40*, 1337-1347.

Kirchhausen, T. (2000). Three ways to make a vesicle. Nat Rev Mol Cell Biol *1*, 187-198.

Krauss, M., Jia, J.Y., Roux, A., Beck, R., Wieland, F.T., De Camilli, P., and Haucke, V. (2008). Arf1-GTP-induced tubule formation suggests a function of Arf family proteins in curvature acquisition at sites of vesicle budding. J Biol Chem *283*, 27717-27723.

Kuehn, M.J., Herrmann, J.M., and Schekman, R. (1998). COPII-cargo interactions direct protein sorting into ER-derived transport vesicles. Nature *391*, 187-190.

Lachmann, J., Barr, F.A., and Ungermann, C. (2012). The Msb3/Gyp3 GAP controls the activity of the Rab GTPases Vps21 and Ypt7 at endosomes and vacuoles. Molecular biology of the cell *23*, 2516-2526.

Lee, M.C., Orci, L., Hamamoto, S., Futai, E., Ravazzola, M., and Schekman, R. (2005). Sar1p N-terminal helix initiates membrane curvature and completes the fission of a COPII vesicle. Cell *122*, 605-617.

Lewandowska, A., Macfarlane, J., and Shaw, J.M. (2013). Mitochondrial association, protein phosphorylation, and degradation regulate the availability of the active Rab GTPase Ypt11 for mitochondrial inheritance. Molecular biology of the cell *24*, 1185-1195.

Lewis, S.M., Poon, P.P., Singer, R.A., Johnston, G.C., and Spang, A. (2004). The ArfGAP Glo3 is required for the generation of COPI vesicles. Molecular biology of the cell *15*, 4064-4072.

Lipatova, Z., Tokarev, A.A., Jin, Y., Mulholland, J., Weisman, L.S., and Segev, N. (2008). Direct interaction between a myosin V motor and the Rab GTPases Ypt31/32 is required for polarized secretion. Mol Biol Cell *19*, 4177-4187.

Lippincott-Schwartz, J., Yuan, L., Tipper, C., Amherdt, M., Orci, L., and Klausner, R.D. (1991). Brefeldin A's effects on endosomes, lysosomes, and the TGN suggest a general mechanism for regulating organelle structure and membrane traffic. Cell *67*, 601-616.

Liu, Y.W., Huang, C.F., Huang, K.B., and Lee, F.J. (2005). Role for Gcs1p in regulation of Arl1p at trans-Golgi compartments. Molecular biology of the cell *16*, 4024-4033.

Lundmark, R., Doherty, G.J., Vallis, Y., Peter, B.J., and McMahon, H.T. (2008). Arf family GTP loading is activated by, and generates, positive membrane curvature. The Biochemical journal *414*, 189-194.

Lynch-Day, M.A., Bhandari, D., Menon, S., Huang, J., Cai, H., Bartholomew, C.R., Brumell, J.H., Ferro-Novick, S., and Klionsky, D.J. (2010). Trs85 directs a Ypt1 GEF, TRAPPIII, to the

phagophore to promote autophagy. Proceedings of the National Academy of Sciences of the United States of America *107*, 7811-7816.

McNew, J.A., Parlati, F., Fukuda, R., Johnston, R.J., Paz, K., Paumet, F., Sollner, T.H., and Rothman, J.E. (2000). Compartmental specificity of cellular membrane fusion encoded in SNARE proteins. Nature *407*, 153-159.

Mellman, I., and Nelson, W.J. (2008). Coordinated protein sorting, targeting and distribution in polarized cells. Nat Rev Mol Cell Biol *9*, 833-845.

Miller, E., Antonny, B., Hamamoto, S., and Schekman, R. (2002). Cargo selection into COPII vesicles is driven by the Sec24p subunit. EMBO J *21*, 6105-6113.

Miller, E.A., Beilharz, T.H., Malkus, P.N., Lee, M.C., Hamamoto, S., Orci, L., and Schekman, R. (2003). Multiple cargo binding sites on the COPII subunit Sec24p ensure capture of diverse membrane proteins into transport vesicles. Cell *114*, 497-509.

Mizuno-Yamasaki, E., Rivera-Molina, F., and Novick, P. (2012). GTPase networks in membrane traffic. Annual review of biochemistry *81*, 637-659.

Monetta, P., Slavin, I., Romero, N., and Alvarez, C. (2007). Rab1b interacts with GBF1 and modulates both ARF1 dynamics and COPI association. Molecular biology of the cell *18*, 2400-2410.

Morozova, N., Liang, Y., Tokarev, A.A., Chen, S.H., Cox, R., Andrejic, J., Lipatova, Z., Sciorra, V.A., Emr, S.D., and Segev, N. (2006). TRAPPII subunits are required for the specificity switch of a Ypt-Rab GEF. Nat Cell Biol *8*, 1263-1269.

Mossessova, E., Corpina, R.A., and Goldberg, J. (2003). Crystal structure of ARF1*Sec7 complexed with Brefeldin A and its implications for the guanine nucleotide exchange mechanism. Mol Cell *12*, 1403-1411.

Mossessova, E., Gulbis, J.M., and Goldberg, J. (1998). Structure of the guanine nucleotide exchange factor Sec7 domain of human arno and analysis of the interaction with ARF GTPase. Cell *92*, 415-423.

Mouratou, B., Biou, V., Joubert, A., Cohen, J., Shields, D.J., Geldner, N., Jurgens, G., Melancon, P., and Cherfils, J. (2005). The domain architecture of large guanine nucleotide exchange factors for the small GTP-binding protein Arf. BMC Genomics *6*, 20.

Nakano, A., and Muramatsu, M. (1989). A novel GTP-binding protein, Sar1p, is involved in transport from the endoplasmic reticulum to the Golgi apparatus. J Cell Biol *109*, 2677-2691.

Natarajan, P., Liu, K., Patil, D.V., Sciorra, V.A., Jackson, C.L., and Graham, T.R. (2009). Regulation of a Golgi flippase by phosphoinositides and an ArfGEF. Nat Cell Biol *11*, 1421-1426.

Novick, P., Ferro, S., and Schekman, R. (1981). Order of events in the yeast secretory pathway. Cell *25*, 461-469.

Novick, P., Field, C., and Schekman, R. (1980). Identification of 23 complementation groups required for post-translational events in the yeast secretory pathway. Cell *21*, 205-215.

Novick, P., and Schekman, R. (1979). Secretion and cell-surface growth are blocked in a temperature-sensitive mutant of Saccharomyces cerevisiae. Proceedings of the National Academy of Sciences of the United States of America *76*, 1858-1862.

Oka, T., and Nakano, A. (1994). Inhibition of GTP hydrolysis by Sar1p causes accumulation of vesicles that are a functional intermediate of the ER-to-Golgi transport in yeast. The Journal of cell biology *124*, 425-434.

Ortiz, D., Medkova, M., Walch-Solimena, C., and Novick, P. (2002). Ypt32 recruits the Sec4p guanine nucleotide exchange factor, Sec2p, to secretory vesicles; evidence for a Rab cascade in yeast. J Cell Biol *157*, 1005-1015.

Palade, G. (1975). Intracellular aspects of the process of protein synthesis. Science *189*, 347-358.

Panic, B., Whyte, J.R., and Munro, S. (2003). The ARF-like GTPases Arl1p and Arl3p act in a pathway that interacts with vesicle-tethering factors at the Golgi apparatus. Curr Biol *13*, 405-410.

Papanikou, E., and Glick, B.S. (2009). The yeast Golgi apparatus: insights and mysteries. FEBS letters *583*, 3746-3751.

Park, S.Y., and Guo, X. (2014). Adaptor Protein Complexes and Intracellular Transport. Bioscience reports.

Payne, G.S., and Schekman, R. (1985). A test of clathrin function in protein secretion and cell growth. Science *230*, 1009-1014.

Peyroche, A., Antonny, B., Robineau, S., Acker, J., Cherfils, J., and Jackson, C.L. (1999). Brefeldin A acts to stabilize an abortive ARF-GDP-Sec7 domain protein complex: involvement of specific residues of the Sec7 domain. Molecular cell *3*, 275-285.

Peyroche, A., Paris, S., and Jackson, C.L. (1996). Nucleotide exchange on ARF mediated by yeast Gea1 protein. Nature *384*, 479-481.

Poon, P.P., Cassel, D., Spang, A., Rotman, M., Pick, E., Singer, R.A., and Johnston, G.C. (1999). Retrograde transport from the yeast Golgi is mediated by two ARF GAP proteins with overlapping function. Embo j *18*, 555-564.

Poon, P.P., Nothwehr, S.F., Singer, R.A., and Johnston, G.C. (2001). The Gcs1 and Age2 ArfGAP proteins provide overlapping essential function for transport from the yeast trans-Golgi network. The Journal of cell biology *155*, 1239-1250.

Poon, P.P., Wang, X., Rotman, M., Huber, I., Cukierman, E., Cassel, D., Singer, R.A., and Johnston, G.C. (1996). Saccharomyces cerevisiae Gcs1 is an ADP-ribosylation factor GTPase-activating protein. Proceedings of the National Academy of Sciences of the United States of America *93*, 10074-10077.

Pylypenko, O., Rak, A., Durek, T., Kushnir, S., Dursina, B.E., Thomae, N.H., Constantinescu, A.T., Brunsveld, L., Watzke, A., Waldmann, H., *et al.* (2006). Structure of doubly prenylated Ypt1:GDI complex and the mechanism of GDI-mediated Rab recycling. Embo j *25*, 13-23.

Rak, A., Pylypenko, O., Durek, T., Watzke, A., Kushnir, S., Brunsveld, L., Waldmann, H., Goody, R.S., and Alexandrov, K. (2003). Structure of Rab GDP-dissociation inhibitor in complex with prenylated YPT1 GTPase. Science *302*, 646-650.

Ramaen, O., Joubert, A., Simister, P., Belgareh-Touze, N., Olivares-Sanchez, M.C., Zeeh, J.C., Chantalat, S., Golinelli-Cohen, M.P., Jackson, C.L., Biou, V., *et al.* (2007). Interactions between conserved domains within homodimers in the BIG1, BIG2, and GBF1 Arf guanine nucleotide exchange factors. The Journal of biological chemistry *282*, 28834-28842.

Randazzo, P.A., Terui, T., Sturch, S., Fales, H.M., Ferrige, A.G., and Kahn, R.A. (1995). The myristoylated amino terminus of ADP-ribosylation factor 1 is a phospholipid- and GTP-sensitive switch. J Biol Chem *270*, 14809-14815.

Rexach, M.F., and Schekman, R.W. (1991). Distinct biochemical requirements for the budding, targeting, and fusion of ER-derived transport vesicles. J Cell Biol *114*, 219-229.

Rojas, A.M., Fuentes, G., Rausell, A., and Valencia, A. (2012). The Ras protein superfamily: Evolutionary tree and role of conserved amino acids. The Journal of cell biology *196*, 189-201.

Rothman, J.E. (1994). Intracellular membrane fusion. Advances in second messenger and phosphoprotein research *29*, 81-96.

Sacher, M., Barrowman, J., Wang, W., Horecka, J., Zhang, Y., Pypaert, M., and Ferro-Novick, S. (2001). TRAPP I implicated in the specificity of tethering in ER-to-Golgi transport. Mol Cell *7*, 433-442.

Sacher, M., Jiang, Y., Barrowman, J., Scarpa, A., Burston, J., Zhang, L., Schieltz, D., Yates, J.R., 3rd, Abeliovich, H., and Ferro-Novick, S. (1998). TRAPP, a highly conserved novel complex on the cis-Golgi that mediates vesicle docking and fusion. EMBO J *17*, 2494-2503.

Saeki, N., Tokuo, H., and Ikebe, M. (2005). BIG1 is a binding partner of myosin IXb and regulates its Rho-GTPase activating protein activity. J Biol Chem *280*, 10128-10134.

Salama, N.R., Yeung, T., and Schekman, R.W. (1993). The Sec13p complex and reconstitution of vesicle budding from the ER with purified cytosolic proteins. EMBO J *12*, 4073-4082.

Santiago-Tirado, F.H., and Bretscher, A. (2011). Membrane-trafficking sorting hubs: cooperation between PI4P and small GTPases at the trans-Golgi network. Trends Cell Biol *21*, 515-525.

Sata, M., Donaldson, J.G., Moss, J., and Vaughan, M. (1998). Brefeldin A-inhibited guanine nucleotide-exchange activity of Sec7 domain from yeast Sec7 with yeast and mammalian ADP ribosylation factors. Proceedings of the National Academy of Sciences of the United States of America *95*, 4204-4208.

Sciorra, V.A., Audhya, A., Parsons, A.B., Segev, N., Boone, C., and Emr, S.D. (2005). Synthetic genetic array analysis of the PtdIns 4-kinase Pik1p identifies components in a Golgi-specific Ypt31/rab-GTPase signaling pathway. Mol Biol Cell *16*, 776-793.

Sclafani, A., Chen, S., Rivera-Molina, F., Reinisch, K., Novick, P., and Ferro-Novick, S. (2010). Establishing a role for the GTPase Ypt1p at the late Golgi. Traffic *11*, 520-532.

Segev, N. (1991). Mediation of the attachment or fusion step in vesicular transport by the GTP-binding Ypt1 protein. Science *252*, 1553-1556.

Segev, N., Mulholland, J., and Botstein, D. (1988). The yeast GTP-binding YPT1 protein and a mammalian counterpart are associated with the secretion machinery. Cell *52*, 915-924.

Setty, S.R., Shin, M.E., Yoshino, A., Marks, M.S., and Burd, C.G. (2003). Golgi recruitment of GRIP domain proteins by Arf-like GTPase 1 is regulated by Arf-like GTPase 3. Curr Biol *13*, 401-404.

Shiba, T., Kawasaki, M., Takatsu, H., Nogi, T., Matsugaki, N., Igarashi, N., Suzuki, M., Kato, R., Nakayama, K., and Wakatsuki, S. (2003). Molecular mechanism of membrane recruitment of GGA by ARF in lysosomal protein transport. Nat Struct Biol *10*, 386-393.

Shin, H.W., Morinaga, N., Noda, M., and Nakayama, K. (2004). BIG2, a guanine nucleotide exchange factor for ADP-ribosylation factors: its localization to recycling endosomes and implication in the endosome integrity. Molecular biology of the cell *15*, 5283-5294.

Singer-Kruger, B., Stenmark, H., Dusterhoft, A., Philippsen, P., Yoo, J.S., Gallwitz, D., and Zerial, M. (1994). Role of three rab5-like GTPases, Ypt51p, Ypt52p, and Ypt53p, in the endocytic and vacuolar protein sorting pathways of yeast. The Journal of cell biology *125*, 283-298.

Singer-Kruger, B., Stenmark, H., and Zerial, M. (1995). Yeast Ypt51p and mammalian Rab5: counterparts with similar function in the early endocytic pathway. J Cell Sci *108 (Pt 11)*, 3509-3521.

Siniossoglou, S., Peak-Chew, S.Y., and Pelham, H.R. (2000). Ric1p and Rgp1p form a complex that catalyses nucleotide exchange on Ypt6p. Embo j *19*, 4885-4894.

Siniossoglou, S., and Pelham, H.R. (2001). An effector of Ypt6p binds the SNARE Tlg1p and mediates selective fusion of vesicles with late Golgi membranes. Embo j *20*, 5991-5998.

Sivars, U., Aivazian, D., and Pfeffer, S.R. (2003). Yip3 catalyses the dissociation of endosomal Rab-GDI complexes. Nature *425*, 856-859.

Smaczynska-de, R., II, Costa, R., and Ayscough, K.R. (2008). Yeast Arf3p modulates plasma membrane PtdIns(4,5)P2 levels to facilitate endocytosis. Traffic *9*, 559-573.

Spang, A., Herrmann, J.M., Hamamoto, S., and Schekman, R. (2001). The ADP ribosylation factor-nucleotide exchange factors Gea1p and Gea2p have overlapping, but not redundant functions in retrograde transport from the Golgi to the endoplasmic reticulum. Mol Biol Cell *12*, 1035-1045.

Stagg, S.M., Gurkan, C., Fowler, D.M., LaPointe, P., Foss, T.R., Potter, C.S., Carragher, B., and Balch, W.E. (2006). Structure of the Sec13/31 COPII coat cage. Nature *439*, 234-238.

Stenmark, H. (2009). Rab GTPases as coordinators of vesicle traffic. Nature reviews Molecular cell biology *10*, 513-525.

Strom, M., Vollmer, P., Tan, T.J., and Gallwitz, D. (1993). A yeast GTPase-activating protein that interacts specifically with a member of the Ypt/Rab family. Nature *361*, 736-739.

Suda, Y., Kurokawa, K., Hirata, R., and Nakano, A. (2013). Rab GAP cascade regulates dynamics of Ypt6 in the Golgi traffic. Proc Natl Acad Sci USA *110*, 18976-18981.

Suvorova, E.S., Duden, R., and Lupashin, V.V. (2002). The Sec34/Sec35p complex, a Ypt1p effector required for retrograde intra-Golgi trafficking, interacts with Golgi SNAREs and COPI vesicle coat proteins. The Journal of cell biology *157*, 631-643.

Ullrich, O., Reinsch, S., Urbe, S., Zerial, M., and Parton, R.G. (1996). Rab11 regulates recycling through the pericentriolar recycling endosome. The Journal of cell biology *135*, 913-924.

Vollmer, P., Will, E., Scheglmann, D., Strom, M., and Gallwitz, D. (1999). Primary structure and biochemical characterization of yeast GTPase-activating proteins with substrate preference for the transport GTPase Ypt7p. European journal of biochemistry / FEBS *260*, 284-290.

Wagner, W., Bielli, P., Wacha, S., and Ragnini-Wilson, A. (2002). Mlc1p promotes septum closure during cytokinesis via the IQ motifs of the vesicle motor Myo2p. Embo j *21*, 6397-6408.

Walch-Solimena, C., Collins, R.N., and Novick, P.J. (1997). Sec2p mediates nucleotide exchange on Sec4p and is involved in polarized delivery of post-Golgi vesicles. J Cell Biol *137*, 1495-1509.

Wang, C.W., Hamamoto, S., Orci, L., and Schekman, R. (2006). Exomer: A coat complex for transport of select membrane proteins from the trans-Golgi network to the plasma membrane in yeast. The Journal of cell biology *174*, 973-983.

Wang, W., and Ferro-Novick, S. (2002). A Ypt32p exchange factor is a putative effector of Ypt1p. Molecular biology of the cell *13*, 3336-3343.

Wennerberg, K., Rossman, K.L., and Der, C.J. (2005). The Ras superfamily at a glance. J Cell Sci *118*, 843-846.

Whyte, J.R., and Munro, S. (2002). Vesicle tethering complexes in membrane traffic. J Cell Sci *115*, 2627-2637.

Will, E., and Gallwitz, D. (2001). Biochemical characterization of Gyp6p, a Ypt/Rab-specific GTPase-activating protein from yeast. The Journal of biological chemistry *276*, 12135-12139.

Wilson, C., Venditti, R., Rega, L.R., Colanzi, A., D'Angelo, G., and De Matteis, M.A. (2011). The Golgi apparatus: an organelle with multiple complex functions. The Biochemical journal *433*, 1-9.

Wilson, D.W., Wilcox, C.A., Flynn, G.C., Chen, E., Kuang, W.J., Henzel, W.J., Block, M.R., Ullrich, A., and Rothman, J.E. (1989). A fusion protein required for vesicle-mediated transport in both mammalian cells and yeast. Nature *339*, 355-359.

Wood, S.A., Park, J.E., and Brown, W.J. (1991). Brefeldin A causes a microtubule-mediated fusion of the trans-Golgi network and early endosomes. Cell *67*, 591-600.

Xu, K.F., Shen, X., Li, H., Pacheco-Rodriguez, G., Moss, J., and Vaughan, M. (2005). Interaction of BIG2, a brefeldin A-inhibited guanine nucleotide-exchange protein, with exocyst protein Exo70. Proceedings of the National Academy of Sciences of the United States of America *102*, 2784-2789.

Yip, C.K., Berscheminski, J., and Walz, T. (2010). Molecular architecture of the TRAPPII complex and implications for vesicle tethering. Nat Struct Mol Biol *17*, 1298-1304.

Yu, I.M., and Hughson, F.M. (2010). Tethering factors as organizers of intracellular vesicular traffic. Annual review of cell and developmental biology *26*, 137-156.

Yu, S., Satoh, A., Pypaert, M., Mullen, K., Hay, J.C., and Ferro-Novick, S. (2006). mBet3p is required for homotypic COPII vesicle tethering in mammalian cells. J Cell Biol *174*, 359-368.

Zanolari, B., Rockenbauch, U., Trautwein, M., Clay, L., Barral, Y., and Spang, A. (2011). Transport to the plasma membrane is regulated differently early and late in the cell cycle in Saccharomyces cerevisiae. J Cell Sci *124*, 1055-1066.

Zhang, C.J., Bowzard, J.B., Anido, A., and Kahn, R.A. (2003). Four ARF GAPs in Saccharomyces cerevisiae have both overlapping and distinct functions. Yeast *20*, 315-330.

Zhao, X., Lasell, T.K., and Melancon, P. (2002). Localization of large ADP-ribosylation factor-guanine nucleotide exchange factors to different Golgi compartments: evidence for distinct functions in protein traffic. Molecular biology of the cell *13*, 119-133.

CHAPTER 2

THE SEC7 ARF-GEF IS RECRUITED TO THE *TRANS*-GOLGI NETWORK BY POSITIVE FEEDBACK[1]

Overview

Arf GTPases are key regulators of both retrograde and anterograde traffic at the Golgi complex. The Golgi-localized Arf activators, Arf-GEFs (guanine exchange factor) of the BIG/GBF family, are poorly understood in terms of both their regulatory and localization mechanisms. We have performed a detailed kinetic characterization of a functional Golgi Arf-GEF, the trans-Golgi network (TGN)-localized Sec7 protein from yeast. We demonstrate that Sec7 is regulated by both autoinhibition and positive feedback. We show that positive feedback arises through the stable recruitment of Sec7 to membranes via its HDS1 domain by interaction with its product, activated Arf1. This interaction mediates localization of Sec7 to the TGN, because deletion of the HDS1 domain in combination with deletion of Arf1 significantly increases cytoplasmic localization of Sec7. Our results lead us to propose a model in which Arf-GEF recruitment is linked to Golgi maturation via Arf1 activation.

[1] Parts of this chapter have been published in Richardson, B.C., McDonold, C.M., and Fromme, J.C. (2012). The Sec7 Arf-GEF is recruited to the trans-Golgi network by positive feedback. Dev Cell *22*, 799-810.

Introduction

The Golgi complex is the primary membrane and protein sorting station in the secretory pathway of eukaryotic cells (De Matteis and Luini, 2008; Glick and Nakano, 2009). Virtually all protein traffic out of the Golgi is controlled by GTPases of the Arf family that act by recruiting effectors, including cargo adaptors and vesicle coats, to sort cargo and generate transport carriers (D'Souza-Schorey and Chavrier, 2006; Donaldson and Jackson, 2011; Gillingham and Munro, 2007; Kahn, 2009). Arf family GTPases are also thought to contribute some of the mechanical force required to deform membranes during transport carrier formation, because activated Arf proteins can tubulate membranes *in vitro* and *in vivo* (Aridor et al., 2001; Beck et al., 2008; Krauss et al., 2008; Lee et al., 2005).

The structural and biochemical mechanism of Arf activation via nucleotide exchange by GEF domains is well characterized (Beraud-Dufour et al., 1998; Goldberg, 1998), and important regulatory features of the peripherally localized Arf-GEFs ARNO/Cytohesin-1/Grp1 have recently been described (DiNitto et al., 2007; Stalder et al., 2011). However, despite the essential function of Arf GTPases in membrane trafficking at the Golgi, their activation at this organelle remains poorly understood. Arf-GEF proteins of the BIG and GBF families are responsible for Golgi-localized Arf activation (Casanova, 2007; Morinaga et al., 1996; Peyroche et al., 1996), but the BIG/GBF family proteins share no detectable sequence homology with the ARNO/Cytohesin-1/Grp1 family outside of the GEF domain. Moreover, the BIG/GBF Arf-GEFs are fundamental regulators of intra-Golgi and Golgi-derived traffic in all eukaryotes, whereas the ARNO/Cytohesin-1/Grp1 Arf-GEFs appear to have cell-type specific functions at the plasma membrane (Klarlund et al., 1997; Kolanus et al., 1996; Venkateswarlu et al., 1998). The importance of the BIG/GBF Arf-GEFs is underscored by the association of mutations in the *BIG2/ARFGEF2* gene with neuronal disease (de Wit et al., 2009; Sheen et al., 2004).

Yeast possess a single member of the BIG subfamily, Sec7, which activates the Arf1 and Arf2 (Arf1/2) GTPases at the *trans*-Golgi network (TGN) (Franzusoff et al., 1991), and two members of the GBF family, Gea1 and Gea2, which activate Arf1/2 at early Golgi compartments (Peyroche et al., 1996; Spang et al., 2001). *SEC7* was among the first genes identified to act in the secretory pathway, and temperature-sensitive *sec7* mutants accumulate greatly exaggerated TGN membrane compartments (Novick et al., 1980; Rambourg et al., 1993), consistent with its role in regulating virtually all anterograde traffic out of the TGN.

The two major unresolved questions regarding the Golgi Arf-GEFs are how their activity is regulated and how they achieve their subcellular localization. We now demonstrate that Sec7 activates Arf1 through a positive feedback mechanism and is also subject to autoinhibitory regulation. Using *in vitro* assays, we show that positive feedback occurs through Arf1-GTP dependent recruitment of Sec7 to the membrane surface via a conserved domain, HDS1. Our data suggest that the HDS1 domain switches from an autoinhibitory state to an activating state upon binding to Arf1-GTP. To probe the physiological significance of our *in vitro* data, we determined that the HDS1 domain also mediates stable interaction between Sec7 and Arf1 *in vivo*. Remarkably, we find that the HDS1 domain cooperates with Arf1 to mediate localization of Sec7 to the TGN *in vivo*. We further determined that the HDS2-4 domains exert an autoinhibitory role and provide additional TGN-directed targeting, possibly through coincidence detection. Our results lead us to propose a model for Arf-GEF recruitment to the Golgi that is intimately linked to Golgi cisternal maturation.

Results

Purification of a Sec7 protein that provides essential SEC7 function

The prototypical member of the BIG and GBF families, Sec7 (for which the "Sec7" GEF domain is named), is 2009 amino acid residues in length, but the GEF domain itself comprises only ~200 amino acids. The remainder of Sec7 is highly conserved through humans. Sequence conservation was previously used to identify conserved regions within the BIG and GBF family members, and these regions have been ascribed domain names based on this conservation (Mouratou et al., 2005; Bui et al., 2009) (Figure 2.1A).

Characterization of this family of Arf-GEFs has been hindered by the difficulty in purifying protein constructs encoding the entirety of the functional gene products. To investigate the function of the non-GEF domains of Sec7, we sought to produce a purified fragment that retained the essential function of the full-length protein. A postdoc in the lab achieved robust expression of a well-behaved N-terminal deletion construct of Sec7 encoding residues 203-2009 (Figure 2.1A,B). The N-terminal 202 amino acids missing from this construct are poorly conserved and are predicted to lack secondary structural elements, so we expected this region to be dispensable for Sec7 function. As *SEC7* is an essential gene in yeast, the Sec7(203-2009) fragment was tested for the ability to complement a *sec7Δ* null mutant. This construct was indeed able to complement the loss of Sec7, indicating that the N-terminal 202 residues are dispensable for growth *in vivo* (Figure 2.1C). Thus, the purified recombinant Sec7(203-2009) protein fragment encodes the full essential function of the endogenous *SEC7* gene product; for simplicity, I will hereafter refer to this purified protein as $Sec7_f$ to denote that this is a fully functional construct.

Figure 2.1: Purification of a functional Sec7 construct uncovers distinct regulatory domains in the C-terminus. (A) Schematic diagram of the Sec7 truncated constructs used for this study, shown with the conserved domain structure of Sec7. The domain names are: DCB, dimerization and cyclophilin binding; HUS, homology upstream of Sec7 domain; GEF, guanine exchange factor (sometimes referred to as the Sec7 domain); HDS, homology downstream of Sec7 domain. Note that the HDS1, 2, 3, and 4 domains are not homologous with each other. **(B)** 5 μg of each construct used in this study was run on a 15% SDS-PAGE gel and stained for total protein. **(C)** Plasmid-borne Sec7 constructs (top to bottom: pCF1045, pCF1046, pCF1136, pCF1135, pRS415) with *SEC7* promoters were tested for their ability to complement a *sec7Δ* mutation via 5-FOA counter-selection plasmid shuffling, using yeast strain CFY409. **(D)** The nucleotide-bound state of Arf1 was monitored by increase in native tryptophan fluorescence. Single reaction curves of myrArf1 activation by the $Sec7_f$, Sec7ΔC, and Sec7GEF constructs in the presence of liposomes. **(E)** Single reaction curves of ΔN17Arf1 activation by the $Sec7_f$, Sec7ΔC, and Sec7GEF constructs in the absence of liposomes. **(F)** The nucleotide-bound state of Arf1 was monitored by increase in native tryptophan fluorescence. Dark lines represent the average of three normalized reactions; lighter surrounding areas represent the corresponding 95% confidence intervals for each time point. **(G)** Quantification of reaction rate from curves in (F). Curves were fit to a single exponential and normalized for measured [Sec7] to obtain the overall reaction rate. Bars are colored as per construct coloring in (A). Error bars represent 95% confidence interval; significance is measured by one-way ANOVA with post-processing to correct for multiple comparisons. **(H)** Quantification of reaction rates in the absence of liposomes. A construct lacking the membrane insertion domain of Arf1 (ΔN17-Arf1) was used to permit exchange in the absence of liposomes. Experiments in (D) and (E) were performed by me; experiments in (F), (G), and (H) were performed by Brian Richardson.

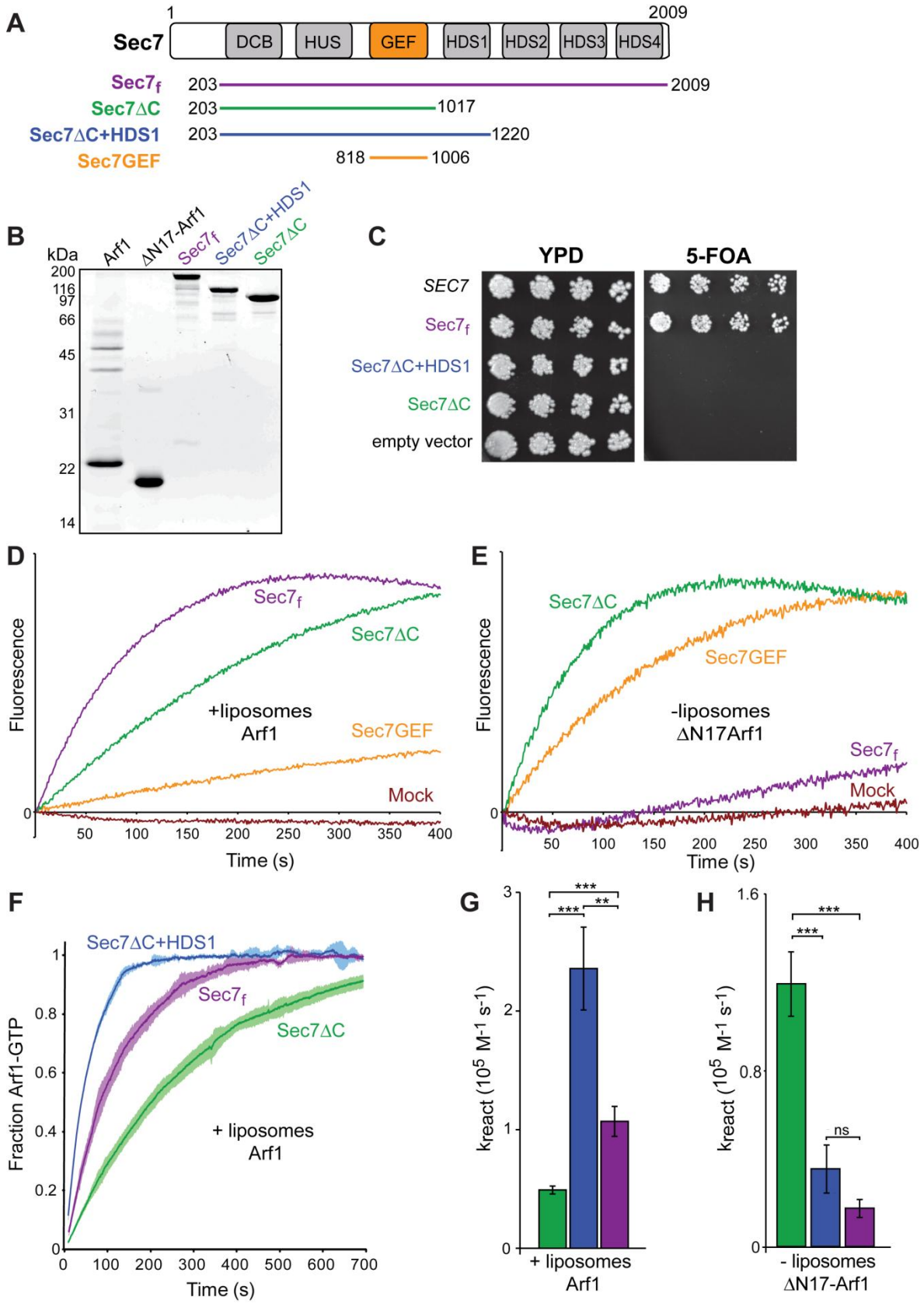
A
Sec7
1
2009
DCB
HUS
GEF
HDS1
HDS2
HDS3
HDS4
Sec7f 203 2009
Sec7ΔC 203 1017
Sec7ΔC+HDS1 203 1220
Sec7GEF 818 1006
B
kDa
Arf1
ΔN17-Arf1
Sec7f
Sec7ΔC+HDS1
Sec7ΔC
200
116
97
66
45
31
22
14
C
YPD
5-FOA
SEC7
Sec7f
Sec7ΔC+HDS1
Sec7ΔC
empty vector
D
Fluorescence
Sec7f
Sec7ΔC
+liposomes
Arf1
Sec7GEF
Mock
Time (s)
E
Fluorescence
Sec7ΔC
Sec7GEF
-liposomes
ΔN17Arf1
Sec7f
Mock
Time (s)
F
Sec7ΔC+HDS1
Sec7f
Sec7ΔC
+ liposomes
Arf1
Fraction Arf1-GTP
Time (s)
G
kreact (10^5 M^-1 s^-1)
***
**
***
+ liposomes
Arf1
H
kreact (10^5 M^-1 s^-1)
***
***
ns
- liposomes
ΔN17-Arf1

Three further recombinant Sec7 fragments were purified for this study: a construct comprising residues 203-1017 (Sec7ΔC), which contains the N-terminal region and the GEF domain, a construct comprising residues 818-1006, which contains just the GEF domain (Sec7GEF), and a construct comprising residues 203-1220 (Sec7ΔC+HDS1), which contains the N-terminal region, the GEF domain, and the conserved HDS1 (homology downstream of Sec7) domain (Figure 2.1A,B). Neither the Sec7ΔC nor the Sec7ΔC+HDS1 construct complemented a *sec7Δ* mutant, indicating that the C-terminus is required for the essential function of Sec7 (Figure 2.1C).

Sec7 GEF activity is stimulated by region(s) outside of the GEF domain

We hypothesized that the non-GEF domains of Sec7 might regulate the activity of the GEF domain. To test this hypothesis, I used native tryptophan fluorescence to monitor Sec7-catalyzed Arf1 nucleotide exchange in real-time. This assay (Higashijima et al., 1987) has been used extensively to investigate the enzymatic kinetics of several different GEF proteins, including activators of Arf-family proteins (Beraud-Dufour et al., 1998; DiNitto et al., 2007; Futai et al., 2004). These experiments were performed using approximately physiological concentrations of GEF (100 nM, based on ~3,700 Sec7 molecules per cell (Ghaemmaghami et al., 2003)) and GTPase (670 nM, based on ~19,000 Arf1 molecules per cell (Ghaemmaghami et al., 2003)).

When we measured the GEF activity of these Sec7 constructs towards Arf1 (N-terminally myristoylated form) in the presence of TGN-like synthetic liposomes (composition presented in Table 2.1), we found that all were considerably more active than the isolated GEF domain (Figures 2.1D,F,G). Furthermore, $Sec7_f$ was significantly more active than Sec7ΔC (Figures

2.1D,F,G). While constructs containing regions C-terminal to the GEF domain but lacking the N-terminal region (residues 1-815) could not be tested due to poor behavior in solution, the results thus far indicate that regions in both the N-terminus and C-terminus enhance the activity of the GEF domain.

Membranes modulate the autoinhibitory or activating potential of the Sec7 C-terminus

Although removing the C-terminus from the $Sec7_f$ construct (to generate Sec7ΔC) results in a loss of activity, reintroducing just the HDS1 domain to generate Sec7ΔC+HDS1 results in a construct with activity even higher than that of $Sec7_f$ (Figure 2.1F,G). Therefore, the HDS2-4 domains have an autoinhibitory function, whereas the HDS1 domain has an activating function, relative to the Sec7ΔC construct.

To determine the role of membranes in the autoregulatory behavior of the C-terminus, we performed the GEF activity assay using an Arf1 construct lacking the amphipathic N-terminal helix (ΔN17-Arf1) as a substrate. In contrast to myristoylated Arf1, ΔN17-Arf1 does not require the presence of biological membranes to become activated (Antonny et al., 1997; Kahn et al., 1992), permitting their removal from the assay. We note that it is not necessarily informative to compare the rates of a given Sec7 construct between reactions with and without liposomes: the different reactions involve different substrates (ΔN17-Arf1 versus Arf1) known to possess different intrinsic activation rates (Antonny et al., 1997). Therefore, we focus our analysis on the relative rates of the different Sec7 constructs for each substrate.

Surprisingly, the absence of membranes resulted in a markedly different activity profile of the constructs. In contrast to its activating role in reactions with Arf1 and liposomes, the HDS1 domain has an autoinhibitory effect in solution, as the activity of Sec7ΔC+HDS1 was less

than that of Sec7ΔC under these conditions (Figures 2.1H). Additionally, $Sec7_f$ was drastically inhibited in the absence of liposomes, as the activity of both Sec7ΔC and Sec7GEF were much higher than that of $Sec7_f$ under these conditions (Figure 2.1E).

Taken together, these results suggest that the HDS1 domain acts as a switch, exerting either an inhibitory or an activating function, and switching between the two states is modulated by membranes.

Activated Arf1 stably recruits Sec7 to membranes through interaction with the conserved HDS1 domain

To further characterize the membrane-dependent switch, we sought to determine the membrane-bound status of the various Sec7 constructs under our reaction conditions. The peripherally-localized Arf-GEFs of the ARNO/Grp1/Cytohesin family contain a Sec7-GEF domain and a C-terminal PH domain that mediates its binding to membranes containing the signaling phospholipids $PI(3,4,5)P_3$ or $PI(4,5)P_2$ (Chardin et al., 1996; Klarlund et al., 2000). Structural elements proximal to the PH domain are autoinhibitory in solution (DiNitto et al., 2007), but the presence of the PH domain significantly increases the activity of the GEF domain in these proteins by enforcing membrane proximity (Chardin et al., 1996; Klarlund et al., 2000). More recently, the PH domain of these proteins has also been shown to interact with the activated, membrane-bound GTPases Arf6, Arf1, and Arl4, enabling it to modulate GEF activity and localization via GTPase cascades or positive feedback (Cohen et al., 2007; DiNitto et al., 2007; Hofmann et al., 2007; Li et al., 2007; Stalder et al., 2011).

Sec7 has no PH domain or other obvious membrane binding motifs. To determine whether $Sec7_f$ can stably associate with membranes, we utilized an *in vitro* membrane-binding assay. Liposomes were incubated with purified proteins in the presence of guanine nucleotides,

and membrane-bound proteins were isolated by floating the liposomes on a sucrose gradient. We tested for stable membrane binding of the four Sec7 constructs and found that none bound autonomously to membranes (Figures 2.2A-E, "GDP" lanes). Surprisingly, $Sec7_f$ and Sec7ΔC+HDS1 instead were recruited to membranes in reactions that also contained activated Arf1 (Arf1 bound to the non-hydrolyzable GTP analog GMP-PNP) (Figures 2.2A,B,D,E, "GTP^*" lanes). In contrast, neither the Sec7GEF nor the Sec7ΔC construct were recruited to membranes under these conditions (Figures 2.2A-C). Similar results were obtained when GTP was used instead of GMP-PNP (data not shown). These results indicate that activated Arf1 stably recruits its activator Sec7 to the membrane surface and that this recruitment requires the HDS1 domain.

Sec7-GEF domains can stably bind their Arf GTPase substrates, but only in their nucleotide-free state, and these enzyme-substrate complexes can dynamically associate with membranes (Beraud-Dufour et al., 1999). However, such an interaction is unlikely to be responsible for the membrane recruitment we observe, as the Sec7GEF construct was not recruited to membranes (Figure 2.2C). Additionally, the interaction we observe is GTP-dependent, which is inconsistent with GEF domain mediated binding, providing further evidence that the membrane recruitment we observe is not due to an interaction between the active site and its substrate or product.

Arf1 activation by Sec7 occurs through HDS1 domain-dependent positive feedback

The observation that Arf1-GTP, the product of Sec7 activity, stably recruits $Sec7_f$ to the membrane surface led us to hypothesize that activation of Arf1 by Sec7 may occur through a

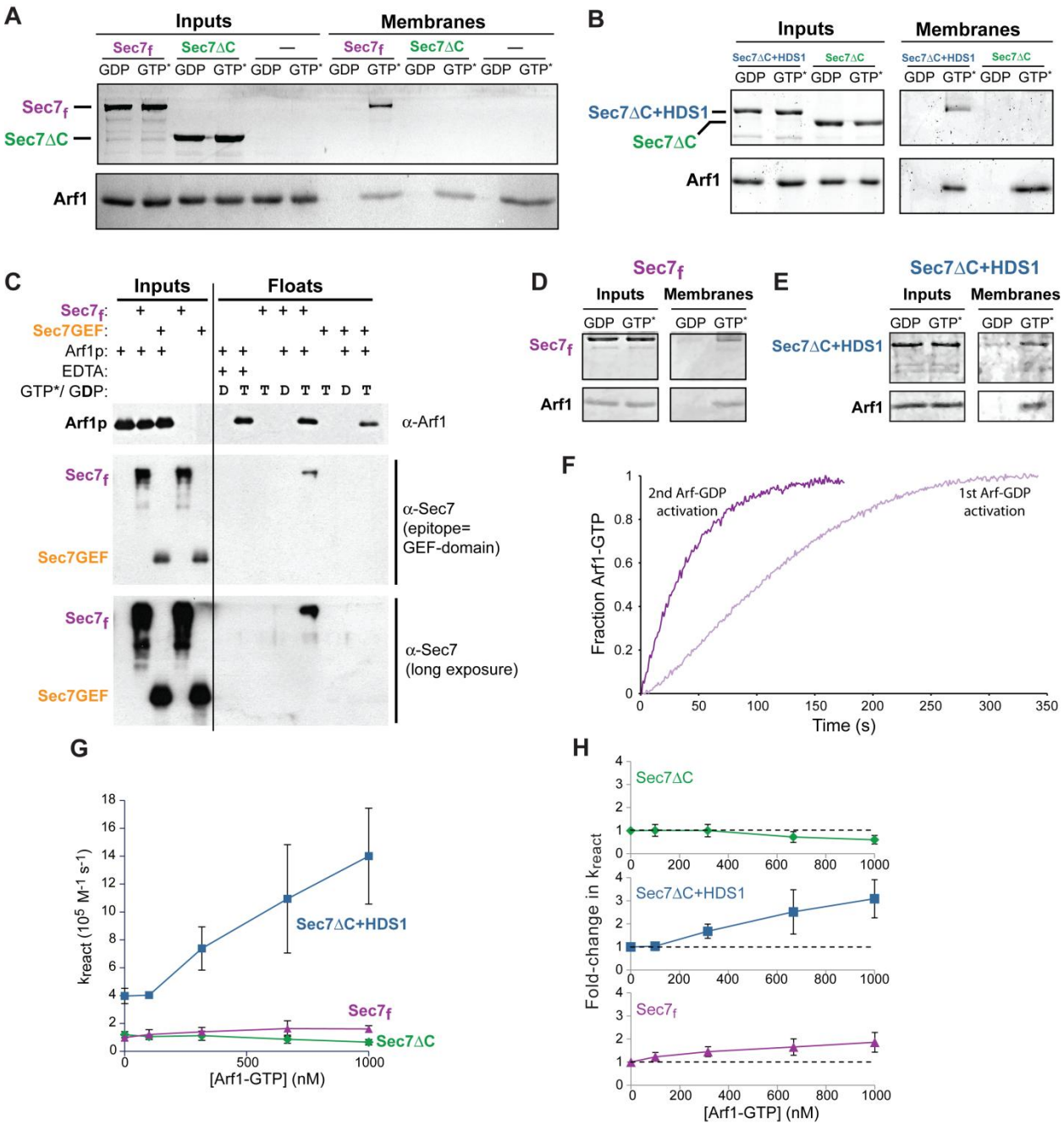

Figure 2.2: The HDS1 domain mediates positive feedback via stable recruitment of Sec7 to membranes. (A), (B) Purified Sec7 constructs were added to liposomes pre-incubated with active (GMP-PNP-bound, denoted GTP*) or inactive (GDP-bound) purified Arf1, and lipid-bound proteins were separated from unbound proteins by flotation on a sucrose gradient. Input (left) and membrane-bound (right) protein content was determined by SDS-PAGE and total protein staining. **(C)** Binding assays performed as in (A),(B) and assessed by Western Blot (performed by me). **(D), (E)** Repeats of liposome binding assays in (A), (B), performed by me. **(G)** A Sec7/liposome/GTP mixture was preincubated with varying amounts of Arf1-GTP as indicated. A constant amount of additional Arf1-GDP (670 nM) was then added and the rate of nucleotide exchange determined. **(H)** Rates from (G) normalized to the rate following a mock (buffer only) preincubation. Experiments (A), (B), (G), and (H) were performed by Brian Richardson.

positive feedback loop, analogous to what has been observed with ARNO (Stalder et al., 2011) and other GEFs (Bose et al., 2001; Butty et al., 2002; Lippe et al., 2001; Margarit et al., 2003). To test this hypothesis, a series of GEF assays were performed in which Arf1-GTP (product) was titrated into the reaction starting conditions, while keeping the amount of Arf1-GDP (substrate) constant. We found that adding increasing amounts of Arf1-GTP to the reaction increased the rates of exchange catalyzed by both $Sec7_f$ and Sec7ΔC+HDS1 (although the effect on $Sec7_f$ is modest), but not Sec7ΔC (Figure 2.2G,H). This effect was seen whether the Arf1-GTP added to the reaction was itself activated by the GEF construct being investigated (as performed for the experiments shown in Figure 2.2F-H), or instead by EDTA-induced nucleotide exchange (data not shown). These results confirm that the product of Sec7 function, Arf1-GTP, stimulates Sec7 activity, indicative of positive feedback.

When we activate Arf1-GDP using low concentrations of $Sec7_f$, then add a second round of Arf1-GDP to the reaction (which now contains both Arf1-GTP and $Sec7_f$), we find a noticeable lag in the first round of Arf1 activation (Figure 2.2F). The shape of the first activation curve indicates that Arf1 activation initially proceeds slowly (a lag phase) before accelerating. This slow initial activation is followed by a round of rapid Arf1 activation upon the addition of more Arf1-GDP (Figure 2.2F). Our interpretation of this phenomenon is that $Sec7_f$ is autoinhibited at the beginning of the time-course until sufficient Arf1 is activated to trigger release of autoinhibition via positive feedback. This observation raised the possibility that, instead of activating $Sec7_f$ and Sec7ΔC+HDS1, Arf1-GTP may simply relieve autoinhibition.

However, the fact that $Sec7_f$ and Sec7ΔC+HDS1 display significantly higher reaction rates than Sec7ΔC (Figure 2.1G) indicates that Arf1-GTP exerts a stimulatory effect. As expected, ΔN17-Arf1-GTP did not recruit $Sec7_f$ to membranes, as ΔN17-Arf1-GTP itself is

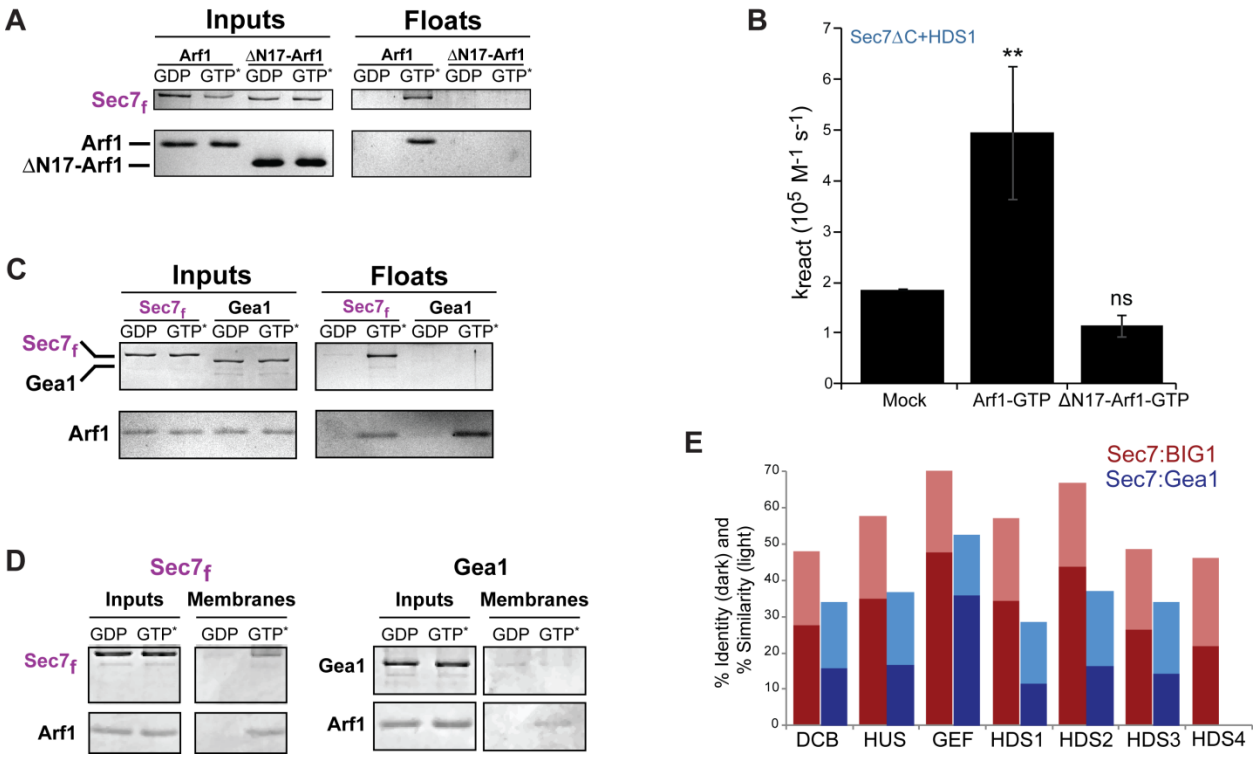

Figure 2.3: Membrane-bound activated Arf1 stably recruits Sec7f, but not Gea1, to membranes.
(A) Liposome flotation comparing Arf1 to ΔN17-Arf1 for recruitment of $Sec7_f$ to membranes.
(B) Sec7ΔC+HDS1 was preincubated with GTP, liposomes, and buffer (mock), Arf1-GTP (670 nM), or ΔN17-Arf1-GTP (670nM) before measuring rate of exchange on Arf1-GDP (670 nM).**(C)**, **(D)** Liposome flotation comparing membrane recruitment of purified $Sec7_f$ to purified full-length Gea1. **(E)** Sec7 conserved domains were aligned pairwise with the corresponding domain in human BIG1 (red) or yeast Gea2 (blue) using MUSCLE (Edgar, 2004). Percent identity and percent similarity of each alignment were calculated using BioEdit; percent similarity is based on the BLOSUM62 substitution matrix. The HDS1 domain is the least conserved domain when comparing between TGN-localized Sec7 and *cis*-Golgi localized Gea2. Experiments in (A), (B), and (C) were performed by Brian Richardson.

not membrane bound (Figure 2.3A). In contrast to the stimulatory effect of Arf1-GTP, an equivalent concentration of ΔN17-Arf1-GTP (670 nM) did not significantly increase the activity of Sec7ΔC+HDS1 (Figure 2.3B). These results suggest that Arf1-GTP must be bound to the membrane surface to exert its full activating effect on the Sec7 constructs. Taken together with the observation that only the two constructs containing the HDS1 domain exhibited positive feedback behavior, this result strongly suggests that positive feedback arises through stable recruitment of Sec7 to the membrane surface by direct interaction between Arf1-GTP and the HDS1 domain.

The early-Golgi localized Arf-GEFs (Gea1/2 in yeast, GBF1 in humans) share a similar domain architecture to the TGN-localized Sec7 and human BIG1/2, and also function on the same Arf GTPase substrates. However, they may be regulated differently given their distinct subcellular location. To assess whether the early-Golgi Arf-GEFs are likely to exhibit positive feedback behavior, we assayed whether activated Arf1 could stably recruit purified yeast Gea1 to membranes using the liposome flotation assay. In contrast to $Sec7_f$, we found that Gea1 was not recruited to liposomes by activated Arf1 (Figure 2.3C,D). Thus, although Gea1/2 and GBF1 possess an HDS1 domain, it may not serve the same function in these proteins as it does in Sec7. Indeed, the HDS1 domain is the least conserved of the recognized homology domains when comparing Gea1 to Sec7, yet is more strongly conserved between Sec7 and its human homolog BIG1 (Figure 2.3E).

The HDS1 domain mediates Sec7 localization to the trans-Golgi network

As Sec7 and Arf1-GTP interact in cell extracts, we hypothesized that this interaction might play a role in localizing Sec7 to the TGN. We examined GFP-Sec7, GFP-Sec7ΔC, and GFP-Sec7ΔC+HDS1 plasmid constructs in cells in which the endogenous *SEC7* gene was intact.

Whereas GFP-Sec7 decorated punctate structures known to correspond to the TGN (Franzusoff et al., 1991), and exhibited very faint cytoplasmic labeling, GFP-Sec7ΔC was exclusively cytoplasmic and nuclear, with no observable punctae (Figure 2.4A). Remarkably, GFP-Sec7ΔC+HDS1 restored partial localization to punctae, with the extent of localization varying among cells (Figure 2.4A). All GFP-Sec7ΔC+HDS1 expressing cells examined exhibited several observable GFP-positive punctae, whereas no GFP-positive punctae were observed in any cells expressing GFP-Sec7ΔC. The HDS1 domain is therefore required to localize the remaining N-terminal regions of Sec7 to punctae under these conditions. Furthermore, these results indicate that the HDS2-4 domains also play a role in localization to punctae, consistent with a report that a 48-amino acid deletion within the HDS4 domain resulted in partial mislocalization of Sec7 (Dehring et al., 2008).

To confirm that the GFP-Sec7ΔC+HDS1 punctae correspond to the TGN, we examined the colocalization of this construct with chromosomal *SEC7-RFP*^{Mars} (Figure 2.4B). Plasmid-borne GFP-Sec7 showed a near complete localization with endogenous Sec7-RFP^{Mars}. Similarly, the colocalization of plasmid-borne GFP-Sec7ΔC+HDS1 punctae with Sec7-RFP^{Mars} was significant. Whereas each GFP-Sec7ΔC+HDS1 puncta was also positive for Sec7-RFP^{Mars}, not every Sec7-RFP^{Mars} punctae was positive for GFP-Sec7ΔC+HDS1, most likely due to the relatively weaker labeling of punctae by this construct. These data indicate that the GFP-Sec7ΔC+HDS1 punctae do indeed correspond to the TGN, although perhaps not all TGN compartments within a cell have detectable levels of GFP-Sec7ΔC+HDS1. Taken together, these results demonstrate that both the HDS1 domain and the HDS2-4 domains play a role in

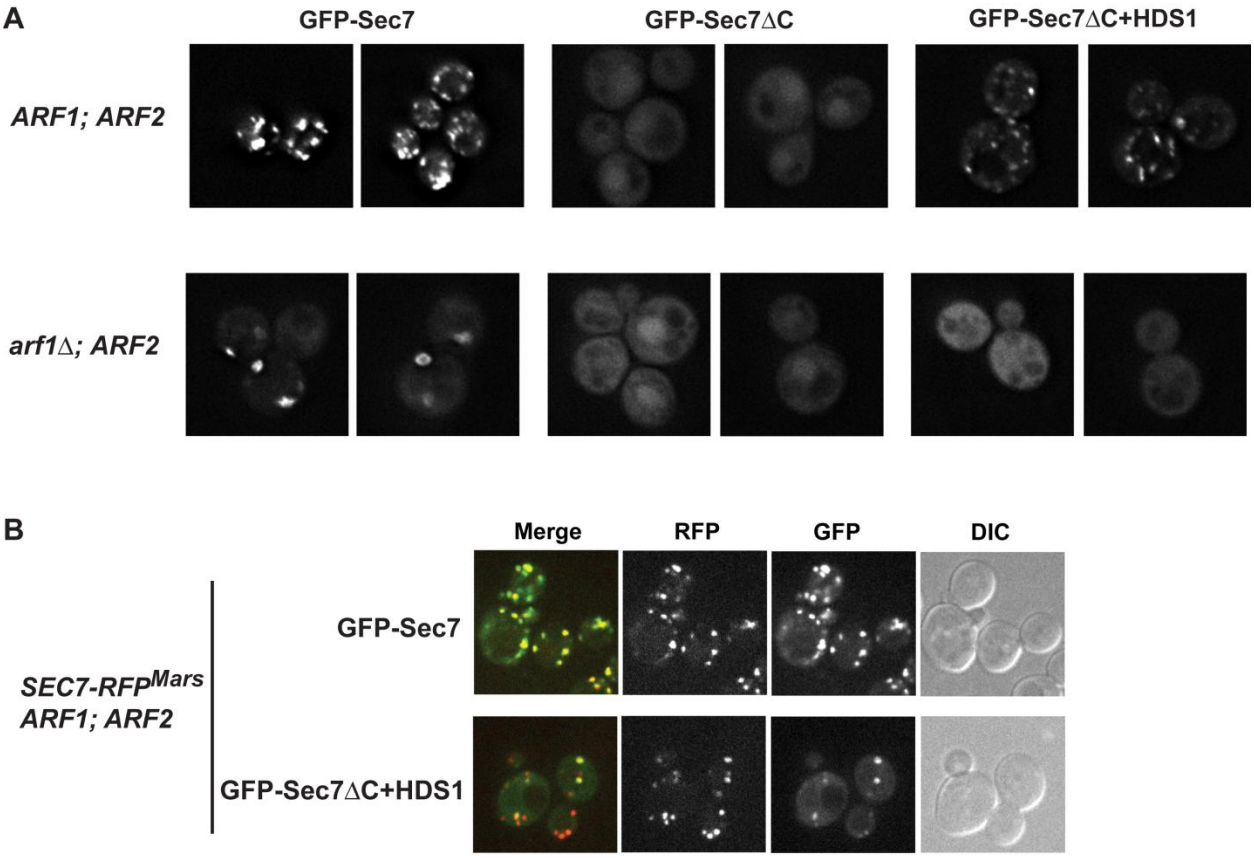

Figure 2.4: The HDS1 domain cooperates with Arf1 to mediate localization of Sec7 to the TGN.
(A) Wild-type yeast cells (CFY103: *ARF1*; *ARF2*; *SEC7*) and *arf1Δ* yeast cells (CFY392: *arf1Δ*; *ARF2*; *SEC7*) expressing plasmid-borne GFP-tagged Sec7 constructs were imaged. Single deconvolved focal planes are shown at equivalent light levels. The plasmids used were pCF1084 (GFP-Sec7), pCF1140 (GFP-Sec7ΔC), and pCF1141 (GFP-Sec7ΔC+HDS1). **(B)** *SEC7-RFP*^{Mars} yeast cells (CFY589) expressing pCF1084 or pCF1141 were imaged to examine the co-localization of GFP and RFP signals by confocal microscopy. Experiments in (B) were performed by Brian Richardson.

localizing Sec7 to the TGN, as loss of HDS2-4 results in partial mislocalization to the cytoplasm and additional loss of HDS1 results in complete mislocalization.

To determine whether the HDS1 domain dependent localization of Sec7 required Arf1, we examined the localization of the GFP-tagged constructs in *arf1*Δ cells. As the *ARF1* gene encodes approximately 90% of the total Arf1 and Arf2 protein in cells, *arf1Δ* strains express ~10% of Arf1/2 relative to *ARF1* strains (Stearns et al., 1990) and represent the best steady-state alternative to the synthetically lethal *arf1Δ arf2Δ* double mutant. Strikingly, we found that the GFP-Sec7ΔC+HDS1 construct is completely mislocalized to the cytoplasm in *arf1*Δ cells, whereas GFP-Sec7 is only slightly mislocalized to the cytoplasm in *arf1Δ* cells, primarily appearing as toroids likely corresponding to enlarged TGN compartments known as Berkeley bodies (Figure 2.4A). Therefore, the HDS1-dependent TGN localization of the GFP-Sec7 constructs is mediated by Arf1.

Discussion

The Golgi is the primary cellular sorting station for protein and membrane secretory traffic. Most of the traffic within and out of the Golgi is controlled by Arf GTPases, yet the Arf-GEFs that activate these GTPases at the Golgi are poorly understood. In this study we have elucidated two key autoregulatory features of the TGN-localized Arf-GEF Sec7: autoinhibition and positive feedback. Both features require the function of a previously uncharacterized domain, the HDS1 domain. Positive feedback arises through interaction of the HDS1 domain with Arf1-GTP, the product of Sec7 activity, resulting in stabilization of Sec7 on the membrane surface (Figure 2.5A,B).

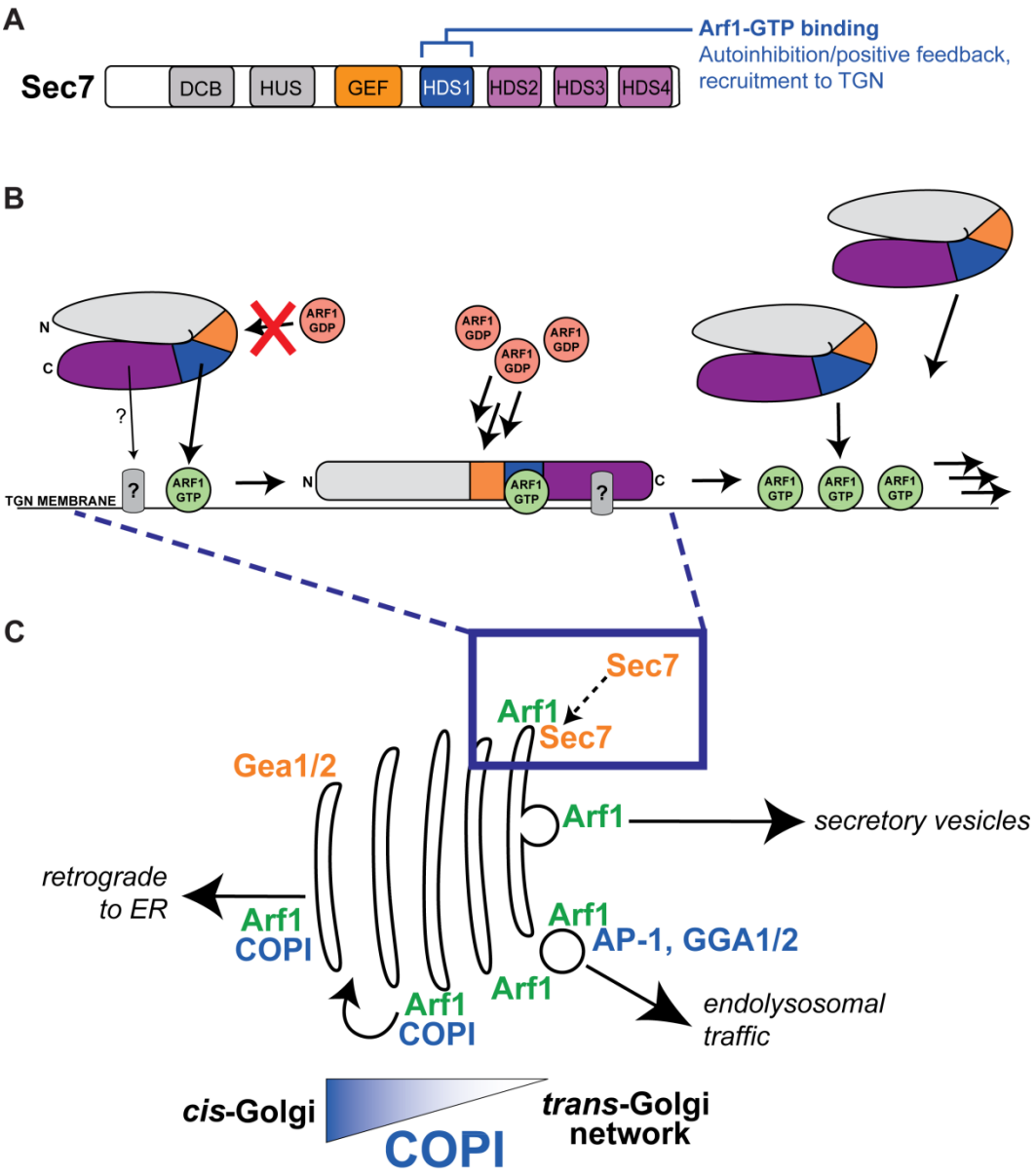

Figure 2.5: Feedback activation model for Sec7 recruitment to the TGN.

(A) Schematic representation of Sec7 homology domains with annotation of the function of the HDS1 domain. **(B)** Model for autoinhibition and positive feedback regulation of Sec7. Although Sec7 is dimeric, for simplicity only one monomer is schematized. Sec7 autoinhibition in solution is represented by a putative intramolecular interaction. Release of autoinhibition is concomitant with recruitment to the TGN membrane by direct interaction of the HDS1 domain (blue) with Arf1-GTP (green circle). An additional factor ("?") may also contribute to the recruitment of Sec7 to the TGN through interaction with the HDS2-4 domains. Positive feedback arises through the generation of more Arf1-GTP by Sec7, which leads to the recruitment of more Sec7, etc. **(C)** Model for Sec7 recruitment to the TGN. Although Arf1-GTP is localized to the entire Golgi, Sec7 might only be recruited to the TGN because COPI may outcompete Sec7 for binding to Arf1-GTP at earlier Golgi compartments.

The rate enhancement that accompanies stable binding of Sec7 to the membrane can be explained by an increased frequency of productive encounters between Sec7, Arf1-GDP, and the membrane surface to form the tripartite enzyme-substrate-membrane complex that is a prerequisite for Arf1 activation. Alternatively, the observed rate enhancement may arise through relief of the autoinhibitory effects of the C-terminus via an allosteric conformational change triggered by binding to Arf1-GTP and concomitant association with the membrane. We favor a hybrid model in which Arf1-GTP recruitment of Sec7 to the membrane by Arf1-GTP results in both allosteric relief of autoinhibition and an increased frequency of productive encounters between Sec7, Arf1-GDP, and the membrane.

The Arf-GEF ARNO requires the presence of an activated Arf GTPase, either Arf6 or Arf1, for robust activity on membranes; when Arf1 is used as an activator and a substrate for ARNO, positive feedback is observed (Stalder et al., 2011). The positive feedback effect that we observed in our assays was less pronounced than that seen for ARNO. For both Sec7 and ARNO, positive feedback also involves relief of autoinhibition. It is possible that the larger positive feedback effect exhibited by ARNO is due to a greater degree of autoinhibition. Indeed, PH domain-proximal elements of ARNO inhibit the activity of its GEF domain by approximately 14-fold (Stalder et al., 2011), whereas we found that the C-terminus of Sec7 inhibited its GEF domain by approximately 7-fold when comparing the rates of $Sec7_f$ and Sec7ΔC in solution. In addition, we were unable to assay Sec7 at very low concentrations (< 50 nM) due to its instability under such conditions. We may have observed a more pronounced positive feedback effect if we had been able to perform the GEF assays at concentrations approaching those used

for ARNO (7.5 nM). Furthermore, our data suggest that a key function of positive feedback for Sec7 is its role in localization of the GEF to the TGN, in addition to its role in rate enhancement. In contrast, positive feedback is not a likely localization mechanism for ARNO, as Arf1, the most likely substrate for ARNO, is primarily localized to the Golgi, but ARNO is primarily localized to the cell periphery. ARNO localization depends instead upon lipid interactions with its PH domain (Venkateswarlu et al., 1998), as well as GTPase cascades (Cohen et al., 2007; DiNitto et al., 2007; Hofmann et al., 2007; Li et al., 2007).

Our data indicate that Arf1-GTP recruits Sec7 to the TGN via interaction with the HDS1 domain. As Sec7 is a major source of Arf1-GTP, what is the origin of the initial Arf1-GTP that recruits Sec7 to the TGN? While residual activity of autoinhibited Sec7 suffices *in vitro*, the early-Golgi Arf-GEFs (Gea1/2 in yeast) might represent a more robust source *in vivo*. As the Golgi matures, Gea1/2 provide the Arf1-GTP needed at the early compartments, most prominently to recruit coatomer to generate COPI vesicles for retrograde cargo sorting. The localization mechanism of Gea1/2 (as well as human GBF1) remains unresolved, although a transmembrane receptor has been proposed (Chantalat et al., 2003), and SNAREs have been shown to recruit Arf1-GDP to the membrane surface (Honda et al., 2005), which may in turn recruit Gea1/2 through a substrate-enzyme interaction. The localization mechanism of the early-Golgi Arf-GEFs is likely distinct from that of Sec7, as we found that Gea1 was not stably recruited to membranes by Arf1-GTP.

Given that Arf1-GTP is present throughout early-Golgi as well as late-Golgi compartments, how does Arf1-GTP specifically recruit Sec7 to the TGN? One possibility is coincidence detection involving an unknown factor binding to Sec7, either to the HDS1 domain or to the N-terminus: although Sec7ΔC+HDS1 is partially mislocalized to the cytoplasm, we found that the visible punctae correspond to the TGN. An alternative model is that Arf1-GTP is

sufficient to provide TGN specificity because Sec7 must compete with other Arf1 effectors for binding to Arf1-GTP (Figure 2.5C). In this scenario, at early Golgi compartments, most of the Arf1-GTP is bound to the COPI coat, which is recruited to the cis- and medial-Golgi by interaction with cargo tails and Arf1-GTP. Therefore, at compartments where COPI cargo is present, the affinity of COPI for the membrane, and thus for Arf1-GTP, may be great enough to effectively outcompete Sec7 for binding to Arf1-GTP. In the maturing Golgi, COPI cargo is relatively absent from later compartments because it has been trafficked to earlier compartments (to the *cis*-Golgi and ER). Free from competition with COPI, Sec7 would be able to bind to Arf1-GTP only at the TGN. Under this speculative model, Arf1-GTP dependent Sec7 recruitment could serve as a checkpoint in Golgi maturation, preventing the premature recruitment of TGN-localized effectors until COPI sorting has completed. Of course, Sec7 would also compete for binding to Arf1-GTP at the TGN with TGN-localized Arf1 effectors, primarily the clathrin adaptors, but perhaps the affinity of these effectors for Arf1-GTP is less than that of coatomer. Future studies involving in-depth characterization of binding constants in the presence of membrane-bound cargo tails may be needed to test this hypothesis.

An intriguing possible consequence of Sec7 positive feedback at the TGN is that it could be used to generate TGN-derived vesicles that traffic to the PM, which have not been clearly demonstrated to require a vesicle coat. Vesiculation could occur through the rapid activation of a high local concentration of Arf1 via Sec7-mediated positive feedback, peaking in activity only after cargos destined for the endolysosomal system have been sorted away from the TGN by Arf1-dependent clathrin-coated vesicles. The reduced fraction of Arf1-GTP bound to clathrin cargo adaptors at the TGN would be free to recruit more Sec7, stimulating positive feedback. Arf1-GTP, at high concentrations, is sufficient to generate the membrane curvature needed for vesiculation (Beck et al., 2008; Krauss et al., 2008), and recently has been shown to be directly

involved in vesicle fission (Beck et al., 2011). Thus, Sec7-mediated positive feedback activation of Arf1 could drive vesiculation of the TGN without the need for a vesicle coat.

Although Arf1 is the primary Arf at the Golgi in yeast cells (Arf2 is redundant and dispensable), there are four paralogous Arfs at the Golgi in human cells. Recent work has indicated that these human paralogs may exhibit some specificity for early versus late Golgi compartments (Ben-Tekaya et al., 2010; Manolea et al., 2010), although this analysis is complicated by robust functional redundancy among the paralogs (Volpicelli-Daley et al., 2005). Therefore in human cells it is possible that GBF1 activates one or two specific Arf paralogs that then serve to recruit BIG1/2 to activate distinct Arf paralogs at the TGN. Despite this important potential distinction, the overall mechanism of GEF recruitment by activated Arf GTPases is very likely conserved between yeast and humans, given the high degree of sequence conservation between Sec7 and BIG1/2, and between the yeast and human Golgi-localized Arfs.

Our results establish autoinhibition and positive feedback as important features of Sec7 regulation, and demonstrate a role for positive feedback in recruitment of Sec7 to the TGN. Our data suggest that the interplay between Arf1 activation and Arf1 effector recruitment must be intimately connected, and the dynamics of competition between GEF and effector for Arf1-GTP binding may play a role in Golgi maturation.

Methods

Plasmids, Strains, and Antibodies

Standard techniques were used for generating yeast strains by homologous recombination (Gauss et al., 2005; Longtine et al., 1998) and by mating. All yeast *SEC7* plasmids encode Sec7 constructs driven by the native *SEC7* promoter. Plasmids are presented in Table 2.2 and yeast strains are presented in Table 2.3.

The anti-Arf1 polyclonal antibody were a kind gift from the Schekman lab. The anti-FLAG monoclonal "M2" antibody and anti-G6PDH (yeast Zwf1) polyclonal antibody were purchased from Sigma. The anti-HA monoclonal "12CA5" antibody was purchased from Roche.

Protein purification

All Sec7 constructs generated for purification contain a C-terminal motif of the GEF domain, "loop>J", recently shown to be important for GEF activity (Lowery et al., 2011). The Bac-to-Bac system (Invitrogen) was used to generate baculoviruses for insect cell expression. Virus was generated in *Sf9* cells (Expression Systems) by transfection of the shuttle vector with Cellfectin II (Invitrogen) followed by two amplification passages. Protein was produced in a 1L culture of *T.ni.* cells at 10^6/ml in ESI-921 media (Expression Systems) grown for 24 hours, infected with virus, and allowed to express for 48 hours. The cells were lysed by sonication in lysis buffer containing 50 mM HEPES pH 7.4, 300 mM KOAc, 20 mM imidazole pH 8.0, 10% glycerol, 10 mM β-ME, with Roche complete protease inhibitors. The lysate was cleared by centrifugation and protein was purified from the cleared lysate by nickel affinity and anion exchange chromatography. Glycerol was added to the purified protein stock to 10% before freezing.

Table 2.1: Plasmids used in this study
Plasmids are listed, along with a description and the source.

Name	Description	Vector Backbone	Source
pET28	T7 promoter-driven expression plasmid		Novagen
pMR1	6xHis-Sec7ΔC (residues 203-1017)	pET28	This study
pBCR389	6xHis-Sec7ΔC+HDS1 (residues 203-1220)	pET28	This study
pCM1	6xHis-GEFdomain (residues 818-1017)	pET28	This study
pCF1163	6xHis-Gea1	pET28	This study
pFastBacHT	Baculovirus plasmid vector		Invitrogen
pBCR314	6xHis-$Sec7_f$ (residues 203-2009)	pFastBacHT	This study
pRS415	centromeric LEU2 plasmid		(Sikorski and Hieter, 1989)
pRS416	centromeric URA3 plasmid		(Sikorski and Hieter, 1989)
pCF1043	*SEC7* (includes ~1 kB of 5'UTR)	pRS416	This study
pCF1045	*SEC7* (includes ~1 kB of 5'UTR)	pRS415	This study
pCF1046	$Sec7_f$ (residues 203-2009) driven by P_{SEC7}	pRS415	This study
pCF1101	3x-HA-Sec7 driven by P_{SEC7}	pRS415	This study
pCF1135	3x-HA-Sec7ΔC (residues 1-1020) driven by P_{SEC7}	pRS415	This study
pCF1136	3x-HA-Sec7ΔC+HDS1 (residues 1-1215) driven by P_{SEC7}	pRS415	This study
pCF1139	3x-HA-Sec7ΔHDS1 (residues 1-1024,1216-2009) driven by P_{SEC7}	pRS415	This study
pCF1210	3x-HA-Sec7 C1116A E1118A G1119A driven by P_{SEC7}	pRS415	This study
pCF1211	3x-HA-Sec7 H1084A V1085A F1089A driven by P_{SEC7}	pRS415	This study
pCF1084	GFP-Sec7 driven by P_{SEC7}	pRS415	This study
pCF1140	GFP-Sec7ΔC (residues 1-1020) driven by P_{SEC7}	pRS415	This study
pCF1141	GFP-Sec7ΔC+HDS1 (residues 1-1215) driven by P_{SEC7}	pRS415	This study
pCF1142	GFP-Sec7ΔHDS1 (residues 1-1024,1216-2009) driven by P_{SEC7}	pRS415	This study
pBCR395	GFP-Sec7 L1097A L1100A driven by P_{SEC7}	pRS415	This study
pBCR396	GFP-Sec7 C1116A E1118A G1119A driven by P_{SEC7}	pRS415	This study
pBCR397	GFP-Sec7 I1124A K1125A I1126A driven by P_{SEC7}	pRS415	This study
pBCR413	GFP-Sec7 E1046A Y1048A driven by P_{SEC7}	pRS415	This study
pBCR414	GFP-Sec7 H1084A V1085A F1089A driven by P_{SEC7}	pRS415	This study
pBCR415	GFP-Sec7 E1154A K1158A N1159A driven by P_{SEC7}	pRS415	This study
pBCR416	GFP-Sec7 S1180A W1181A K1182A D1183A driven by P_{SEC7}	pRS415	This study

Table 2.2: Yeast strains used in this study
Strains are listed, along with the genotype and the source.

Name	Description	Source
SEY6210	*MATα his3-Δ200 leu2-3,112 lys2-801 trp1-Δ901 ura3-52 suc2-Δ9*	(Robinson et al., 1988)
SEY6210.1	*MATa his3-Δ200 leu2-3,112 lys2-801 trp1-Δ901 ura3-52 suc2-Δ9*	(Robinson et al., 1988)
CFY362	SEY621.1 *SEC7-3xFLAG-6XHis::TRP1*	This study
CFY392	SEY6210 *arf1Δ::HIS3*	(Gaynor and Emr, 1997)
CFY589	SEY6210.1 *SEC7-RFP^{Mars}::TRP1*	Emr Lab, unpublished
CFY403	SEY6210.1 *arg4Δ::KANMX*	Emr Lab, unpublished
CFY512	CFY403 *SEC7-3xHA::TRP1*	This study
CFY743	CFY403 *6xHA-SEC7*	This study
BY4742	*MATα his3-Δ1 leu2-Δ0 lys2-Δ0 ura3-Δ0*	(Brachmann et al., 1998)
CFY409	BY4742 *sec7Δ::KANMX* +pCF1043	This study*
CFY863	CFY409 *arf1Δ::HIS3*	This study

*****Derived from BY4743 *SEC7*/*sec7Δ::KANMX* diploid strain (Giaever et al., 2002)

His-tagged bacterial expression constructs were created using the pET28 vector backbone. The expression vectors were transformed into Rosetta2 cells and grown in 8L TB to an OD of ~3.5, followed by decrease of temperature to 18°C, induction of expression with 250 μM IPTG, and overnight expression. Cells were lysed by sonication in lysis buffer containing 50 mM HEPES pH 7.4, 450 mM KOAc, 20 mM imidazole pH 8.0, 10% glycerol, 10 mM β-ME, 1 mM PMSF; for ΔN17-Arf1, the lysis buffer also included 1 mM $MgCl_2$. The lysate was cleared by centrifugation and protein was purified from the cleared lysate by nickel affinity, anion exchange, and gel filtration chromatography into a final buffer of 20 mM HEPES pH 7.4, 150 mM NaCl, 2 mM DTT, with additional 1 mM MgCl2 for ΔN17-Arf1.

Recombinant myristoylated yeast Arf1 was obtained following a previously published protocol (Ha et al., 2005). Briefly, Arf1 and N-myristoyl transferase were coexpressed overnight in *E. coli* in the presence of myristate (Sigma) at 18°C, and the culture was lysed by sonication and cleared by ultracentrifugation. Lysate from 1 L culture was incubated with 30 ml DEAE resin (GE Healthcare) in batch; unbound protein was concentrated and then purified by gel filtration (Superdex 10/300 GL, GE Healthcare) and hydrophobic interaction chromatography (HiTrap Phenyl HP, GE Healthcare) to obtain uniformly myristoylated Arf1.

Preparation of Liposomes

Unilamellar liposomes were generated from a mixture of lipids (Table 2.1) approximating the endogenous TGN lipid composition determined in a published lipidomics study (Klemm et al., 2009), plus added DiR near-infrared dye (Avanti Polar Lipids) to aid in visualization and quantitation of lipids. Following vacuum drying, lipid films were hydrated in 20 mM HEPES pH

Table 2.3: Lipid formulation of liposomes used in this study
Shown are the amounts (in mol %) of each lipid in the lipid mix.

Mol %	Lipid
24%	DOPC
6%	POPC
7%	DOPE
3%	POPE
1%	DOPS
2%	POPS
1%	DOPA
2%	POPA
29%	PI (liver-derived)
1%	PI(4)P
2%	CDP-DAG
4%	PO-DAG
2%	DO-DAG
5%	C18-Ceramide
10%	Cholesterol
1%	DiR (fluorescent lipid)

7.4, 150 mM KOAc, followed by extrusion through 100 nm filters (Whatman) to generate liposomes.

Liposome flotation assays

To assess Arf1-mediated recruitment, liposomes were incubated with 10 μg Arf1 in the presence of 625 μM EDTA and 125 μM GMPPNP nonhydrolyzable GTP analog for one hour to insert activated Arf1 into the membrane. The exchange reaction was stopped with 2.5 mM $MgCl_2$, and the liposomes with bound Arf1 were incubated for one hour with 10 μg of purified Sec7 construct. Liposomes were separated from unbound protein by sucrose gradient ultracentrifugation similar to published procedures (Matsuoka et al., 1998): sucrose was added to the binding reaction to 1M, layered with .75 M sucrose followed by sucrose-free buffer, and spun at 100,000 rpm for 20 minutes at 20ºC in a TLA-100 ultracentrifuge rotor. The top layer was collected and bound proteins assessed by SDS-PAGE, with loading normalized for lipid recovery as measured by DiR fluorescence.

Arf1 nucleotide exchange kinetics assay

The nucleotide-bound state of Arf1 was monitored in real-time by native tryptophan fluorescence (297.5 nm excitation, 340 nm emission), similar to published procedures (Antonny et al., 1997; Higashijima et al., 1987). The native tryptophan fluorescence exchange assay was set up by sequentially adding liposomes at 200 μM final total lipid concentration, 100 nM Sec7 construct, Arf1 construct at varying concentrations as indicated, and 200 μM GTP to prewarmed 20 mM HEPES pH 7.4, 150 mM KOAc, 1 mM $MgCl_2$. Tryptophan fluorescence at 297.5 nm excitation and 340 nm emission was monitored for stability during setup. After addition of the

final component, tryptophan fluorescence was monitored for 10 to 40 minutes, depending on reaction conditions, to obtain the exchange trace. Triplicate traces were fit to a single exponential curve as described below. Due to documented variability in exchange rates for different batches of liposomes (Stalder et al., 2011), all reactions shown within any one figure panel were performed using a single batch of liposomes.

Due to slow linear drift of the fluorescence trace clearly visible after completion of the reaction, presumably the result of gradual liposome aggregation, curves of fluorescence vs. time were fit using GraphPad Prism software to a single exponential curve with an additional linear term:

$$Fluorescence = (Baseline\ fluorescence) + (Plateau\ fluorescence) * (1 - e^{-kreact*[Sec7]*time}) - (Drift * time)$$

Occasional spikes in the fluorescence traces were minimized by automatic outlier elimination in the single exponential fit. To account for pipetting error and differences between Sec7 preparations, measurement of the native Sec7 fluorescence during reaction setup and comparison to a standard curve permitted the exact [Sec7] of a given reaction to be determined. The traces shown in Figures 1D and S1D were transformed from raw fluorescence quantification to fraction of Arf1 with bound GTP by normalization to the fit baseline fluorescence and plateau fluorescence, and removal of the linear drift.

Immunoprecipitations

Cell pellets (15 OD-equivalents of log-phase cells) were resuspended in 800 ul of either "Mg^{2+} lysis buffer" (50 mM Tris pH 7.5, 150 mM NaCl, 0.2% NP-40, 1 mM EDTA, 5 mM Mg^{2+}, 1 mM PMSF, 1X Roche protease inhibitor cocktail), or "EDTA lysis buffer" (50 mM Tris pH 7.5, 150 mM NaCl, 0.2% NP-40, 5 mM EDTA, 1 mM PMSF, 1X Roche protease inhibitor cocktail). The cell suspensions were mechanically disrupted by bead-beating (500 µl glass beads)

and the lysates were cleared by centrifugation at 14,000 g for 5 minutes. The supernatants were incubated with 10 ul of anti-HA resin (Sigma) for four hours at 4°C. The resin was washed 3 times with lysis buffer before the addition of 30 µl sample buffer. Samples were heated to 55°C for 15 minutes before separation by SDS-PAGE and analysis by immunoblot.

Microscopy

Cells were grown in synthetic dropout media and imaged in log phase (OD_{600} ~ 0.5) after spotting onto coverslips in growth media. Live cells were imaged at room temperature on two different microscopes.

For all Figures except 5B we used a DeltaVision RT wide-field deconvolution microscope (Applied Precision) with a PlanApo 100x objective (1.35 NA; Olympus) and a digital camera (Cool Snap HQ; Photometrics). Images acquired on this microscope were deconvolved ("conservative" setting, 6 cycles), and single deconvolved focal planes are shown. For Figure 5B, we used a CSU-X spinning disk (Intelligent Imaging Innovations) with spherical aberration correction device, with a 63x 1.4 NA objective on an inverted microscope (DMI6000B; Leica) and QuantEM EMCCD camera (Photometrics) controlled by Slidebook 5.0 (Intelligent Imaging Innovations). Single confocal sections are shown.

For all microscopy experiments, exposure times and image processing were identical for each sample within an experiment. Care was taken to ensure that light levels were scaled equivalently among all samples within an experiment when exporting from the imaging software, and when subsequently processed within ImageJ and Photoshop (adjusting only light level min/max settings for clarity).

REFERENCES

Antonny, B., Beraud-Dufour, S., Chardin, P., and Chabre, M. (1997). N-terminal hydrophobic residues of the G-protein ADP-ribosylation factor-1 insert into membrane phospholipids upon GDP to GTP exchange. Biochemistry *36*, 4675-4684.

Aridor, M., Fish, K.N., Bannykh, S., Weissman, J., Roberts, T.H., Lippincott-Schwartz, J., and Balch, W.E. (2001). The Sar1 GTPase coordinates biosynthetic cargo selection with endoplasmic reticulum export site assembly. J Cell Biol *152*, 213-229.

Beck, R., Prinz, S., Diestelkotter-Bachert, P., Rohling, S., Adolf, F., Hoehner, K., Welsch, S., Ronchi, P., Brugger, B., Briggs, J.A., *et al.* (2011). Coatomer and dimeric ADP ribosylation factor 1 promote distinct steps in membrane scission. J Cell Biol *194*, 765-777.

Beck, R., Sun, Z., Adolf, F., Rutz, C., Bassler, J., Wild, K., Sinning, I., Hurt, E., Brugger, B., Bethune, J., *et al.* (2008). Membrane curvature induced by Arf1-GTP is essential for vesicle formation. Proc Natl Acad Sci USA *105*, 11731-11736.

Ben-Tekaya, H., Kahn, R.A., and Hauri, H.P. (2010). ADP ribosylation factors 1 and 4 and group VIA phospholipase A regulate morphology and intraorganellar traffic in the endoplasmic reticulum-Golgi intermediate compartment. Molecular biology of the cell *21*, 4130-4140.

Beraud-Dufour, S., Paris, S., Chabre, M., and Antonny, B. (1999). Dual interaction of ADP ribosylation factor 1 with Sec7 domain and with lipid membranes during catalysis of guanine nucleotide exchange. J Biol Chem *274*, 37629-37636.

Beraud-Dufour, S., Robineau, S., Chardin, P., Paris, S., Chabre, M., Cherfils, J., and Antonny, B. (1998). A glutamic finger in the guanine nucleotide exchange factor ARNO displaces Mg2+ and the beta-phosphate to destabilize GDP on ARF1. EMBO J *17*, 3651-3659.

Bose, I., Irazoqui, J.E., Moskow, J.J., Bardes, E.S., Zyla, T.R., and Lew, D.J. (2001). Assembly of scaffold-mediated complexes containing Cdc42p, the exchange factor Cdc24p, and the effector Cla4p required for cell cycle-regulated phosphorylation of Cdc24p. J Biol Chem *276*, 7176-7186.

Brachmann, C.B., Davies, A., Cost, G.J., Caputo, E., Li, J., Hieter, P., and Boeke, J.D. (1998). Designer deletion strains derived from Saccharomyces cerevisiae S288C: a useful set of strains and plasmids for PCR-mediated gene disruption and other applications. Yeast *14*, 115-132.

Butty, A.C., Perrinjaquet, N., Petit, A., Jaquenoud, M., Segall, J.E., Hofmann, K., Zwahlen, C., and Peter, M. (2002). A positive feedback loop stabilizes the guanine-nucleotide exchange factor Cdc24 at sites of polarization. EMBO J *21*, 1565-1576.

Casanova, J.E. (2007). Regulation of Arf activation: the Sec7 family of guanine nucleotide exchange factors. Traffic *8*, 1476-1485.

Chantalat, S., Courbeyrette, R., Senic-Matuglia, F., Jackson, C.L., Goud, B., and Peyroche, A. (2003). A novel Golgi membrane protein is a partner of the ARF exchange factors Gea1p and Gea2p. Mol Biol Cell *14*, 2357-2371.

Chardin, P., Paris, S., Antonny, B., Robineau, S., Beraud-Dufour, S., Jackson, C.L., and Chabre, M. (1996). A human exchange factor for ARF contains Sec7- and pleckstrin-homology domains. Nature *384*, 481-484.

Cohen, L.A., Honda, A., Varnai, P., Brown, F.D., Balla, T., and Donaldson, J.G. (2007). Active Arf6 recruits ARNO/cytohesin GEFs to the PM by binding their PH domains. Mol Biol Cell *18*, 2244-2253.

D'Souza-Schorey, C., and Chavrier, P. (2006). ARF proteins: roles in membrane traffic and beyond. Nature reviews Molecular cell biology *7*, 347-358.

De Matteis, M.A., and Luini, A. (2008). Exiting the Golgi complex. Nature reviews Molecular cell biology *9*, 273-284.

de Wit, M.C., de Coo, I.F., Halley, D.J., Lequin, M.H., and Mancini, G.M. (2009). Movement disorder and neuronal migration disorder due to ARFGEF2 mutation. Neurogenetics *10*, 333-336.

Dehring, D.A., Adler, A.S., Hosseini, A., and Hicke, L. (2008). A C-terminal sequence in the guanine nucleotide exchange factor Sec7 mediates Golgi association and interaction with the Rsp5 ubiquitin ligase. The Journal of biological chemistry *283*, 34188-34196.

DiNitto, J.P., Delprato, A., Gabe Lee, M.T., Cronin, T.C., Huang, S., Guilherme, A., Czech, M.P., and Lambright, D.G. (2007). Structural basis and mechanism of autoregulation in 3-phosphoinositide-dependent Grp1 family Arf GTPase exchange factors. Molecular cell *28*, 569-583.

Donaldson, J.G., and Jackson, C.L. (2011). ARF family G proteins and their regulators: roles in membrane transport, development and disease. Nature reviews Molecular cell biology *12*, 362-375.

Edgar, R.C. (2004). MUSCLE: multiple sequence alignment with high accuracy and high throughput. Nucleic Acids Res *32*, 1792-1797.

Franzusoff, A., Redding, K., Crosby, J., Fuller, R.S., and Schekman, R. (1991). Localization of components involved in protein transport and processing through the yeast Golgi apparatus. J Cell Biol *112*, 27-37.

Futai, E., Hamamoto, S., Orci, L., and Schekman, R. (2004). GTP/GDP exchange by Sec12p enables COPII vesicle bud formation on synthetic liposomes. EMBO J *23*, 4146-4155.

Gauss, R., Trautwein, M., Sommer, T., and Spang, A. (2005). New modules for the repeated internal and N-terminal epitope tagging of genes in Saccharomyces cerevisiae. Yeast *22*, 1-12.

Gaynor, E.C., and Emr, S.D. (1997). COPI-independent anterograde transport: cargo-selective ER to Golgi protein transport in yeast COPI mutants. J Cell Biol *136*, 789-802.

Ghaemmaghami, S., Huh, W.K., Bower, K., Howson, R.W., Belle, A., Dephoure, N., O'Shea, E.K., and Weissman, J.S. (2003). Global analysis of protein expression in yeast. Nature *425*, 737-741.

Giaever, G., Chu, A.M., Ni, L., Connelly, C., Riles, L., Veronneau, S., Dow, S., Lucau-Danila, A., Anderson, K., Andre, B., *et al.* (2002). Functional profiling of the Saccharomyces cerevisiae genome. Nature *418*, 387-391.

Gillingham, A.K., and Munro, S. (2007). The small G proteins of the Arf family and their regulators. Annual review of cell and developmental biology *23*, 579-611.

Glick, B.S., and Nakano, A. (2009). Membrane traffic within the Golgi apparatus. Annual review of cell and developmental biology *25*, 113-132.

Goldberg, J. (1998). Structural basis for activation of ARF GTPase: mechanisms of guanine nucleotide exchange and GTP-myristoyl switching. Cell *95*, 237-248.

Ha, V.L., Thomas, G.M., Stauffer, S., and Randazzo, P.A. (2005). Preparation of myristoylated Arf1 and Arf6. Methods Enzymol *404*, 164-174.

Higashijima, T., Ferguson, K.M., Sternweis, P.C., Ross, E.M., Smigel, M.D., and Gilman, A.G. (1987). The effect of activating ligands on the intrinsic fluorescence of guanine nucleotide-binding regulatory proteins. J Biol Chem *262*, 752-756.

Hofmann, I., Thompson, A., Sanderson, C.M., and Munro, S. (2007). The Arl4 family of small G proteins can recruit the cytohesin Arf6 exchange factors to the plasma membrane. Curr Biol *17*, 711-716.

Honda, A., Al-Awar, O.S., Hay, J.C., and Donaldson, J.G. (2005). Targeting of Arf-1 to the early Golgi by membrin, an ER-Golgi SNARE. J Cell Biol *168*, 1039-1051.

Kahn, R.A. (2009). Toward a model for Arf GTPases as regulators of traffic at the Golgi. FEBS Lett *583*, 3872-3879.

Kahn, R.A., Randazzo, P., Serafini, T., Weiss, O., Rulka, C., Clark, J., Amherdt, M., Roller, P., Orci, L., and Rothman, J.E. (1992). The amino terminus of ADP-ribosylation factor (ARF) is a critical determinant of ARF activities and is a potent and specific inhibitor of protein transport. J Biol Chem *267*, 13039-13046.

Klarlund, J.K., Guilherme, A., Holik, J.J., Virbasius, J.V., Chawla, A., and Czech, M.P. (1997). Signaling by phosphoinositide-3,4,5-trisphosphate through proteins containing pleckstrin and Sec7 homology domains. Science *275*, 1927-1930.

Klarlund, J.K., Tsiaras, W., Holik, J.J., Chawla, A., and Czech, M.P. (2000). Distinct polyphosphoinositide binding selectivities for pleckstrin homology domains of GRP1-like proteins based on diglycine versus triglycine motifs. J Biol Chem *275*, 32816-32821.

Klemm, R.W., Ejsing, C.S., Surma, M.A., Kaiser, H.J., Gerl, M.J., Sampaio, J.L., de Robillard, Q., Ferguson, C., Proszynski, T.J., Shevchenko, A., *et al.* (2009). Segregation of sphingolipids and sterols during formation of secretory vesicles at the trans-Golgi network. J Cell Biol *185*, 601-612.

Kolanus, W., Nagel, W., Schiller, B., Zeitlmann, L., Godar, S., Stockinger, H., and Seed, B. (1996). Alpha L beta 2 integrin/LFA-1 binding to ICAM-1 induced by cytohesin-1, a cytoplasmic regulatory molecule. Cell *86*, 233-242.

Krauss, M., Jia, J.Y., Roux, A., Beck, R., Wieland, F.T., De Camilli, P., and Haucke, V. (2008). Arf1-GTP-induced tubule formation suggests a function of Arf family proteins in curvature acquisition at sites of vesicle budding. J Biol Chem *283*, 27717-27723.

Lee, S.Y., Yang, J.S., Hong, W., Premont, R.T., and Hsu, V.W. (2005). ARFGAP1 plays a central role in coupling COPI cargo sorting with vesicle formation. J Cell Biol *168*, 281-290.

Li, J., Peters, P.J., Bai, M., Dai, J., Bos, E., Kirchhausen, T., Kandror, K.V., and Hsu, V.W. (2007). An ACAP1-containing clathrin coat complex for endocytic recycling. J Cell Biol *178*, 453-464.

Lippe, R., Miaczynska, M., Rybin, V., Runge, A., and Zerial, M. (2001). Functional synergy between Rab5 effector Rabaptin-5 and exchange factor Rabex-5 when physically associated in a complex. Mol Biol Cell *12*, 2219-2228.

Longtine, M.S., McKenzie, A., 3rd, Demarini, D.J., Shah, N.G., Wach, A., Brachat, A., Philippsen, P., and Pringle, J.R. (1998). Additional modules for versatile and economical PCR-based gene deletion and modification in Saccharomyces cerevisiae. Yeast *14*, 953-961.

Lowery, J., Szul, T., Seetharaman, J., Jian, X., Su, M., Forouhar, F., Xiao, R., Acton, T.B., Montelione, G.T., Lin, H., *et al.* (2011). A novel C-terminal motif within the Sec7 domain of guanine nucleotide exchange factors regulates ARF binding and activation. J Biol Chem.

Manolea, F., Chun, J., Chen, D.W., Clarke, I., Summerfeldt, N., Dacks, J.B., and Melancon, P. (2010). Arf3 is activated uniquely at the trans-Golgi network by brefeldin A-inhibited guanine nucleotide exchange factors. Molecular biology of the cell *21*, 1836-1849.

Margarit, S.M., Sondermann, H., Hall, B.E., Nagar, B., Hoelz, A., Pirruccello, M., Bar-Sagi, D., and Kuriyan, J. (2003). Structural evidence for feedback activation by Ras.GTP of the Ras-specific nucleotide exchange factor SOS. Cell *112*, 685-695.

Matsuoka, K., Orci, L., Amherdt, M., Bednarek, S.Y., Hamamoto, S., Schekman, R., and Yeung, T. (1998). COPII-coated vesicle formation reconstituted with purified coat proteins and chemically defined liposomes. Cell *93*, 263-275.

Morinaga, N., Tsai, S.C., Moss, J., and Vaughan, M. (1996). Isolation of a brefeldin A-inhibited guanine nucleotide-exchange protein for ADP ribosylation factor (ARF) 1 and ARF3 that contains a Sec7-like domain. Proc Natl Acad Sci USA *93*, 12856-12860.

Novick, P., Field, C., and Schekman, R. (1980). Identification of 23 complementation groups required for post-translational events in the yeast secretory pathway. Cell *21*, 205-215.

Peyroche, A., Paris, S., and Jackson, C.L. (1996). Nucleotide exchange on ARF mediated by yeast Gea1 protein. Nature *384*, 479-481.

Rambourg, A., Clermont, Y., and Kepes, F. (1993). Modulation of the Golgi apparatus in Saccharomyces cerevisiae sec7 mutants as seen by three-dimensional electron microscopy. Anat Rec *237*, 441-452.

Robinson, J.S., Klionsky, D.J., Banta, L.M., and Emr, S.D. (1988). Protein sorting in Saccharomyces cerevisiae: isolation of mutants defective in the delivery and processing of multiple vacuolar hydrolases. Mol Cell Biol *8*, 4936-4948.

Sheen, V.L., Ganesh, V.S., Topcu, M., Sebire, G., Bodell, A., Hill, R.S., Grant, P.E., Shugart, Y.Y., Imitola, J., Khoury, S.J., *et al.* (2004). Mutations in ARFGEF2 implicate vesicle trafficking in neural progenitor proliferation and migration in the human cerebral cortex. Nature Genet *36*, 69-76.

Sikorski, R.S., and Hieter, P. (1989). A system of shuttle vectors and yeast host strains designed for efficient manipulation of DNA in Saccharomyces cerevisiae. Genetics *122*, 19-27.

Spang, A., Herrmann, J.M., Hamamoto, S., and Schekman, R. (2001). The ADP ribosylation factor-nucleotide exchange factors Gea1p and Gea2p have overlapping, but not redundant functions in retrograde transport from the Golgi to the endoplasmic reticulum. Mol Biol Cell *12*, 1035-1045.

Stalder, D., Barelli, H., Gautier, R., Macia, E., Jackson, C.L., and Antonny, B. (2011). Kinetic studies of the Arf activator Arno on model membranes in the presence of Arf effectors suggest control by a positive feedback loop. J Biol Chem *286*, 3873-3883.

Stearns, T., Kahn, R.A., Botstein, D., and Hoyt, M.A. (1990). ADP ribosylation factor is an essential protein in Saccharomyces cerevisiae and is encoded by two genes. Mol Cell Biol *10*, 6690-6699.

Venkateswarlu, K., Oatey, P.B., Tavare, J.M., and Cullen, P.J. (1998). Insulin-dependent translocation of ARNO to the plasma membrane of adipocytes requires phosphatidylinositol 3-kinase. Curr Biol *8*, 463-466.

Volpicelli-Daley, L.A., Li, Y., Zhang, C.J., and Kahn, R.A. (2005). Isoform-selective effects of the depletion of ADP-ribosylation factors 1-5 on membrane traffic. Mol Biol Cell *16*, 4495-4508.

INSIGHTS INTO SEC7 RECRUITMENT TO THE TRANS-GOLGI NETWORK

Overview

The Sec7 Arf-GEF is an important regulator of membrane trafficking at the *trans*-Golgi network (TGN). Sec7 is a peripheral membrane protein, and the proper localization of Sec7 to the TGN is essential for its function. Arf1-GTP helps recruit Sec7 to the TGN via the HDS1 domain; however, Arf1 is not the only factor that mediates the TGN localization of Sec7, as Sec7 is only slightly mislocalized in *arf1*Δ cells. The temperature-sensitive mutant *sec7-1* becomes cytoplasmic at 36°C. I have determined that the *sec7-1* mutant protein is capable of dimerization and can dimerize with wild-type Sec7 to regain proper localization to the TGN. I performed a screen for genes whose overexpression could rescue growth of *sec7-1* at the restrictive temperature using a galactose-induced expression library and have confirmed that overexpression of Ypt1, a Golgi-localized Rab GTPase, rescues the temperature sensitivity of the *sec7-1* mutant. Additionally, I have determined that loss of the HDS4 domain of Sec7 results in partial mislocalization to the cytoplasm.

Introduction

The Arf family of small GTPases control nearly all protein traffic out of the Golgi by recruiting effectors such as cargo adaptors, coat proteins, and lipid modifying enzymes (Donaldson and Jackson, 2011; Gillingham and Munro, 2007). The BIG/GBF families of Arf-GEFs activate Arf at the Golgi and are vital regulators of Golgi trafficking pathways in all eukaryotes (Casanova, 2007). However, the mechanisms of Arf-GEF recruitment and regulation at the Golgi remain poorly understood.

While we have gained insight into the mechanisms of Arf-GEF regulation and determined that Sec7 is recruited to the TGN by positive feedback, it is clear that other factors are involved in recruiting Sec7 to the TGN (Richardson et al., 2012). To gain further insight into Sec7 regulation, I took advantage of the *sec7-1* temperature sensitive mutant, which mislocalizes to the cytoplasm at higher temperatures. A dosage suppression screen has been successfully used to identify regulators of the GEF Sec2, which recruits the Rab GTPase Sec4 to secretory vesicles at the TGN. The screen identified Ypt31/32 as regulators of Sec2, and further investigation determined that Ypt32 recruits Sec2 to secretory vesicles, enabling Sec2 to activate Sec4 (Ortiz et al., 2002). I therefore used a similar approach to identify suppressors of the *sec7-1* mutant.

Here I report the results of a high copy suppressor screen for factors involved in recruiting Sec7 to the TGN. I screened for genes whose overexpression suppressed the growth defect of *sec7-1* at 36°C. One of the identified suppressors, *YPT1*, encodes a Rab GTPase involved in intra-Golgi and ER to Golgi trafficking. My findings confirm a previous study that identified Ypt1 as a high copy suppressor of *sec7-1* (Jones et al., 1999). The genetic interaction between Sec7 and Ypt1 suggests that Sec7 might be regulated by Ypt1 and hints at potential crosstalk between the Rab- and Arf-mediated trafficking pathways at the Golgi.

Results

Sec7 is recruited to the TGN through a positive feedback mechanism by binding to Arf1-GTP via its HDS1 domain; however, this interaction is only partially responsible for the TGN localization of Sec7 *in vivo*, as Sec7 is only slightly mislocalized in the absence of Arf1 (Richardson et al., 2012). Additional factors are likely to be involved in recruiting Sec7 to the TGN; therefore, I characterized the *sec7-1* temperature-sensitive mutant and performed a screen for genes that can rescue the growth of *sec7-1* at the restrictive temperature.

Mislocalization of sec7-1 is rescued by dimerization with wild-type Sec7

The BIG/GBF Arf-GEFs form homodimers in vivo, and this dimerization is at least partially mediated through the DCB (dimerization and cyclophilin binding) domain in the N-terminus (Ramaen et al., 2007). We sequenced the *sec7-1* mutant and found that it encodes an S402L substitution in the DCB domain. To establish whether this mutation disrupts the ability of *sec7-1* to dimerize, I compared the size of wild-type Sec7 to *sec7-1* by gel filtration chromatography and determined that *sec7-1* remains a homodimer; one caveat is that the experiment was performed at 4°C rather than at the restrictive temperature (Figure 3.1A). Thus, this mutation does not appear to affect the ability of *sec7-1* to homodimerize, and instead may disrupt an additional function of this domain that perhaps acts together with dimerization to achieve proper localization.

To confirm that the loss of TGN localization is not due to a loss of dimerization, I tested whether wild-type Sec7 could dimerize with *sec7-1* and bring it to the TGN. I determined that the presence of untagged, endogenously-expressed Sec7 rescued the mislocalization of GFP-*sec7-1* (Figure 3.1B). I then tested whether this rescue was a result of a dimerization interaction

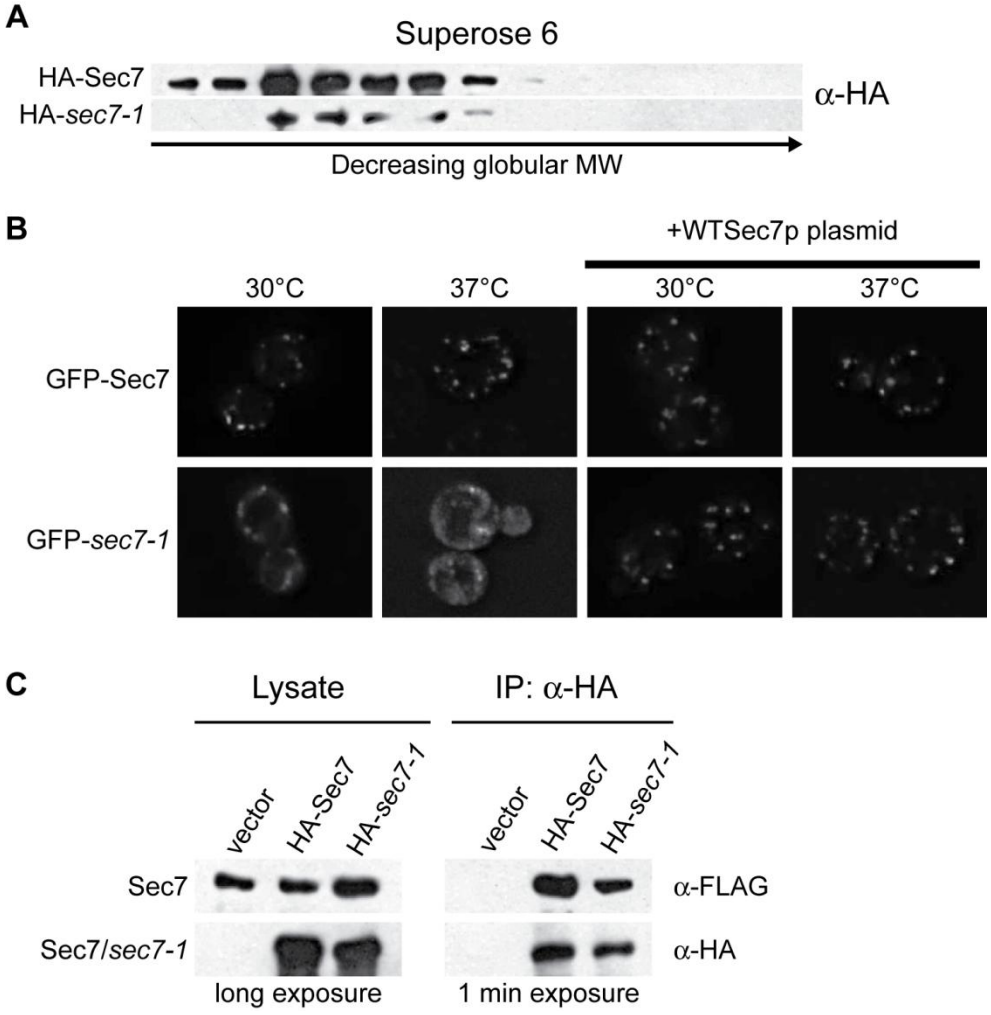

Figure 3.1: The *sec7-1* mutant affects localization without disrupting dimerization
(A) Gel filtration sizing of wild-type Sec7 and *sec7-1*. **(B)** Plasmid-borne wild-type Sec7 rescued the localization of GFP-*sec7-1*, but loss of Sec7 via 5-FOA plasmid shuffling resulted in mislocalization of *sec7-1*. **(C)** Wild-type FLAG-tagged Sec7 co-immunoprecipitates with either HA-tagged Sec7 or HA-tagged *sec7-1*.

between the wild-type Sec7p and *sec7-1*p, and found that Sec7 co-immunoprecipitates with *sec7-1* (Figure 3.1C). Taken together, these data suggest that *sec7-1* is in the proper conformational and dimerization state, indicating that the mutation specifically affects localization. Therefore, the *sec7-1* allele is an ideal candidate for a dosage suppression screen.

A high copy suppressor screen for genes that rescue sec7-1

To identify factors involved in Sec7 localization, I performed a genetic screen for high copy suppressors of *sec7-1* temperature sensitivity using a *GAL1*-regulated cDNA expression library, which contains plasmids carrying oriented yeast cDNAs under the control of the inducible *GAL1* promoter. Approximately 50,000 transformants were plated and incubated at 36°C, yielding 11 colonies that grew at the restrictive temperature. Genes were successfully identified for 10 of the 11 isolated colonies, representing five unique suppressors: *YPT1*, *SMY1*, *YCP4*, *CDC43*, and *SGT2* (Table 3.1). My results confirm a previous study in which overexpression of *YPT1* via a 2-μm plasmid rescued the growth of a *sec7-1* strain (Jones et al., 1999). The gene-containing plasmids were retransformed into the *sec7-1* strain to confirm suppression of the *sec7-1* temperature sensitivity (Figure 3.2). Only *SMY1* overexpression failed to rescue the growth of *sec7-1* cells. One explanation for this is that the *SMY1* isolates contained a second cDNA-containing plasmid; one of the three isolated *SMY1* colonies was confirmed to contain a second plasmid carrying *VMA3*, which encodes a subunit of the vacuolar H(+)-ATPase.

I also attempted to assess the ability of the isolated suppressors to rescue the localization defect of GFP-*sec7-1*. However, growth in galactose-containing medium appeared to affect the localization of GFP-*sec7-1* in this strain background, and this analysis proved to be uninformative (data not shown).

Table 3.1: Genes identified from a high copy suppressor screen

Gene	# of isolated colonies	Protein description
Ycp4	4	Unknown function; has structural similarity to flavodoxins
Smy1	3	Kinesin-like myosin passenger-protein; interacts with Myo2 and controls actin cable structure and dynamics
Ypt1	1	Small GTPase of the Rab family; involved in trafficking pathways at the Golgi
Cdc43	1	Beta subunit of geranylgeranyltransferase type I; catalyzes geranylgeranylation to the cysteine residue in proteins containing a C-terminal CaaX sequence
Sgt2	1	Glutamine-rich cytoplasmic co-chaperone; serves as a scaffold for factors that mediate posttranslational insertion of tail-anchored proteins into the ER membrane

*Protein descriptions modified from yeastgenome.org

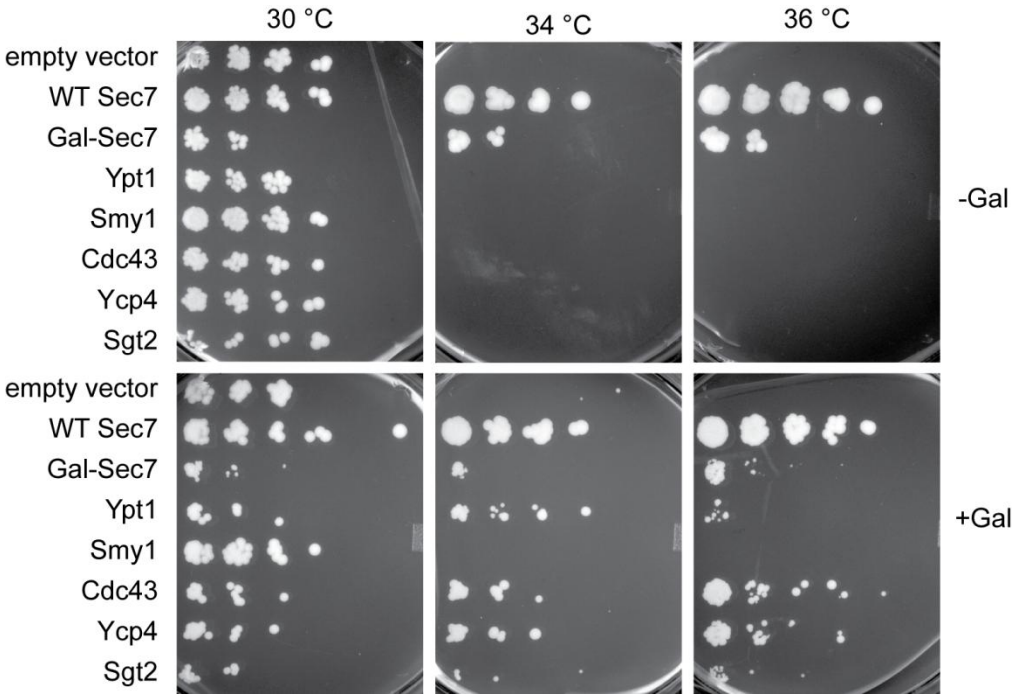

Figure 3.2: High copy suppression of *sec7-1* temperature sensitivity
Overexpression of isolated gene-containing plasmids in cells carrying the *sec7-1* mutant allele. Suppression by the isolated *SMY1*-containing plasmid was not confirmed.

The HDS4 domain mediates Sec7 localization to the trans-Golgi network

Our previous results have demonstrated that deletion of the HDS2-4 domains from the C-terminus of Sec7 results in a partial cytoplasmic mislocalization, while deletion of the entire C-terminus results in a complete loss of TGN punctae (Richardson et al., 2012). To further characterize the role of the C-terminal HDS domains in Sec7 localization, I examined GFP-tagged constructs of two further Sec7 constructs: the first comprises residues 1-1799 and lacks the HDS4 domain (Sec7ΔHDS4), and the second comprises residues 1-1515 and lacks both the HDS3 and HDS4 domains (Sec7ΔHDS3/4) (Figure 3.3A). Similar to Sec7ΔC+HDS1, both Sec7ΔHDS4 and Sec7ΔHDS3/4 displayed partial mislocalization to the cytoplasm while still retaining localization to TGN punctae (Figure 3.3B). Thus, the HDS4 domain is necessary for the full localization of Sec7 to the TGN.

Discussion

Using a high copy suppressor screen, I have confirmed that *YPT1* is a suppressor of the *sec7-1* mutation. The small GTPase Ypt1 is another important regulator of Golgi trafficking events and is involved in tethering incoming ER-derived and intra-Golgi vesicles (Bacon et al., 1989; Cao et al., 1998; Segev, 1991; Suvorova et al., 2002). While this genetic interaction had been previously identified (Jones et al., 1999), no further studies of the connection between Ypt1 and Sec7 or the implications of this connection for the Rab and Arf pathways at the Golgi have been conducted. The nature of the connection between Ypt1 and Sec7 will be explored in greater detail in the following chapter.

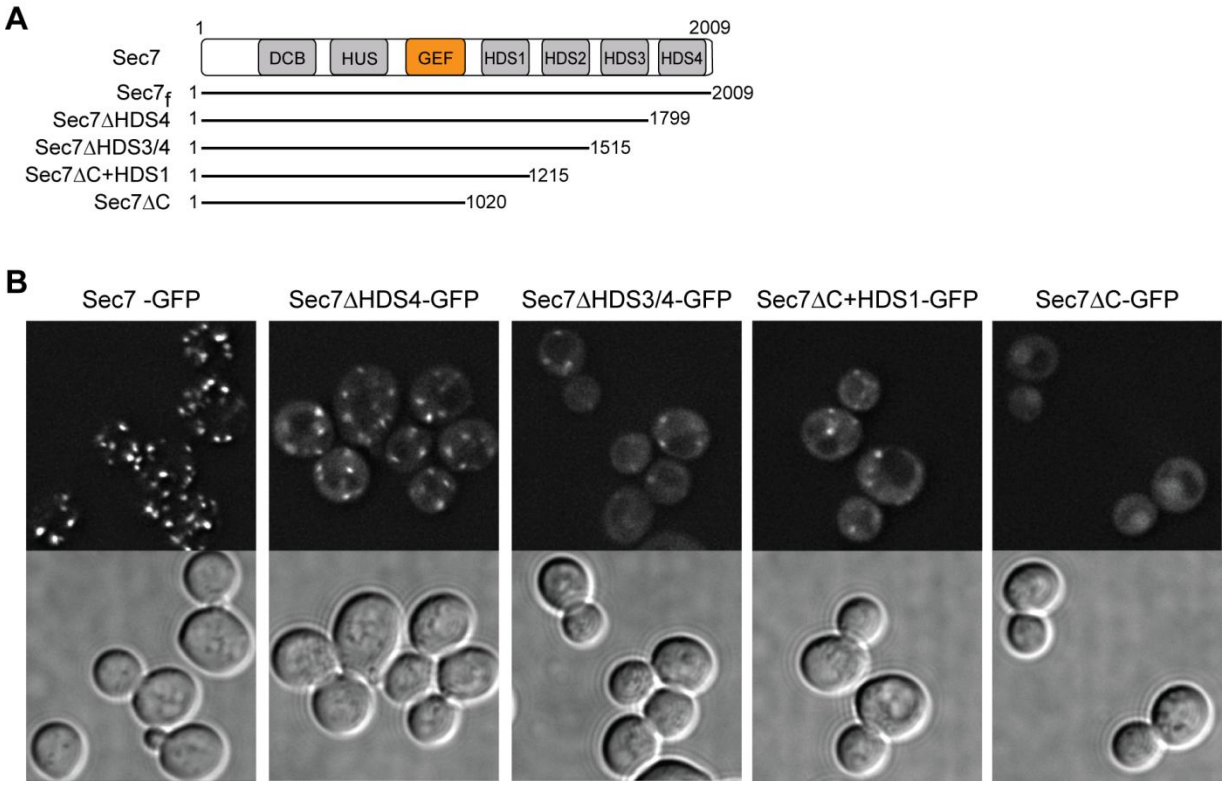

Figure 3.3: Localization of GFP-tagged Sec7 truncation constructs
(A) Schematic diagram of the truncated Sec7 constructs **(B)** Localization of plasmid-borne GFP-tagged Sec7 truncations in cells expressing the endogenous *SEC7* gene.

Several factors could have limited the recovery of suppressors from this screen. First, while my screen recovered a previously identified suppressor of *sec7-1*, *SEC7* itself was not recovered. Increasing the number of transformants may yield further *sec7-1* suppressors, including *SEC7* itself. I confirmed by PCR that *SEC7* was represented in the library; however, overexpression of *SEC7* is detrimental to yeast viability, and overexpression of *SEC7* in the *sec7-1* strain only weakly suppressed the growth phenotype (Figure 3.2). Second, the *sec7-1* mutation may disrupt the binding sites of regulatory proteins and prevent their association with Sec7. Therefore, it is possible that other suppressors were missed by my screen. Performing a targeted screen of known Golgi-localized proteins may yield additional regulators of Sec7 that were missed by this screen.

Methods

Plasmids and strains

Plasmids and strains were constructed using standard techniques and are described in Table 3.2 and Table 3.3, respectively.

Antibodies

The anti-FLAG monoclonal "M2" antibody was purchased from Sigma, and the anti-HA monoclonal antibody "12CA5" was purchased from Roche.

Gel filtration chromatography

Strains carrying either wild-type Sec7 or *sec7-1* were grown to log phase at 30°C and then shifted to 37°C for 1 hour before pelleting. Cells were resuspended in 1 mL lysis buffer (1x PBS, 10mM DTT, 1x Roche protease inhibitor cocktail) and mechanically disrupted by bead-beating (500 uL glass beads). Cell lysates were cleared two times by centrifugation at 14,000 g for 5 minutes at 4°C, then run over a gel filtration column at 4°C (Superose 6 10/30 GL, GE Healthcare). Proteins from sequential fractions were separated by SDS-PAGE and analyzed by immunoblot.

Immunoprecipitations

Cell pellets (25 OD-equivalents of log-phase cells) were resuspended in 1 mL of lysis buffer (50 mM Tris pH 7.5, 150 mM NaCl, 0.2% NP-40, 5 mM EDTA, 1 mM PMSF, 1X Roche protease inhibitor cocktail). The cell suspensions were mechanically disrupted by bead-beating (500 µl glass beads), and the lysates were cleared by centrifugation at 14,000 g for 5 minutes at

Table 3.2: Plasmids used in this study
Plasmids are listed, along with a description and the source.

Name	Description	Vector Backbone	Source
pRS415	centromeric LEU2 plasmid		(Sikorski and Hieter, 1989)
pRS416	centromeric URA3 plasmid		(Sikorski and Hieter, 1989)
Gal1-Sec7	Yeast ORF collection clone with Gal1 promoter, URA3 plasmid	BG1805-amp	Open Biosystems
pCF1043	*SEC7* (includes ~1 kB of 5'UTR)	pRS416	(Richardson et al., 2012)
pCF1101	3x-HA-Sec7 driven by P_{SEC7}	pRS415	(Richardson et al., 2012)
pCF1085	3x-HA-*sec7-1* driven by P_{SEC7}	pRS415	this study
pCF1084	GFP-Sec7 driven by P_{SEC7}	pRS415	(Richardson et al., 2012)
pCF1105	GFP-*sec7-1* driven by P_{SEC7}	pRS415	this study
pCF1140	GFP-Sec7ΔC (residues 1-1020) driven by P_{SEC7}	pRS415	(Richardson et al., 2012)
pCF1141	GFP-Sec7ΔC+HDS1 (residues 1-1215) driven by P_{SEC7}	pRS415	(Richardson et al., 2012)
pCF1156	GFP-Sec7ΔHDS2/3 (residues 1-1250) drive by P_{SEC7}	pRS415	this study
pCF1157	GFP-Sec7ΔHDS4 (residues 1-1799) driven by P_{SEC}	pRS415	this study
pCM21	plasmid isolated from *GAL1* library carrying Ycp4		this study
pCM22	plasmid isolated from *GAL1* library carrying Smy1		this study
pCM23	plasmid isolated from *GAL1* library carrying Ypt1		this study
pCM24	plasmid isolated from *GAL1* library carrying Cdc43		this study
pCM25	plasmid isolated from *GAL1* library carrying Sgt2		this study

Table 3.3: Yeast strains used in this study
Strains are listed, along with the genotype and the source.

Name	Genotype	(Strain construction method)	Source
SEY6210	*MATα his3-Δ200 leu2-3,112 lys2-801 trp1-Δ901 ura3-52 suc2-Δ9*		(Robinson et al., 1988)
SEY6210.1	*MATa his3-Δ200 leu2-3,112 lys2-801 trp1-Δ901 ura3-52 suc2-Δ9*		(Robinson et al., 1988)
RSY298	*MATa, ade2-1 his3-11,15 leu2-3,112 trp1-1 ura3-1 sec7-1*		R. Schekman
BY4742	*MATα his3-Δ1 leu2-Δ0 lys2-Δ0 ura3-Δ0*		(Brachmann et al., 1998)
CFY362	SEY6210.1 *SEC7-3xFLAG-6XHis::TRP1*	(PCR integration into SEY6210.1)	This study
CFY409	BY4742 sec7Δ::KANMX +pCF1043		(Richardson et al., 2012)

4°C. The supernatants were incubated with 10 ul of anti-HA resin (Sigma) for four hours at 4ºC. The resin was washed three times with lysis buffer before the addition of 15 µl sample buffer. Samples were heated to 55ºC for 15 minutes before separation by SDS-PAGE and immunoblot analysis.

High copy suppressor screen

The high copy suppressor screen was performed screen using a *GAL1*-regulated cDNA expression library, which contains plasmids carrying oriented yeast cDNAs under the control of the *GAL1* promoter (Liu et al., 1992). The *sec7-1* strain (*MATa, ade2-1; his3-11,15; leu2-3,112; trp1-1; ura3-1*) was grown in raffinose liquid medium and transformed with the cDNA library. Cells were plated onto selective media at a density of ~100 colonies per plate. Transformants were replica plated onto selective media containing either glucose or galactose and screened for growth at 35°C. To confirm that suppression was dependent on the cDNA-carrying plasmid, suppressors were streaked onto galactose plates containing 5-FOA to select for loss of the plasmid and tested for growth at 35°C. Plasmids from confirmed suppressors were isolated from yeast using the Zymoprep Yeast Plasmid Miniprep Kit and then amplified in bacteria. The cDNA inserts were amplified by PCR and sequenced to identify the gene(s) responsible for the suppression.

Microscopy

Cells were grown in synthetic dropout media and imaged in log phase (OD_{600} ~ 0.5) after spotting onto coverslips in growth media. Live cells were imaged at room temperature using a DeltaVision RT wide-field deconvolution microscope (Applied Precision) with a PlanApo 100x

objective (1.35 NA; Olympus) and a digital camera (Cool Snap HQ; Photometrics). Acquired images acquired were deconvolved ("conservative" setting, 6 cycles), and single deconvolved focal planes are shown. Exposure times and image processing were identical for each sample within an experiment, and light levels were scaled equivalently among all samples within an experiment when processed within ImageJ (adjusting only light level min/max settings for clarity).

REFERENCES

Bacon, R.A., Salminen, A., Ruohola, H., Novick, P., and Ferro-Novick, S. (1989). The GTP-binding protein Ypt1 is required for transport in vitro: the Golgi apparatus is defective in ypt1 mutants. J Cell Biol *109*, 1015-1022.

Cao, X., Ballew, N., and Barlowe, C. (1998). Initial docking of ER-derived vesicles requires Uso1p and Ypt1p but is independent of SNARE proteins. EMBO J *17*, 2156-2165.

Casanova, J.E. (2007). Regulation of Arf activation: the Sec7 family of guanine nucleotide exchange factors. Traffic *8*, 1476-1485.

Donaldson, J.G., and Jackson, C.L. (2011). ARF family G proteins and their regulators: roles in membrane transport, development and disease. Nature reviews Molecular cell biology *12*, 362-375.

Gillingham, A.K., and Munro, S. (2007). The small G proteins of the Arf family and their regulators. Annual review of cell and developmental biology *23*, 579-611.

Jones, S., Jedd, G., Kahn, R.A., Franzusoff, A., Bartolini, F., and Segev, N. (1999). Genetic interactions in yeast between Ypt GTPases and Arf guanine nucleotide exchangers. Genetics *152*, 1543-1556.

Liu, H., Krizek, J., and Bretscher, A. (1992). Construction of a GAL1-regulated yeast cDNA expression library and its application to the identification of genes whose overexpression causes lethality in yeast. Genetics *132*, 665-673.

Ortiz, D., Medkova, M., Walch-Solimena, C., and Novick, P. (2002). Ypt32 recruits the Sec4p guanine nucleotide exchange factor, Sec2p, to secretory vesicles; evidence for a Rab cascade in yeast. J Cell Biol *157*, 1005-1015.

Ramaen, O., Joubert, A., Simister, P., Belgareh-Touze, N., Olivares-Sanchez, M.C., Zeeh, J.C., Chantalat, S., Golinelli-Cohen, M.P., Jackson, C.L., Biou, V., *et al.* (2007). Interactions between conserved domains within homodimers in the BIG1, BIG2, and GBF1 Arf guanine nucleotide exchange factors. The Journal of biological chemistry *282*, 28834-28842.

Richardson, B.C., McDonold, C.M., and Fromme, J.C. (2012). The Sec7 Arf-GEF is recruited to the trans-Golgi network by positive feedback Dev Cell *22*, 799-810.

Segev, N. (1991). Mediation of the attachment or fusion step in vesicular transport by the GTP-binding Ypt1 protein. Science *252*, 1553-1556.

Suvorova, E.S., Duden, R., and Lupashin, V.V. (2002). The Sec34/Sec35p complex, a Ypt1p effector required for retrograde intra-Golgi trafficking, interacts with Golgi SNAREs and COPI vesicle coat proteins. The Journal of cell biology *157*, 631-643.

CHAPTER 4

FOUR GTPASES DIFFERENTIALLY REGULATE THE SEC7 ARF-GEF TO DIRECT TRAFFIC AT THE *TRANS*-GOLGI NETWORK[2]

Overview

Traffic through the Golgi complex is controlled by small GTPases of the Arf and Rab families. Guanine nucleotide exchange factor (GEF) proteins activate these GTPases to control Golgi function, yet the full assortment of signals regulating these GEFs is unknown. The Golgi Arf-GEF Sec7 and the homologous BIG1/2 proteins are effectors of the Arf1 and Arl1 GTPases. We demonstrate that Sec7 is also an effector of two Rab GTPases, Ypt1 (Rab1) and Ypt31/32 (Rab11), signifying unprecedented signaling cross-talk between GTPase pathways. The molecular basis for the role of Ypt31/32 and Rab11 in vesicle formation has remained elusive. We find that Arf1, Arl1, and Ypt1 primarily affect the membrane localization of Sec7, whereas Ypt31/32 exerts a dramatic stimulatory effect on the nucleotide exchange activity of Sec7. The convergence of multiple signaling pathways on a master regulator reveals a mechanism for balancing incoming and outgoing traffic at the Golgi.

[2] Parts of this chapter will be published in McDonold, C.M., and Fromme, J.C. (2014). Four GTPases differentially regulate the Sec7 Arf-GEF to direct traffic at the *trans*-Golgi network. Dev Cell (accepted).

Introduction

The Golgi complex is the primary sorting organelle of the eukaryotic secretory pathway. Traffic through the Golgi depends on the action of small GTPases of the Arf and Rab families (Barr, 2009; Donaldson and Jackson, 2011). Arf proteins primarily regulate outgoing vesicle biogenesis pathways by recruiting vesicle coat proteins and lipid-modifying enzymes. Rab proteins primarily regulate the transport, tethering, and fusion of incoming vesicles. Notable exceptions include Rab6 and the Rab11 homologs Ypt31/32, which also appear to play direct roles in vesicle biogenesis (Benli et al., 1996; Jedd et al., 1997; Miserey-Lenkei et al., 2010), although the role of Ypt31/32 in vesicle biogenesis is unknown. GEFs activate Arf and Rab proteins to govern incoming and outgoing traffic at the Golgi (Mizuno-Yamasaki et al., 2012), but it is unknown how these GEFs are regulated by organelle status and cargo flux. In particular, there is scant evidence of significant coordination between Arf and Rab pathways at the Golgi.

Multiple Arf-dependent vesicle pathways sort cargos from the trans-Golgi network (TGN) to endosomes, the lysosome, and the plasma membrane (PM). Cargo sorting at the TGN depends upon Arf activation by the Arf-GEF Sec7 in yeast and its homologs BIG1/2 in mammalian cells (Casanova, 2007). Sec7 is regulated through positive feedback by Arf1 (Richardson et al., 2012), and BIG1/2 is regulated by both Arf and Arl1 GTPases (Christis and Munro, 2012; Lowery et al., 2013).

Here I report that in addition to being an effector of Arf1 and Arl1, Sec7 is also an effector of two Rab proteins, Ypt1 (Rab1) and Ypt31/32 (Rab11). Therefore, four distinct GTPases directly regulate Sec7. I show that Ypt1 primarily affects the localization of Sec7 and exerts a modest affect on Sec7 activity. In contrast, Ypt31/32 exerts a dramatic stimulatory effect on the activity of Sec7. TGN cargo sorting in yeast appears to occur sequentially, and levels of

Ypt31/32 peak during cargo sorting. Disrupting either Ypt31/32 function or decreasing Golgi Arf levels lowers the fidelity of cargo sorting, but to different extents. These findings indicate that Ypt31/32 stimulation of Sec7 activity is a critical driver of cargo sorting at the TGN, providing an explanation for the role of Ypt31/32 and Rab11 family members in vesicle biogenesis. Given the roles of Arl1 and Ypt1 in vesicle tethering, I propose that Sec7 serves as a master regulator to balance incoming and outgoing traffic at the Golgi.

Results

Sec7 localization and activity is regulated by several conserved C-terminal HDS (Homology Downstream of Sec7) domains. The HDS1 domain exerts an autoinhibitory effect that is relieved by binding to Arf1-GTP on the membrane surface. The HDS2-4 domains are also autoinhibitory, but it is unknown how this autoinhibition is relieved (Richardson et al., 2012). An unknown protein might bind to this region to relieve autoinhibition; therefore, I performed a targeted screen of candidate Golgi-localized proteins, testing for factors that either affected Sec7 membrane localization in vivo or could recruit Sec7 to membranes *in vitro*.

Sec7 is an effector of the Ypt1 and Ypt31/32 Rab GTPases

Both Rab and Arf GTPases are active at membrane surfaces. Using purified membrane-anchored GTPases to mimic the physiological context of Rab and Arf function, we found that both Ypt1 and Ypt31 Rab proteins recruited a purified Sec7 construct, $Sec7_f$ (encoding residues 203-2009, the essential primary sequence (Richardson et al., 2012)), to liposomes in a nucleotide-dependent manner (Figures 4.1A and 4.2A-D). Arl1 also recruited $Sec7_f$ to liposomes

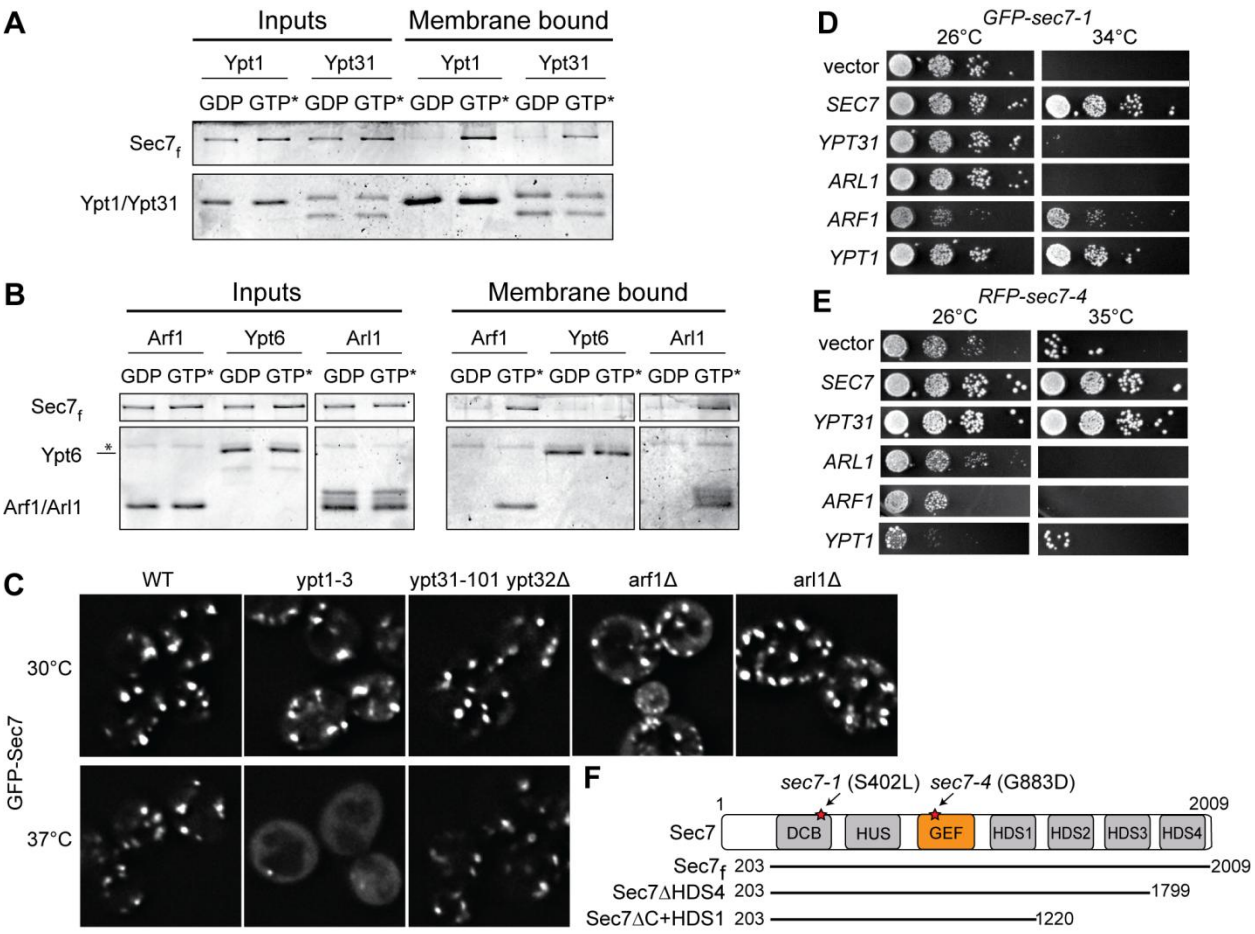

Figure 4.1: Sec7 is an effector of four different Golgi GTPases.
(A) Liposome flotation assays showing activated Ypt1 and Ypt31 recruit purified $Sec7_f$ to liposomes. GTP* = GMP-PNP (active GTPase). **(B)** Activated Arf1 and Arl1, but not Ypt6, recruit purified $Sec7_f$ to liposomes. *, contaminant. Purified Rab GTPases bind to membranes regardless of their nucleotide state via a 7xHis tag, which is not present on purified Arf1 or Arl1. **(C)** Localization of an extra copy of GFP-Sec7 in yeast cells harboring the indicated mutations. For temperature-sensitive mutants, images are shown for both permissive (30°C) and restrictive (37°C) temperatures. **(D-E)** Overexpression of indicated GTPases via 2-μm plasmids in temperature-sensitive yeast cells carrying (D) GFP-*sec7-1* or (E) RFP-*sec7-4* mutant alleles. **(F)** Schematic diagram of the Sec7 conserved domain structure and Sec7 truncated constructs; stars denote the approximate locations of the specified mutations. See also Figure 4.2.

Figure 4.2: Purified proteins and localization of Sec7-GFP in mutant strains.

(A) 15% SDS-PAGE gel of 0.5 μg of each purified GTPase. The faster-migrating species in some of the preparations is likely due to proteolysis at the N-terminus, consistent with the disordered N-terminus of yeast Ypt31 (Ignatev et al., 2008). **(B)** 8% SDS-PAGE gel of 1.5 μg of each purified Sec7 construct. **(C)** anti-His immunoblot of purified GTPases. **(D)** anti-His immunoblot of purified GEF constructs before and after TEV cleavage to remove the 6xHis tag (pre-TEV sample for Sec7ΔC+HDS1 not shown).

(E) Localization of an extra copy of GFP-Sec7 in yeast strains harboring the indicated gene deletions or temperature-sensitive mutations. Of the 20 strains tested, the mutants with at least partial cytoplasmic mislocalization are: *ypt1-3*, *arf1*Δ, *arl3*Δ, *sys1*Δ, *trs33*Δ, *trs85*Δ, *ypt6*Δ, and *gyp6*Δ. Certain strains exhibited a brighter GFP-Sec7 signal (*arl1*Δ*, arl3*Δ*, drs2*Δ*, gyp2*Δ*, gmh1*Δ*, sys1*Δ*, syt1*Δ), presumably due to upregulated expression. Although knockdown of Arl1 in metazoan cells results in mislocalization of BIG1/2 (Christis and Munro, 2012), GFP-Sec7 is not significantly mislocalized to the cytoplasm in *arl1*Δ yeast cells. This result was also observed previously (Setty et al., 2004). **(F)** Co-localization analysis with Sys1-DsRed confirms that the GFP-Sec7 punctae correspond to Golgi compartments. Sys1 is a resident Golgi transmembrane protein that partially co-localizes with Sec7, but some DsRed signal is also visible in the cytoplasm (presumably due to partial proteolysis of the fusion protein) and the vacuole. The GFP channel in (F) and (G) is shown at different light levels compared to (E), for clarity of colocalization.

(G) Same as in (F), for GFP-tagged Sec7 alleles after 30 min at 37°C. Note that Sys1 appears to accumulate in enlarged structures after perturbation of Sec7 function, especially in the GFP-*sec7-1* strain. Experiments in (F) and (G) were performed by Chris Fromme.

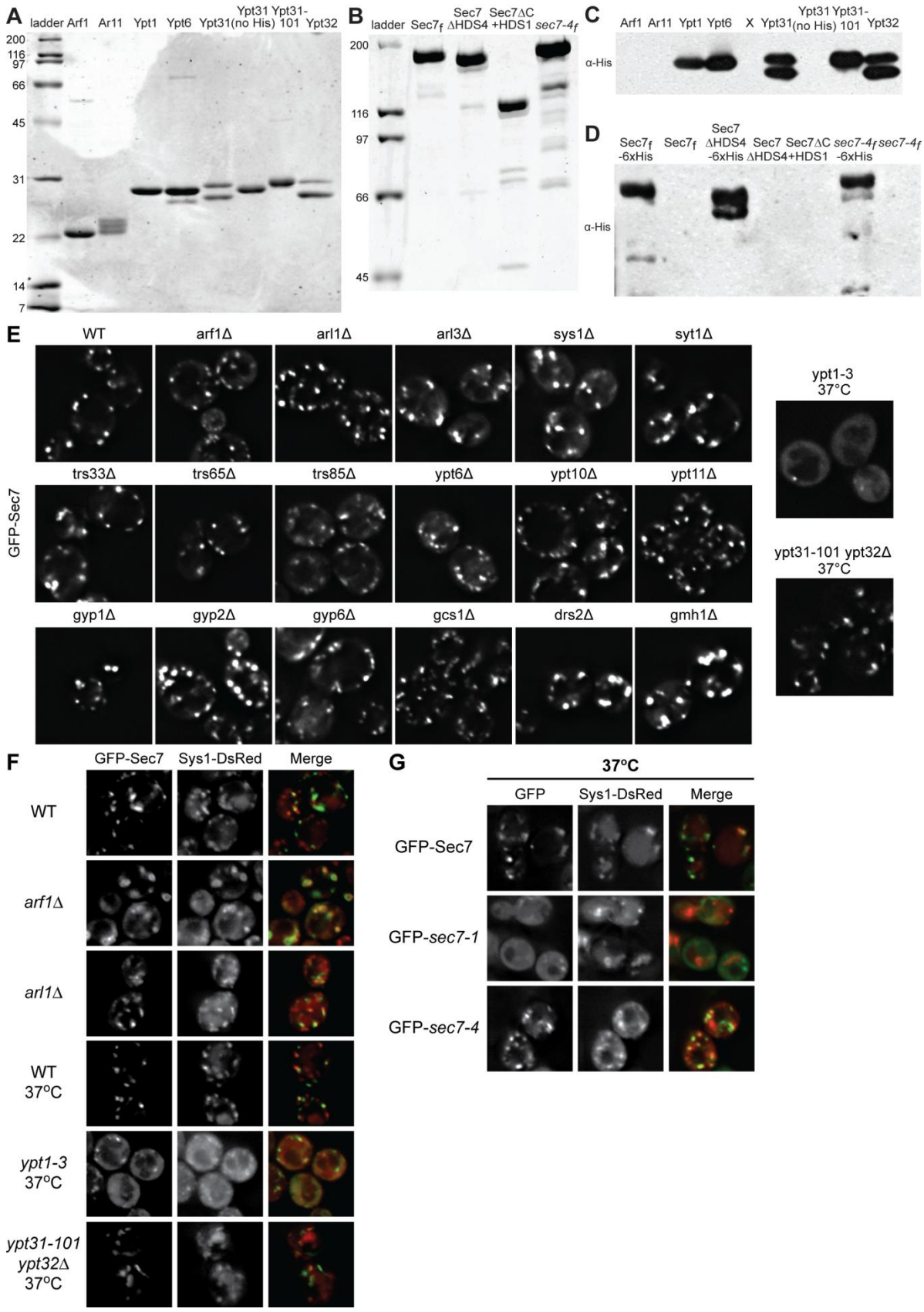
A
ladder Arf1 Ar11 Ypt1 Ypt6 Ypt31 Ypt31(no His) Ypt31-101 Ypt32
200
116
97
66
45
31
22
14
7
B
ladder Sec7f Sec7 ΔHDS4 Sec7ΔC +HDS1 sec7-4f
200
116
97
66
45
C
Arf1 Ar11 Ypt1 Ypt6 X Ypt31 Ypt31(no His) Ypt31-101 Ypt32
α-His
D
Sec7f -6xHis
Sec7f
Sec7 ΔHDS4 -6xHis
Sec7 ΔHDS4+HDS1
Sec7ΔC
sec7-4f -6xHis
sec7-4f
α-His
E
WT
arf1Δ
arl1Δ
arl3Δ
sys1Δ
syt1Δ
trs33Δ
trs65Δ
trs85Δ
ypt6Δ
ypt10Δ
ypt11Δ
GFP-Sec7
gyp1Δ
gyp2Δ
gyp6Δ
gcs1Δ
drs2Δ
gmh1Δ
ypt1-3 37°C
ypt31-101 ypt32Δ 37°C
F
GFP-Sec7
Sys1-DsRed
Merge
WT
arf1Δ
arl1Δ
WT 37°C
ypt1-3 37°C
ypt31-101 ypt32Δ 37°C
G
37°C
GFP
Sys1-DsRed
Merge
GFP-Sec7
GFP-sec7-1
GFP-sec7-4

(Figure 4.1B), confirming the conservation of the interaction between Arl1 and BIG1/2 (Christis and Munro, 2012). Another Golgi-localized Rab, Ypt6, did not recruit $Sec7_f$ to liposomes. This result, together with the observed nucleotide-dependence, establishes the specificity of the interactions (Figure 4.1B).

We imaged Sec7 in mutant strains (Figure 4.2E) to assess the importance of these interactions for localization to the TGN. Sec7-GFP was largely mislocalized to the cytoplasm in a *ypt1-3* temperature sensitive (ts) strain at the restrictive temperature (Figures 4.1C and 4.2F); however, this mutation has many effects on the Golgi, so it is possible that this effect is indirect. Sec7-GFP exhibited normal localization in *ypt31-101 ypt32*Δ cells at the restrictive temperature (Figures 4.1C and 4.2F), indicating that the Ypt31/32 interaction is not required for Sec7 localization to the TGN membrane.

A previous study found allele-specific genetic interactions between Sec7 and both Ypt1 and Ypt31/32: overexpression of Ypt1 suppressed the ts-growth phenotype of the *sec7-1* mutant, and overexpression of Ypt31 or Ypt32 suppressed the ts-growth phenotype of the *sec7-4* mutant (Jones et al., 1999). We confirmed these results and also tested whether overexpression of the other Sec7-interacting proteins, Arf1 and Arl1, was able to suppress the growth phenotypes. Arf1 overexpression partially suppressed the *sec7-1* but not the *sec7-4* mutant (Figure 4.1D,E); interpretation of this result is complicated because Arf1-GTP is both a regulator and product of Sec7. The *sec7-4* mutant encodes a G883D substitution within the catalytic GEF domain (Deitz et al., 2000), and the isolated GEF domain harboring this mutation exhibits reduced catalytic activity (Jones et al., 1999). We sequenced the *sec7-1* mutant and determined that it encodes a single S402L amino acid substitution in the DCB (Dimerization and Cyclophilin Binding) domain (Figure 4.1F).

At the restrictive temperature, we observed that GFP-*sec7-4* localized to punctate structures similar to the TGN localization of wild-type GFP-Sec7. In contrast, GFP-*sec7-1* was mislocalized to the cytoplasm under the same conditions (Figures 4.3A and 4.2G). Remarkably, overexpression of Ypt1 suppressed the mislocalization phenotype of GFP-*sec7-1*, restoring the punctate appearance (Figure 4.3B). The primary established role of Ypt1 is to regulate the tethering of ER-derived vesicles with the cis-Golgi (Bacon et al., 1989; Cao et al., 1998; Segev, 1991; Wang et al., 2000). However, Ypt1 alleles that specifically affect fusion of endosomal vesicles with the late Golgi have been described (Sclafani et al., 2010), providing evidence that Ypt1 acts at both early and late Golgi compartments. Our results suggest that Ypt1 also plays a role in Sec7 localization to the TGN through a direct physical interaction.

Mutations in the SEC7 or YPT31/32 genes result in similar enlarged Golgi morphology phenotypes (Benli et al., 1996; Jedd et al., 1997; Novick et al., 1980). Given the suppression of the *sec7-4* growth defect by Ypt31/32 overexpression, we tested whether Ypt31/32 could alleviate the catalytic deficiency of the *sec7-4* mutant. We introduced the *sec7-4* mutation into the purified $Sec7_f$ construct (Figure 4.2B). Using an *in vitro* GEF activity assay measuring the kinetics of Arf1 activation, we observed that the *sec7-4*$_f$ mutant protein exhibits considerably reduced catalytic activity relative to the wild-type protein at the permissive temperature (30°C) (Figure 4.3C,D). Arf1 activation by *sec7-4*$_f$ displayed sigmoidal kinetics (Figure 4.3C), indicative of a positive feedback effect under these conditions. Strikingly, the presence of activated Ypt31 in the reaction increased the activity of *sec7-4*$_f$ to a level exceeding that of the wild-type $Sec7_f$ construct (Figure 4.3D). Ypt31 also exerted a strong stimulatory effect on the activity of the wild-type $Sec7_f$ protein (Figures 4.3D and 4.4A). These data indicate that overexpression of Ypt31/32 suppressed the *sec7-4* growth defect by rescuing its catalytic

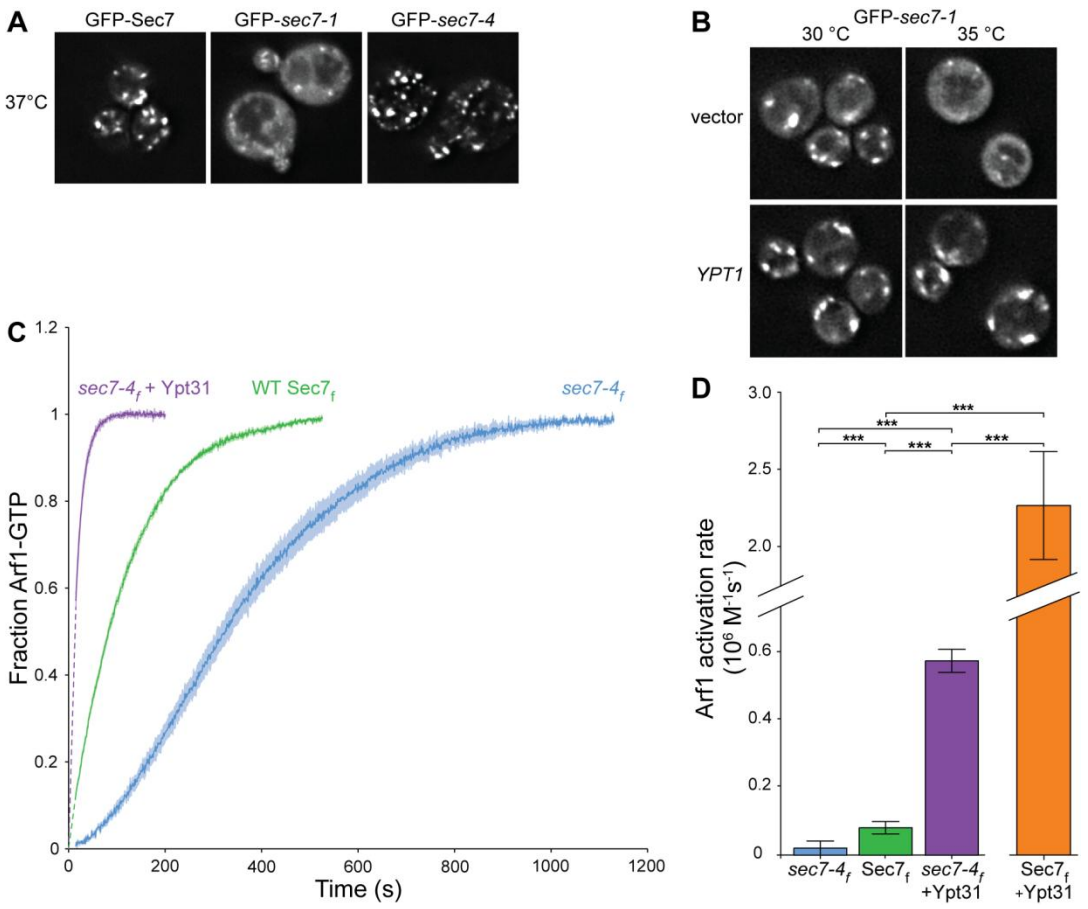

Figure 4.3: Overexpression of Ypt1 and Ypt31 rescues Sec7 allele-specific phenotypes.
(A) Localization of GFP-tagged Sec7, *sec7-1*, and *sec7-4* after 20 min incubation at restrictive temperature (37°C). **(B)** Localization of GFP-*sec7-1* in cells overexpressing Ypt1 at both permissive (30°C) and restrictive (35°C) temperatures. **(C)** Activation of Arf1 (measured via tryptophan fluorescence) by 100 nM WT $Sec7_f$, $sec7\text{-}4_f$, or $sec7\text{-}4_f$ in the presence of 500 nM activated Ypt31. Dark lines represent the average of 3 normalized reactions; lighter shaded areas represent the corresponding 95% confidence intervals (CI); dashed lines represent data not captured but inferred from curve-fitting.
(D) Quantification of Arf1 activation rates from curves in (C). Data for WT $Sec7_f$ + Ypt31 is included for comparison. The activation curve for this sample is not shown in (C) because it was acquired using a different concentration (30 nM) of the GEF. Error bars represent 95% CIs for n=3.

activity. Taken together, our results demonstrate that Sec7 is an effector of both Ypt1 and Ypt31/32 and that these interactions are physiologically relevant.

The four GTPase regulators exert different effects on Sec7 activity

To gain mechanistic insight into the regulation of Sec7, we compared the activity of $Sec7_f$ in the presence of each regulator. Ypt31 and Ypt32 exerted a strong stimulatory effect on $Sec7_f$, and Ypt1 also stimulated $Sec7_f$ to a significant degree (Figures 4.4A and 4.5A-D). Ypt6 had no effect on $Sec7_f$ activity (Figure 4.5B). Stimulation by Arf1 is most evident at higher concentrations of Arf1 or when the autoinhibitory HDS2-4 domains are removed (Figure 4.4B and (Richardson et al., 2012)). The stimulatory effect of Ypt31 was dependent upon nucleotide activation and was reduced by introduction of the *ypt31-101* mutation (Figure 4.4C,D). These results establish Ypt31/32 as a potent regulator of Sec7 catalytic activity.

Removing the membrane anchor from Ypt31 eliminated its stimulatory activity (Figure 4.4D). This result indicates that either proximity of the Rab to the membrane is important for this effect or that the Sec7-Ypt31 interaction is diminished if Ypt31 is not membrane anchored.

Ypt1 and Ypt31 both require the HDS2-3 domains for binding to $Sec7_f$, suggesting that they bind directly to this region (Figure 4.4E,F). The effects of Ypt1 and Ypt31 combine to generate an additive stimulatory effect (Figure 4.5E), implying that Ypt1 and Ypt31 bind simultaneously to different sites within the HDS2-3 domains.

Removal of the HDS4 domain resulted in a Sec7 construct (Sec7ΔHDS4) with activity similar to that of a construct lacking the HDS2-4 domains (Sec7ΔC+HDS1) (Figure 4.4B,G), indicating that the HDS4 domain is the primary determinant for autoinhibition within the HDS2-4 domains.

Figure 4.4: Each GTPase plays a distinct role in Sec7 activation, with Ypt31 exerting the largest stimulatory effect.

(A) Rates of Arf1 activation by $Sec7_f$ in the presence of membrane-bound, activated GTPases or buffer ("mock"). n=3. **(B)** Arf1 activation by purified Sec7ΔC+HDS1. n=3. **(C)** Arf1 activation by $Sec7_f$ in the presence of GDP-bound or GTP-bound Ypt31. n=4. **(D)** Arf1 activation by $Sec7_f$ in the presence of activated membrane-bound Ypt31 or *ypt31-101*, or soluble Ypt31. n=3. **(E**,**F)** Liposome floatation assays showing Ypt1- and Ypt31-dependent recruitment of purified $Sec7_f$ (E) and Sec7ΔHDS4 (F), but not of purified Sec7ΔC+HDS1 (E); GTP* = GMP-PNP (active GTPase). **(G)** Arf1 activation by purified Sec7ΔHDS4. n=3. **(H)** Arf1 activation by membrane-anchored $Sec7_f$. n=3. **(I)** Model of Sec7 recruitment to the TGN and regulation of GEF activity by four GTPases. Sec7 is dimeric, but a monomer is shown for simplicity. This model is based on the findings from this study and previous reports (Christis and Munro, 2012; Richardson et al., 2012). See also Figure 4.5.In (A)-(D),(G),(H), error bars represent 95% CIs for the indicated n.

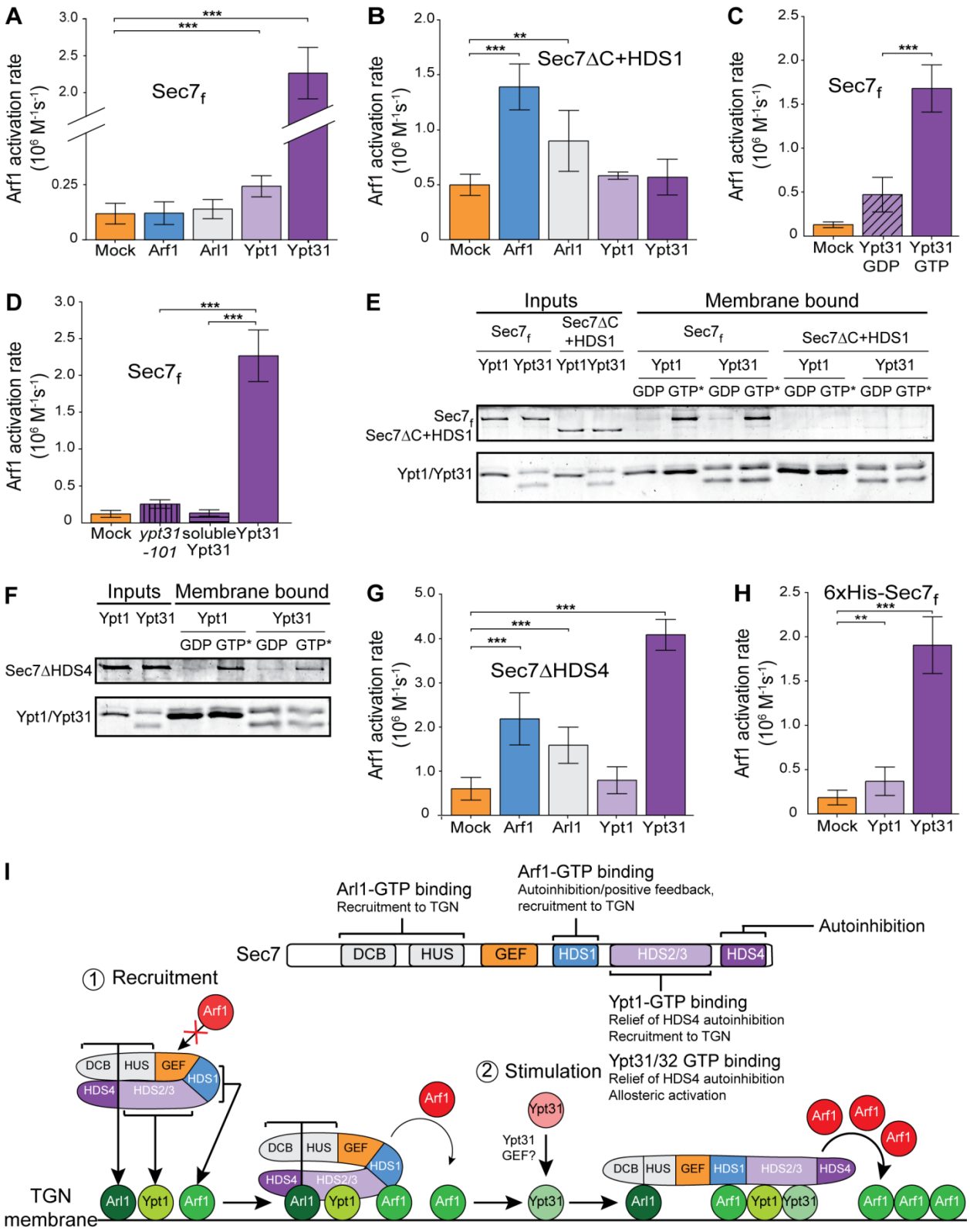
A
Arf1 activation rate (10^6 M^-1s^-1)
Sec7f
Mock Arf1 Arl1 Ypt1 Ypt31
B
Sec7ΔC+HDS1
Mock Arf1 Arl1 Ypt1 Ypt31
C
Sec7f
Mock Ypt31 GDP Ypt31 GTP
D
Sec7f
Mock ypt31-101 soluble Ypt31
E
Inputs
Membrane bound
Sec7f
Sec7ΔC +HDS1
Ypt1 Ypt31 Ypt1 Ypt31
GDP GTP* GDP GTP* GDP GTP* GDP GTP*
Sec7f
Sec7ΔC+HDS1
Ypt1/Ypt31
F
Inputs
Membrane bound
Ypt1 Ypt31 Ypt1 Ypt31
GDP GTP* GDP GTP*
Sec7ΔHDS4
Ypt1/Ypt31
G
Sec7ΔHDS4
Mock Arf1 Arl1 Ypt1 Ypt31
H
6xHis-Sec7f
Mock Ypt1 Ypt31
I
Arl1-GTP binding
Recruitment to TGN
Arf1-GTP binding
Autoinhibition/positive feedback, recruitment to TGN
Autoinhibition
Sec7
DCB HUS GEF HDS1 HDS2/3 HDS4
Ypt1-GTP binding
Relief of HDS4 autoinhibition
Recruitment to TGN
① Recruitment
Arf1
② Stimulation
Ypt31
Ypt31 GEF?
Ypt31/32 GTP binding
Relief of HDS4 autoinhibition
Allosteric activation
TGN membrane
Arl1 Ypt1 Arf1

Figure 4.5: In vitro assay data and controls.
(A) Example fluorescence trace of Arf1 activation by $Sec7_f$ in the presence of activated Ypt1. Insets, from left to right: Ypt1 activation by EDTA-triggered nucleotide exchange, $Sec7_f$ membrane recruitment and stimulation by activated Ypt1, and Arf1 activation by $Sec7_f$. Liposomes and buffer are present from the beginning of the trace.**(B)** Arf1 activation rates by $Sec7_f$ in the presence of activated of Rab GTPases at various concentrations. n=3-5. **(C)** Summary table of GEF activity assay results. **(D)** Comparison of Arf1 activation by $Sec7_f$ in the presence of 100 nM activated Ypt31 or Ypt32. n=4. **(E)** Arf1 activation by $Sec7_f$ in the presence of either 50 nM activated Ypt1, 50nM Ypt31, 50nM each of Ypt1 and Ypt31 (added simultaneously to the same population of liposomes), or 100nM of Ypt31. n=3.**(F)** Arf1 activation by $Sec7_f$ in the presence of either 250 nM activated Arl1, 250nM Ypt1, 250 nM each of Arl1 and Ypt1 (added simultaneously to the same population of liposomes), 500 nM Arl1, or 500 nM Ypt1. n=3.
(G) Comparison of Arf1 activation by $Sec7_f$ or membrane-anchored his-$Sec7_f$. n=3.
In (B, D-G), error bars represent 95% CIs for the indicated n.

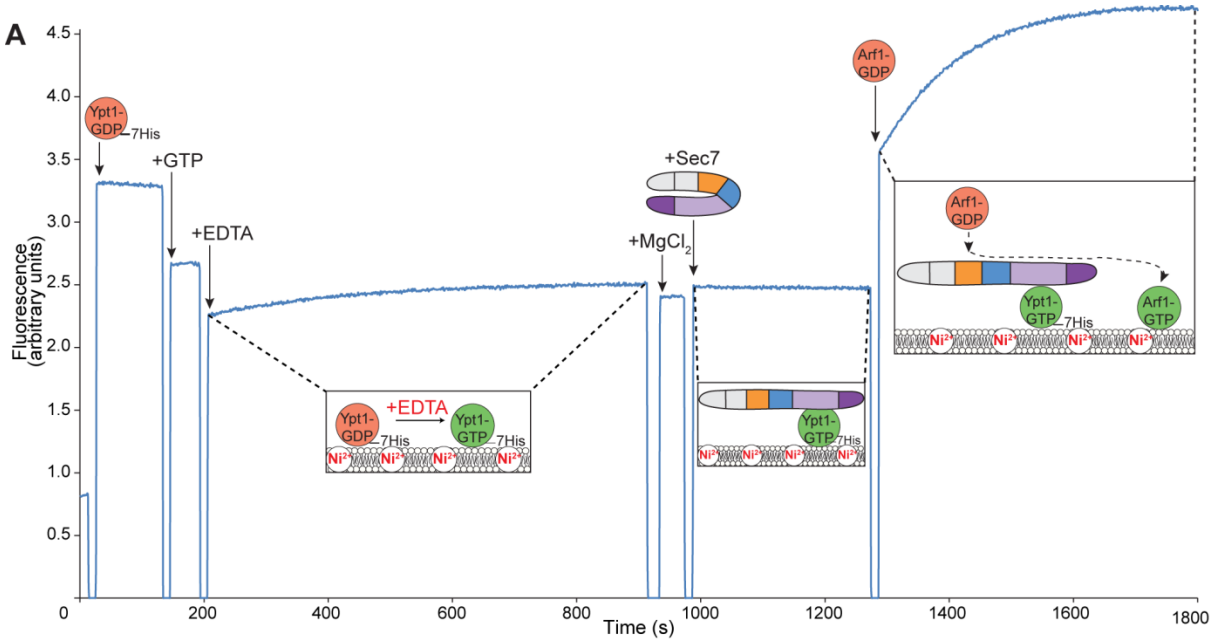

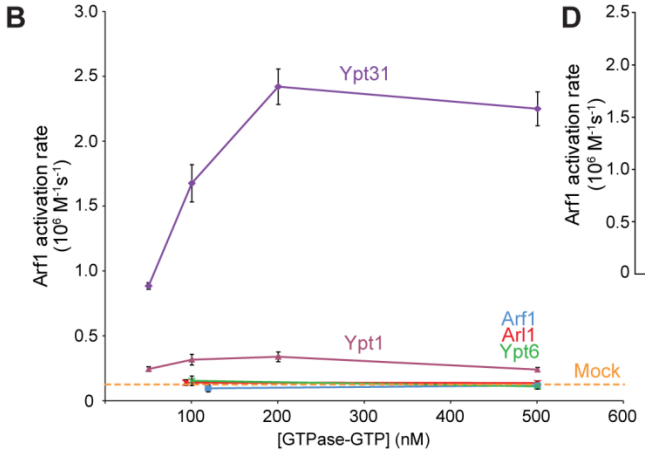

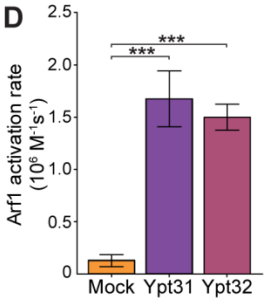

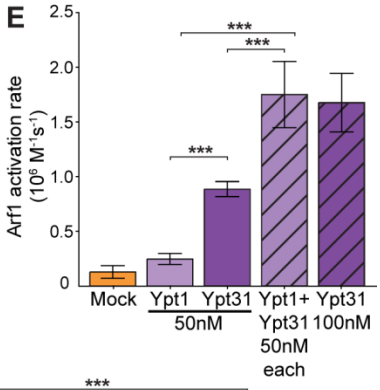

C **Summary of Sec7 GEF activity assays**
GTPase at 500 nM unless otherwise indicated

Construct	Experiment	Result
$Sec7_f$	Stimulation by Arf1	none
	Stimulation by Arl1	none
	Stimulation by Ypt1	2-fold
	Stimulation by Ypt6	none
	Stimulation by Ypt31	20-fold at 500 nM 13-fold at 100 nM
	Stimulation by Ypt32	12-fold at 100 nM
	Stimulation by ypt31-101	2-fold
	Stimulation by soluble Ypt31	none
Sec7ΔHDS4	Increase in activity relative to $Sec7_f$	5-fold
	Stimulation by Arf1	3.5-fold
	Stimulation by Arl1	2.5-fold
	Stimulation by Ypt1	none
	Stimulation by Ypt31	7-fold
Sec7ΔC+HDS1	Increase in activity relative to $Sec7_f$	4-fold
	Stimulation by Arf1	3-fold
	Stimulation by Arl1	2-fold
	Stimulation by Ypt1	none
	Stimulation by Ypt31	none
6xHis-$Sec7_f$	Increase in activity relative to $Sec7_f$	1.5-fold
	Stimulation by Ypt1	2-fold
	Stimulation by Ypt31	10-fold

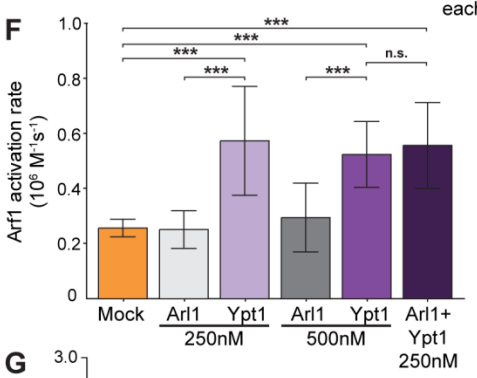

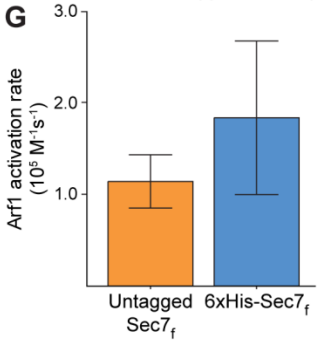

Arf1, Arl1, and Ypt31 stimulated the activity of Sec7ΔHDS4, whereas Ypt1 did not (Figure 4.4G). This indicates that the stimulatory effect of Ypt1 is not observable once autoinhibition by the HDS4 domain is relieved, whereas stimulation by Arf1 or Arl1 is more significant in the absence of HDS4 domain autoinhibition. Arf1 and Arl1 stimulated the activity of Sec7ΔC+HDS1 (Figure 4.4B), whereas Ypt31 exerted no effect, consistent with the lack of Ypt31 binding to this construct (Figure 4.4E).

In light of the *in vivo* localization data reported here and previously published (Richardson et al., 2012), the *in vitro* GEF assay results (summarized in Figure 4.5C) signify that Arf1 and Ypt1 mediate recruitment of Sec7 to the TGN and partially relieve autoinhibition (of the HDS1 and HDS4 domains, respectively). Arl1 was weaker than Arf1 in relieving HDS1 domain autoinhibition (Figure 4.4B,G), and did not increase the activity of Ypt1-stimulated $Sec7_f$ (Figure 4.5F). These results are consistent with a role for Arl1 in recruitment of Sec7 to the membrane surface, which appears weaker than the roles of both Arf1 and Ypt1. Given its function in localization of the Sec7 homologs BIG1/2 (Christis and Munro, 2012), Arl1 may provide TGN compartment specificity for Sec7 through coincidence with Arf1 and Ypt1.

Ypt31 likely exerts an allosteric effect, perhaps inducing Sec7 to adopt a hyperactive conformation. To test this hypothesis, we measured the activity of $Sec7_f$ anchored to the membrane via a histidine tag. Membrane anchoring almost doubled the activity of the $Sec7_f$ construct (Figure 4.5G). Ypt1 and Ypt31 each provided further stimulation of the activity of membrane-anchored $Sec7_f$ (Figure 4.4H), consistent with both Ypt1 and Ypt31 inducing more active conformations of Sec7. Taken together, these results allow us to construct a model for how the four GTPases recruit Sec7 to the TGN and regulate its activity: Sec7 is initially recruited

to the TGN membrane by Ypt1, Arf1, and Arl1 in coincidence, resulting in a basal level of Sec7 activity. Subsequent binding to Ypt31/32 stimulates Sec7 activity (Figure 4.4I).

Ypt31/32 levels peak during Sec7-dependent cargo sorting events

Our data indicate that Ypt31 is the key regulator of Sec7 GEF activity for Arf1 activation at the TGN. If true, then the appearance of Ypt31 at the TGN should be coincident with Arf1-dependent cargo sorting events. We therefore used live-cell imaging to establish the dynamics of Sec7 at the TGN relative to its regulators and relative to cargos whose sorting depends upon Sec7 activity. As others have reported (Jian et al., 2010), we found that tagging Arf1 or Arl1 inactivated these proteins, so we limited our analysis of regulators to Ypt1 and Ypt31.

The yeast Golgi is very dynamic, with a lifetime of a few minutes (Losev et al., 2006; Matsuura-Tokita et al., 2006; Rivera-Molina and Novick, 2009). Two waves of cargo adaptors are recruited to the TGN, separated by only a few seconds (Daboussi et al., 2012). Our time-lapse imaging revealed that ~500 nm TGN compartments, labeled by Sec7, disintegrate into several smaller structures (Figure 4.6A-C). These structures appear to be membranous, as they co-label with the integral membrane v-SNARE protein Snc1 (Figure 4.6D), which marks secretory vesicles destined for the PM. We interpret these small, highly mobile structures to be nascent vesicles or vesicle precursors.

In support of the role of Ypt1 in Sec7 recruitment, we observed that Ypt1 levels peak before Sec7 levels, whereas Ypt31/32 levels peak soon after Sec7 levels (Figures 4.6E,F and 4.7A,D; (Suda et al., 2013)). We examined three cargos: Kex2, a furin protease that cycles between the TGN and endosomes; Tlg1, a Golgi t-SNARE that also cycles between the TGN and endosomes, and Snc1. Kex2 (and presumably Tlg1) is sorted by the Arf1-dependent GGA and

Figure 4.6: Sec7-dependent cargo sorting events are sequential and coincide with the peak of Ypt31 levels.

(A) Live-cell imaging of GFP-Sec7-labeled TGN compartments disintegrating into smaller, fast-moving structures. **(B)** Timelapse subseries (1 sec intervals) of the box from (A), a single Golgi compartment. **(C)** Normalized quantification of the GFP-Sec7 signal in the box from (A). **(D)** Timelapses (5 sec intervals) from strains expressing Sec7-6xDsRed and different Sec7-dependent cargos, aligned by measured Sec7 disappearance time. A strain expressing both GFP-Sec7 and Sec7-6xDsRed serves as a control.

(E) Timelapses (1 sec intervals) from strains expressing Sec7-6xDsRed and GFP-Ypt1 or GFP-Ypt31.

(F) Quantification of the peak-to-peak times. Error bars represent s.e.m. for n=5. **(G)** Quantification of the relative disappearance time for cargos. Error bars represent s.e.m. for n=4 to 6. **(H)** Model for the dynamics of Sec7-dependent events at the late Golgi. Sec7 disappearance is set to t=0. Peak times and sorting times are set relative to t=0. Sorting times denote when >80% of the cargo has exited the TGN. For simplicity, a single time (-11 s) is used to denote sorting of Kex2 (-13.5 s) and Tlg1 (-9 s). Times are denoted as approximate (~) when derived from two sequential relative comparisons. For example, the timing of Sec7 peak levels was measured relative to Sec7 disappearance (Figure S3E), while the peak levels of the Rab proteins were measured relative to the peak of Sec7 (Panel F). Dotted lines and arrows represent events not measured, but inferred from this study and others, for example, the timing of PI(4)P appearance relative to Sec7 (Ortiz et al., 2002; Daboussi et al., 2012). We envision that Sec7 must leave the membrane surface of a secretory vesicle (perhaps triggered by inactivation of Arf1 and Arl1 by the Gcs1 ArfGAP) before Ypt31/32 can recruit Sec2, leading to Sec4 activation and recruitment of the Myo2 (Myosin V) motor. See also Figures 4.7 and 4.8. Experiments in this Figure were performed by Chris Fromme.

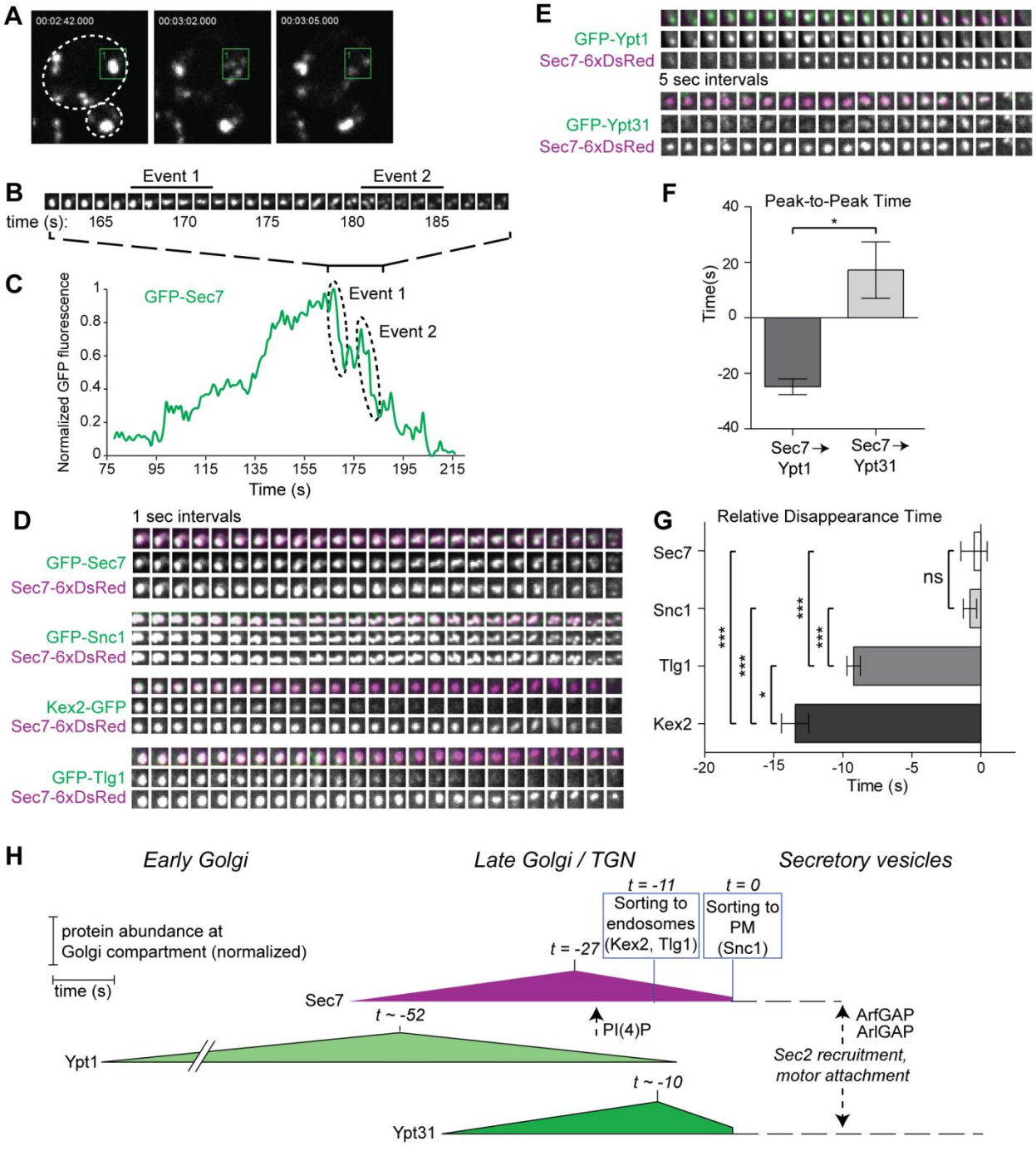
A
00:02:42.000
00:03:02.000
00:03:05.000
B
Event 1
Event 2
time (s): 165 170 175 180 185
C
GFP-Sec7
Event 1
Event 2
Normalized GFP fluorescence
Time (s)
D
1 sec intervals
GFP-Sec7
Sec7-6xDsRed
GFP-Snc1
Sec7-6xDsRed
Kex2-GFP
Sec7-6xDsRed
GFP-Tlg1
Sec7-6xDsRed
E
GFP-Ypt1
Sec7-6xDsRed
5 sec intervals
GFP-Ypt31
Sec7-6xDsRed
F
Peak-to-Peak Time
Time(s)
Sec7→ Ypt1
Sec7→ Ypt31
G
Relative Disappearance Time
Sec7
Snc1
Tlg1
Kex2
ns
Time (s)
H
Early Golgi
Late Golgi / TGN
Secretory vesicles
protein abundance at Golgi compartment (normalized)
time (s)
t = -11
t = 0
Sorting to endosomes (Kex2, Tlg1)
Sorting to PM (Snc1)
t = -27
Sec7
t ~ -52
PI(4)P
ArfGAP
ArlGAP
Sec2 recruitment, motor attachment
Ypt1
t ~ -10
Ypt31

Figure 4.7: Fluorescence quantitation of time-lapse imaging and controls.
(A) Normalized fluorescence plotted versus time for the timelapses shown in Figure 4E. **(B)** The same for timelapses shown in Figure 4D. **(C)** Immunoblots to show expression levels of GFP-tagged Rab proteins relative to endogenous levels. The strain with GFP-Ypt31 integrated at the *YPT31* locus (CFY1805, which preserves the endogenous *YPT31* gene) was used to generate the data presented in Figure 4, Figure S3A, and Movie S3. G6PDH (Zwf1) serves as a loading control. **(D)** Sec7 peak-to-peak times for strains with GFP-Ypt31 on a low expression plasmid, GFP-Ypt31 integrated at the *YPT31* locus, and GFP-Ypt32 integrated at the *URA3* locus. Error bars represent s.e.m for n=3 to 5. **(E)** Sec7 peak-to-disappearance times are plotted indicating mean (26.6 seconds) and s.e.m. for 26 measurements. **(F)** Average disappearance time versus average maximum fluorescence intensity for cargos. Experiments in this Figure were performed by Chris Fromme.

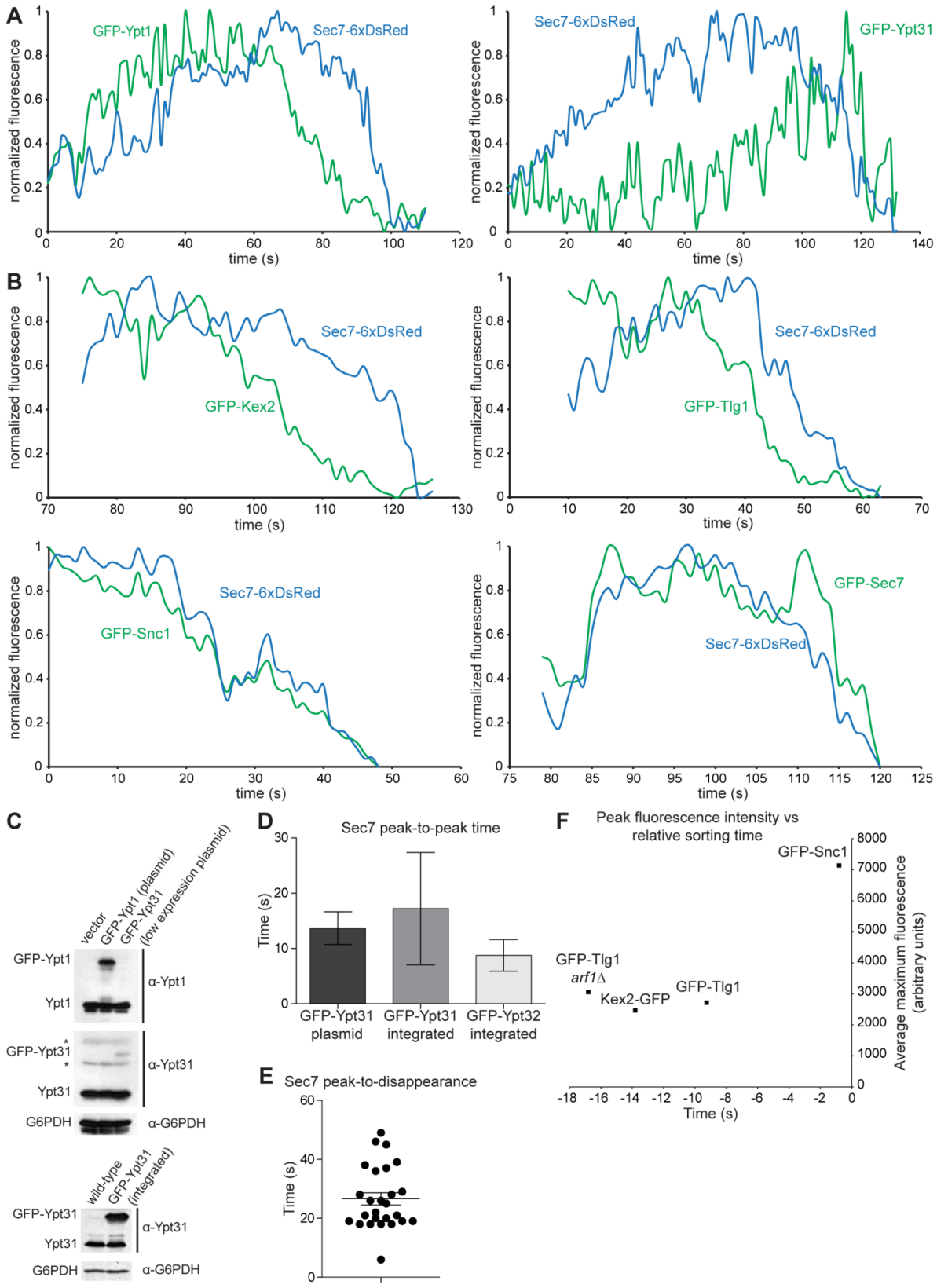
A
GFP-Ypt1
Sec7-6xDsRed
normalized fluorescence
time (s)
Sec7-6xDsRed
GFP-Ypt31
B
Sec7-6xDsRed
GFP-Kex2
GFP-Tlg1
GFP-Snc1
GFP-Sec7
C
vector
GFP-Ypt1 (plasmid)
GFP-Ypt31 (low expression plasmid)
GFP-Ypt1
Ypt1
α-Ypt1
GFP-Ypt31
Ypt31
α-Ypt31
G6PDH
α-G6PDH
wild-type
GFP-Ypt31 (integrated)
D
Sec7 peak-to-peak time
Time (s)
GFP-Ypt31 plasmid
GFP-Ypt31 integrated
GFP-Ypt32 integrated
E
Sec7 peak-to-disappearance
F
Peak fluorescence intensity vs relative sorting time
GFP-Snc1
GFP-Tlg1 arf1Δ
Kex2-GFP
GFP-Tlg1
Average maximum fluorescence (arbitrary units)

AP-1 clathrin adaptors (Abazeed and Fuller, 2008); the sorting machinery for Snc1 is unknown. For each cargo, we measured the time between its disappearance from a Golgi compartment (interpreted as sorting) and the ultimate disintegration of the same compartment. We observed a pattern in which Kex2 was sorted first, followed by Tlg1, then Snc1 (Figures 4.6E,G and 4.7B). Sorting of all three cargos occurred within 15 seconds, consistent with the timing reported for clathrin adaptor progression (Daboussi et al., 2012). Thus, Sec7-dependent cargo sorting events appear to occur sequentially, as previously proposed (Daboussi et al., 2012), with the bulk of sorting to endosomes occurring before sorting to the PM.

Our analysis indicates that Kex2 and Tlg1 sorting occurs soon after Sec7 levels peak, when Ypt31 levels are rising. Disruption of Ypt31/32 function alters the steady-state distribution of Kex2 and Snc1 (Chen et al., 2005). Similarly, we found that lowering Golgi Arf levels by ~90% alters the steady state localization of Kex2 and the kinetics of Tlg1 cargo sorting (Figure 4.8A-D). Our results lead to a model in which abundant Arf1-GTP, generated by Ypt31/32 stimulation of Sec7 and enhanced by positive feedback, is required for the fidelity of sequential cargo sorting events (Figure 4.6H). Vesicles formed later in the sequence would carry more Ypt31/32, enriching these Rab proteins specifically on secretory vesicles. An attractive feature of this model is that after vesicle biogenesis, Sec7 dissociation from a secretory vesicle would allow Ypt31/32 to recruit its known effectors Sec2 and Myo2 (Daboussi et al., 2012; Lipatova et al., 2008; Ortiz et al., 2002), priming the vesicle for motor-driven transport and eventual fusion with the PM.

Figure 4.8: Disruption of Ypt31/32 function results in a similar, but distinct, cargo sorting phenotype compared to lowering Golgi Arf levels.
(A) Images showing Kex2-GFP overlapping significantly with the TGN (marked by Sec7-6xDsRed) in wild-type cells. Virtually all TGN localization of Kex2 is lost in both *ypt31-101 ypt32*Δ and *arf1*Δ cells (*S. cerevisiae* possesses two highly homologous Golgi-localized Arf proteins, Arf1 and Arf2. The *arf1*Δ strain expresses ~10% of Arf1/2 relative to wild-type cells (Stearns et al., 1990)). Imaging was performed at 26°C for all strains. **(B)** GFP-Snc1 localization to the PM is diminished in *ypt31-101 ypt32*Δ cells, but not significantly mislocalized in *arf1*Δ cells. **(C)** GFP-Tlg1 displays increased localization to the vacuole in *ypt31-101 ypt32*Δ. In *arf1*Δ cells, there is slight mislocalization of Tlg1 to the vacuole, but a significant portion remains TGN-localized. **(D)** The significant portion of GFP-Tlg1 localizing to the TGN in *arf1*Δ cells allowed us to measure the sorting dynamics of GFP-Tlg1 in this mutant compared to wild-type cells. Error bars represent s.e.m. for n=5 (mutant) or n=4 (wild-type).**(E)** Context for the main findings of this study: a schematic of the Golgi complex, showing major outgoing and incoming trafficking pathways (solid arrows), and the key GTPases. Blue-labeled GTPases regulate the tethering of incoming vesicles. Green-labeled GTPases regulate formation of outgoing vesicles. Magenta-labeled Arf1 represents the inactive form, which must be activated (dashed arrow) by its GEF, Sec7, at the TGN. Prior to this study, the Ypt31/32 Rab proteins had an unknown role in vesicle formation. **(F)** The major finding of this study, that four GTPases differentially regulate Sec7. We propose that Sec7 is regulated by a two-stage process in which initial recruitment of Sec7 relies upon three GTPases, and subsequent activation requires the Ypt31/32 GTPase. In the absence of incoming traffic, we expect the signals from Ypt1 and Arl1 will be lower, thus dampening recruitment and activation of Sec7. It remains unknown how activation of Ypt31/32 is regulated. Experiments in this Figure were performed by Chris Fromme.

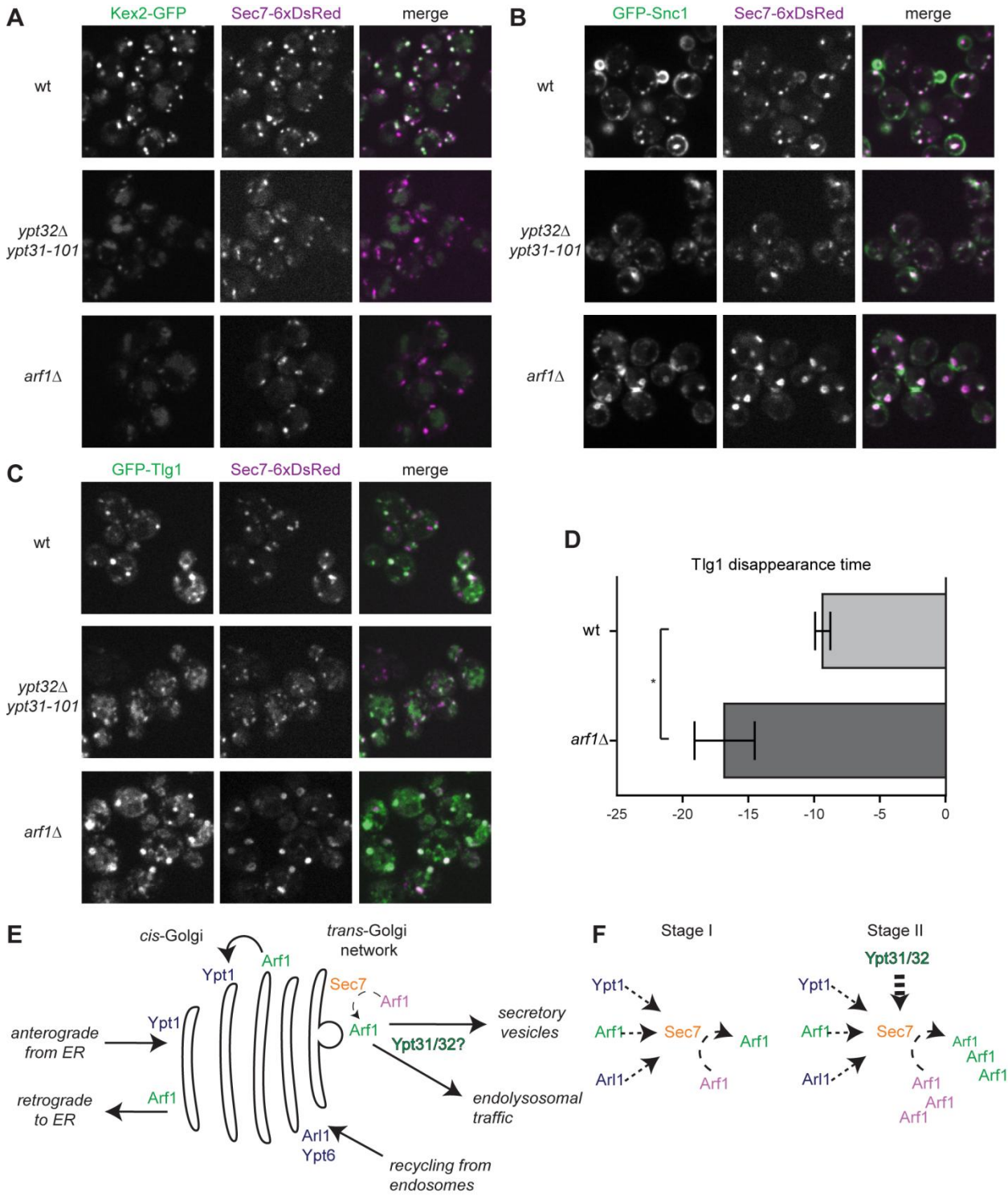
A
Kex2-GFP
Sec7-6xDsRed
merge
wt
ypt32Δ ypt31-101
arf1Δ
B
GFP-Snc1
Sec7-6xDsRed
merge
wt
ypt32Δ ypt31-101
arf1Δ
C
GFP-Tlg1
Sec7-6xDsRed
merge
wt
ypt32Δ ypt31-101
arf1Δ
D
Tlg1 disappearance time
wt
arf1Δ
*
-25
-20
-15
-10
-5
0
E
cis-Golgi
trans-Golgi network
Arf1
Ypt1
Sec7
Arf1
anterograde from ER
Ypt1
Arf1
Ypt31/32?
secretory vesicles
retrograde to ER
Arf1
endolysosomal traffic
Arl1
Ypt6
recycling from endosomes
F
Stage I
Ypt1
Arf1
Sec7
Arf1
Arl1
Arf1
Stage II
Ypt31/32
Ypt1
Arf1
Sec7
Arf1
Arf1
Arf1
Arl1
Arf1
Arf1
Arf1

Discussion

Crosstalk has previously been demonstrated between Arf and Rab pathways during endocytosis (Chesneau et al., 2012), on endosomes (D'Souza et al., 2014; Inoue et al., 2008; Kobayashi and Fukuda, 2012), and at the early Golgi (Chen et al., 2011). Our findings reveal an unprecedented level of crosstalk between Arf and Rab GTPase pathways at the TGN and establish Sec7 as a GTPase signaling hub.

Previous studies identified a role for Ypt31/32 and Rab11 in vesicle formation (Benli et al., 1996; Jedd et al., 1997; Ullrich et al., 1996). Our results provide a mechanistic explanation for Ypt31/32 function in vesicle biogenesis through direct stimulation of Sec7 activity. Cells therefore use a single regulator (Ypt31/32) to drive two coupled events at the TGN: vesicle formation and motor-dependent transport of secretory vesicles. Given the high degree of homology between Ypt31/32 and Rab11-family members (including Rab4 and Rab14), and between Sec7 and the BIG1/2 Arf-GEFs in other organisms, we expect that a similar mechanism operates to generate vesicles at the TGN and recycling endosomes in metazoan cells.

We have also identified Ypt1 as a key regulator of Sec7 membrane localization and activity, underscoring the importance of Ypt1 and Rab1 in regulating multiple aspects of Golgi function. As other known effectors of both Ypt1 and Arl1 mediate tethering of incoming vesicles at the Golgi (Cao et al., 1998; Panic et al., 2003; Setty et al., 2003), direct regulation by these GTPases suggests that Sec7 provides a mechanistic link between incoming and outgoing vesicle traffic (Figure 4.8E,F).

We found that the *sec7-1* allele encodes a mutation that results in cytoplasmic mislocalization. It is possible that this mutation disrupts the interaction between Sec7 and one of the regulatory GTPases or between Sec7 and the membrane surface. Ypt1 overexpression likely

restores membrane localization of the *sec7-1* protein by strengthening the Ypt1-Sec7 interaction, compensating for whichever interaction is diminished by the *sec7-1* mutation. However, we cannot rule out the possibility that Sec7 function is also regulated indirectly by the effect of Ypt1 on Golgi morphology.

The regulation of Sec7 GEF activity is complex. Both the HDS1 and HDS4 domains exert autoinhibitory effects (this work and (Richardson et al., 2012)). Relief of HDS1 domain autoinhibition appears to require recruitment to the membrane surface by binding to either Arf1-GTP or Arl1-GTP, while relief of HDS4 domain autoinhibition appears to require binding of either Ypt1-GTP or Ypt31/32-GTP. The stimulatory effect of Ypt31/32 is greater than that obtained by removal of the HDS4 domain, implying that Ypt31/32 triggers allosteric activation in addition to relief of autoinhibition. Our previous work demonstrated that the membrane surface itself plays an important role in stimulating Sec7 activity (Richardson et al., 2012), but so far no specific lipid requirement has been identified. Future studies will be needed to determine the mechanistic details underlying membrane recruitment and progression of Sec7 from inactive to fully active states.

Our data, together with previous reports (Christis and Munro, 2012; Lowery et al., 2013; Richardson et al., 2012), indicate that Arf1, Arl1, and Ypt1 each play a role in recruiting Sec7 to the Golgi. Subsequent binding to Ypt31/32 further stimulates the activity of Sec7, and this appears necessary to faithfully drive Sec7-dependent cargo sorting events. This idea is supported by the loss of cargo-sorting fidelity in both *ypt31/32* and *arf1* mutant cells.

Regulation by multiple GTPases is a mechanism to ensure precise spatiotemporal regulation of Sec7 activity. We envision that the integration of four different GTPase signals by Sec7 may enable regulation of TGN cargo sorting in response to various cellular stimuli,

including stresses such as nutrient deprivation or changes in secretory cargo load. A full understanding of the signaling logic of the Golgi complex will require mechanistic investigations of each of the Arf and Rab GEFs that together control the function of this organelle.

Methods

Plasmid constructs, yeast strains and genetic methods

Plasmids and strains were constructed using standard techniques and are described in Table 4.1. Strains were generated by standard techniques and are described in Table 4.2.

Antibodies

The anti-Ypt1 (Preuss et al., 1992) and anti-Ypt31 (Jedd et al., 1997) antisera used for Figure S3C were gifts from N. Segev. The anti-G6PDH antibody was purchased from Sigma (A9521).

Protein purification

As reported previously, removal of the first 202 residues of Sec7 greatly improved protein expression and did not compromise the essential function(s) of the protein (Richardson et al., 2012). The $Sec7_f$ and Sec7ΔC+HDS1 constructs were purified as previously described (Richardson et al., 2012), with the addition of treatment by TEV-protease to remove the 6xHis-tag prior to the final chromatography step. Removal of the tag was confirmed by immunoblot (Figure 4.2D). The *sec7-4*$_f$ and Sec7ΔHDS4 constructs were purified using the same procedure as $Sec7_f$. We were not able to purify a well-behaved construct for the HDS2-3 domain region. In our experience the conserved N-terminal domains of Sec7 appear to be required for expression and purification of truncation constructs.

C-terminal 7xHis-tagged yeast Rab protein expression constructs were created using the pGEX-6P vector backbone. Constructs were designed so that the C-terminal cysteine residues

Table 4.1: Plasmids used in this study

Name	Description	Vector Backbone	Source
pNmt1	Nmt1 (S. ce.)	pCYC	(Duronio et al., 1990)
pArf1	Arf1 (S. ce.)	pET3c	(Weiss et al., 1989)
pCF1184	Arl1 (S. ce.)	pET23	this study
Ypt1-7His	Ypt1 with C-terminal his-tag and cleavable GST-fusion	pGEX-6P	T. Bretscher
pCM14	Ypt6 with C-terminal his-tag and cleavable GST-fusion	pGEX-6P	this study
pCM15	Ypt31 with C-terminal his-tag and cleavable GST-fusion	pGEX-6P	this study
pCM16	Ypt31 “soluble” (no his-tag) with cleavable GST-fusion	pGEX-6P	this study
pCM17	*ypt31-101* with C-terminal his-tag and cleavable GST-fusion	pGEX-6P	this study*
Ypt32-7His	Ypt32 with C-terminal his-tag and cleavable GST-fusion	pGEX-6P	T. Bretscher
pBCR314	6xHis-Sec7$_f$ (residues 203-2009)	pFastBacHT	(Richardson et al., 2012)
pBCR389	6xHis-Sec7ΔC+HDS1 (residues 203-1220)	pET28	(Richardson et al., 2012)
pCM18	6xHis-Sec7ΔHDS4 (residues 203-1799)	pFastBacHT	this study
pCF1257	6xHis-*sec7-4$_f$* (residues 203-2009, G883D)	pFastBacHT	this study
pRS304	yeast integration vector with *TRP1* marker		(Sikorski and Hieter, 1989)
pRS305	yeast integration vector with *LEU2* marker		(Sikorski and Hieter, 1989)
pRS415	yeast centromeric plasmid with *LEU2* marker		(Sikorski and Hieter, 1989)
pRS416	yeast centromeric plasmid with *URA3* marker		(Sikorski and Hieter, 1989)
pRS426	yeast 2-micron (high copy) vector with *URA3* marker		(Sikorski and Hieter, 1989)
pCF1043	*SEC7* (includes ~1 kB of 5’UTR)	pRS416	(Richardson et al., 2012)

Table 4.1 (continued)

Name	Description	Vector Backbone	Source
pCF1084	GFP-Sec7 driven by P_{SEC7}	pRS415	(Richardson et al., 2012)
pCF1105	GFP-sec7-1 driven by P_{SEC7}	pRS415	this study
pCF1106	GFP-sec7-4 driven by P_{SEC7}	pRS415	this study
pCF1191	GFP-Sec7 (driven by P_{SEC7}) integration plasmid	pRS305	this study
pCF1197	GFP-sec7-1 (driven by P_{SEC7}) integration plasmid	pRS305	this study
pCF1246	RFP^{MARS}-sec7-4 (driven by P_{SEC7}) integration plasmid	pRS304	this study
pCF1258	*SEC7* gene	pRS426	this study
VSB284	*YPT31* gene	pRS426	(Sciorra et al., 2005)
pCF1259	*ARL1* gene	pRS426	this study
pCF1261	*ARF1* gene	pRS426	this study
pCF1263	*YPT1* gene	pRS426	this study
GFP-Tlg1	GFP-Tlg1	pRS416	(Xu et al., 2013)
GFP-Ypt1	GFP-Ypt1	pRS415	(Buvelot Frei et al., 2006)
VSB311	GFP-Ypt31	pRS415	Sciorra et al., 2005)
GFP-Snc1	GFP-Snc1 integration plasmid	pRS306	(Lewis et al., 2000)
pRC678	GFP-Ypt31 integration plasmid	pRS306	(Buvelot Frei et al., 2006)
pRC679	GFP-Ypt32 integration plasmid	pRS306	(Buvelot Frei et al., 2006)
Sec7-6xDsRed	Sec7-6xDsRed integration plasmid (URA3)		(Losev et al., 2006)
Sys1-DsRed	Sys1-DsRed	pRS416	T. Graham

*The *ypt31-101* mutation was originally reported in (Sciorra et al., 2005). This allele has the following mutations: K43R, K127N

Table 4.2: Yeast strains used in this study

Name	Genotype	(Strain construction method)	Source
SEY6210	*MATα his3-Δ200 leu2-3,112 lys2-801 trp1-Δ901 ura3-52 suc2-Δ9*		(Robinson et al., 1988)
SEY6210.1	*MATa his3-Δ200 leu2-3,112 lys2-801 trp1-Δ901 ura3-52 suc2-Δ9*		(Robinson et al., 1988)
BY4741	*MATa his3-Δ1 leu2-Δ0 met15-Δ0 ura3-Δ0*		(Brachmann et al., 1998)
BY4742	*MATα his3-Δ1 leu2-Δ0 lys2-Δ0 ura3-Δ0*		(Brachmann et al., 1998)
BYgeneΔ	*BY4741 geneΔ::KanMX*		(Giaever et al., 2002)
VSY468	*SEY6210 ypt31-101::URA3 ypt32Δ::TRP1*		(Sciorra et al., 2005)
CFY409	BY4742 *sec7Δ::KANMX* +pCF1043		(Richardson et al., 2012)
CBY474	*MATa ade2 can1-100 leu2-3,112 trp1-1 ura3-1 ypt1-3*		(Cao et al., 1998)
CFY1037	*SEY6210 GFP-Sec7::LEU2*	(integration of pCF1191 into SEY6210)	this study
CFY1111	*SEY6210.1 GFP-sec7-1::LEU2*	(integration of pCF1197 into SEY6210.1)	this study
CFY1319	*SEY6210 ypt31-101::URA3::ura3 ypt32Δ::TRP1*	(5-FOA selection of VSY468)	this study
CFY1499	*SEY6210.1 RFP^{MARS}-sec7-4:TRP1*	(integration of pCF1246 into SEY6210.1)	this study
CFY1681	*SEY6210.1 Sec7-6xDsRed::URA3*	(integration of Sec7-6xDsRed into SEY6210.1)	this study
CFY1689	*SEY6210.1 Sec7-6xDsRed::URA3::ura3*	(5-FOA selection of CFY1681)	this study
CFY1690	*SEY6210.1 Sec7-6xDsRed::URA3 Kex2-GFP::HIS3*		this study
		(PCR integration into CFY1681)	
CFY1711	*SEY6210.1 Sec7-6xDsRed::URA3::ura3 ura3::GFP-Snc1::URA3*		this study
		(GFP-Snc1 plasmid integration into CFY1689)	
CFY1752	*SEY6210.1 Sec7-6xDsRed::URA3 Kex2-GFP::HIS3 arf1Δ::KanMX*		this study
		(PCR integration into CFY1690)	
CFY1754	*SEY6210.1 Sec7-6xDsRed::URA3::ura3 ura3::GFP-Snc1::URA3 arf1Δ::KanMX*		this study
		(PCR integration into CFY1711)	

Table 4.2 (continued)

Name	Genotype	(Strain construction method)	Source
CFY1754	*SEY6210.1 Sec7-6xDsRed::URA3::ura3 ura3::GFP-Snc1::URA3 arf1Δ::KanMX*	(PCR integration into CFY1711)	this study
CFY1764	*SEY6210.1 Sec7-6xDsRed::URA3::ura3 arf1Δ::KanMX*	(PCR integration into CFY1689)	this study
CFY1780	*SEY6210 ypt31-101::URA3::ura3 ypt32Δ::TRP1 Sec7-6xDsRed::URA3*	(integration of Sec7-6xDsRed into CFY1319)	this study
CFY1784	*SEY6210 GFP-Ypt31::URA3*	(GFP-Ypt31 plasmid integration into SEY6210)	this study
CFY1786	*SEY6210 ura3::GFP-Ypt32::URA3*	(GFP-Ypt32 plasmid integration into SEY6210)	this study
CFY1805	*SEY6210 GFP-Ypt31::URA3 Sec7-6xDsRed::URA3::ura3*	(made by mating/sporulation CFY1689 x CFY1784)	this study
CFY1806	*SEY6210 ura3::GFP-Ypt1::URA3 Sec7-6xDsRed::URA3::ura3*	(made by mating/sporulation CFY1689 x CFY1786)	this study
CFY1811	*SEY6210 ypt31-101::URA3::ura3 ypt32Δ::TRP1 Sec7-6xDsRed::URA3*::ura3	(5-FOA selection of CFY1780)	this study
CFY1817	*SEY6210 ypt31-101::URA3::ura3 ypt32Δ::TRP1 Sec7-6xDsRed::URA3 Kex2-GFP::HIS3*	(PCR integration into CFY1780)	this study
CFY1819	*SEY6210 ypt31-101::URA3::ura3 ypt32Δ::TRP1 Sec7-6xDsRed::URA3*::ura3 *ura3::GFP-Snc1::URA3*	(GFP-Snc1 plasmid integration into CFY1811)	this study

(prenylated *in vivo*) were replaced with a 7xHis-tag for membrane anchoring. These constructs were purified using the GST tag, which was removed by PreScission protease treatment. The expression vectors were transformed into Rosetta2 (Novagen) *E. coli* cells and grown in 1-2L TB at 37°C to an OD of ~3.0. The temperature was then decreased to 18°C, expression was induced with 500 μM IPTG, and cells were grown overnight. Cells were lysed by sonication in lysis buffer containing 1xPBS, 2 mM MgCl2, and 5 mM β-Me. The lysate was centrifuged, and protein was purified from the cleared lysate by glutathione resin (G Biosciences) followed by cleavage with PreScission protease overnight at 4°C in a buffer containing 50 mM Tris-HCl pH 7.5, 150 mM NaCl, 1 mM EDTA, 2 mM MgCl2, and 5 mM β-Me. The eluate containing the purified protein was then collected and exchanged into a buffer containing 20 mM Tris-HCl pH 8, 100 nM NaCl, 2 mM MgCl2, and 1 mM DTT before use in GEF activity assays. We note that there are two distinct species in some of the purifications. Analysis by anti-His-tag immunoblot indicated that the faster migrating species are likely N-terminal proteolytic products (Figure 4.2C). The structure of yeast Ypt31 demonstrated that the N-terminal nine amino acids are disordered (Ignatev et al., 2008).

Myristoylated Arf1 was purified as reported (Ha et al., 2005). For purification of myristoylated Arl1, a plasmid encoding full-length yeast Arl1 was introduced into BL21(DE3) *E. coli* cells together with the Nmt1 plasmid encoding the N-myristoyl transferase enzyme. Growth and expression was the same as for Arf1. Following cell lysis (in 15 mL lysis buffer per 1 liter cell pellet: 25 mM Tris pH 7.5, 100 mM NaCl, 1 mM MgCl2, 10 mM ßME, 1 mM PMSF) by sonication, the lysate was clarified by centrifugation. The supernatant was incubated with SP-sepharose (GE Healthcare) resin (1 ml resin per 7 mg protein in lysate). The unbound fraction was applied to a MonoQ column (GE Healthcare), and a 100 mM to 1 M NaCl gradient (25 mM

Tris pH 8.0, 2 mM MgCl2, 1 mM DTT) was run. Peak fractions were pooled and run on a Superdex 200 column (GE Healthcare). Peak fractions were then run on a HiTrap Phenyl column (GE Healthcare), using a 3 M to 0 M NaCl gradient (20 mM Tris pH 8.0, 2 mM MgCl2, 1 mM DTT). We note that the purified protein runs as three species on an SDS-PAGE gel.

Liposome preparation

TGN-like liposomes were prepared as described (Richardson et al., 2012), except they also contained 5% Ni2+-DOGS for binding His-tagged proteins. Liposomes were extruded through 100 nm filters.

Liposome floatation (binding) assays

Flotation assays were performed as described (Richardson et al., 2012), using 4 ug of each protein and 0.3 mM of liposomes per 75 ul binding reaction. The His-tags at the C-termini of the Rab proteins allow these proteins to be bound to the liposomes regardless of their activation state. In contrast, the Arf1 and Arl1 proteins only bind to liposomes when activated, due to a conformational change that exposes an N-terminal membrane-inserting helix. 15% PAGE gels were stained with IRDye (Li-Cor) and imaged on a Li-Cor Odyssey instrument. Gel images were processed with the ImageJ despeckle filter and min/max levels were adjusted in Photoshop for clarity.

GEF activity assays

Tryptophan fluorescence GEF assays were performed at 30°C as described (Richardson et al., 2012). Figure 4.5A presents an example of a single replicate. Unless otherwise indicated,

most assays were performed with 500 nM GTPase activators, 30 nM GEF construct, and 400 nM myrArf1-GDP substrate. Assays in Figure 4.3C,D used 100nM GEF construct. Assays in Figures 4.4C and 4.5B,D,E used either 100 nM GTPase activator or the concentration specified in the figure and 50 nM GEF construct. Liposomes batches were pooled, and the same pool was used for all GEF assays, except for those in Figures 4.4C and 4.5B,D,E, which were performed with a separate pool of liposomes.

Microscopy

See Table 4.3 for which strains and plasmids were used for each experiment. Images in the same figure panel are shown at the same light levels.

Cells were grown in synthetic media and imaged in log phase (OD600 ~ 0.4) on glass coverslips or in glass-bottomed dishes. Images shown in Figures 4.1, 4.2, and 4.3 were obtained using a DeltaVision RT wide-field microscope (Applied Precision). Single focal planes are shown after deconvolution in softWoRx (Applied Precision).

Images shown in Figures 4.6 and 4.8 were obtained using an Andor Revolution spinning disk confocal microscope with dual cameras for simultaneous red/green image acquisition. For each tine series, a single focal plane was imaged under reduced laser power to minimize photobleaching. 500 ms exposures were acquired every second for four minutes at 26°C. Image processing for these data was done using the SlideBook software (3I).

Peak-to-peak times were determined similar to a previous report (Daboussi et al., 2012), being careful to only analyze compartments that remained spatially resolved from other

Table 4.3: Strains and plasmids used in microscopy and growth experiments.

Experiment (Figure #)	Strain(s) and plasmid(s) used
Figure 4.1C	BY4741, BYarf1Δ, BYarl1Δ, SEY6210, VSY468, CBY474, each with pCF1084
Figure 4.1D	CFY1111 with pRS426, pCF1258, pCF1259, pCF1261, pCF1263, or VSB284
Figure 4.1E	CFY1499 with pRS426, pCF1258, pCF1259, pCF1261, pCF1263, or VSB284
Figure 4.2E	CBY474, VSY468, BY4171, BYgeneΔ, each with pCF1084
Figure 4.2F	BY4741, BYarf1Δ, BYarl1Δ, SEY6210, VSY468, CBY474, each with pCF1084 and Sys1-DsRed
Figure 4.2G	CFY409 with shuffled pCF1084, pCF1105, or pCF1106, each with Sys1-DsRed
Figure 4.3A	CFY409 with shuffled pCF1084, pCF1105, or pCF1106
Figure 4.3B	CFY1111 with pRS426 or pCF1263
Figure 4.6A-C	CFY1037
Figure 4.6D	CFY1681+pCF1084, CFY1711, CFY1690, CFY1689+GFP-Tlg1
Figure 4.6E	CFY1689+GFP-Ypt1, CFY1805
Figure 4.7C,D	CFY1689+GFP-Ypt1, CFY1689+GFP-Ypt31, CFY1805, CFY1806
Figure 4.8A-D	CFY1690, CFY1689+GFP-TLG1, CFY1711, CFY1752, CFY1754, CFY1764+GFP-Tlg1, CFY1811+GFP-Tlg1, CFY1817, CFY1819

compartments and within the observed focal plane for the duration of the analysis time. Peak times were determined after photobleach correction and normalization of the fluorescence signal. The typical amount of photobleaching during a 4 minute time course was ~15% for Sec7-6xDsRed and ~40-50% for the GFP-tagged proteins. Relative disappearance times were determined using compartments which met the above criteria and for which the disintegration of the Sec7 marker was observable during the time-course. For compartments meeting these criteria, the time of disappearance was chosen as the timepoint when the normalized fluorescence signal dropped below 20% of its maximum value for the duration of the analysis time. We note that although we were only able to quantify several compartments due to the selection criteria, we observed that virtually all compartments exhibited qualitatively similar maturation kinetics.

We tested two different GFP-Ypt31 constructs, one with an expression level much lower than endogenous Ypt31, and another with an expression level that was higher (Figure 4.7C). Both constructs exhibited similar dynamics relative to Sec7 (Figure 4.7D), despite differing in expression level by an order of magnitude. The data shown in Figure 4.6 was collected using the strain with higher GFP-Ypt31 expression level. Both the GFP-Ypt1 and GFP-Ypt31 fusions were previously shown to be functional (Buvelot Frei et al., 2006).

We were concerned that the measured disappearance times might simply be an artifact of either photobleaching or the intensity of the fluorescence signal (i.e., cargos with weak fluorescent signal may appear to be sorted earlier). Photobleaching was judged not to be a concern, as other compartments within the same cell remained fluorescent after the disappearance of signal from the measured compartment. To test the possibility of artifacts due to fluorescence intensity, we plotted relative disappearance time versus maximum fluorescence intensity values, averaged for each cargo or mutant strain. There was no significant correlation between compartment

fluorescence intensity and disappearance time (Figure 4.7F), although Snc1 was the most intense and had the latest disappearance. For example, the intensity of GFP-Tlg1 at Golgi compartments is increased in the *arf1*Δ strain relative to wild-type cells, likely owing to the enlargement of the Golgi in this strain, yet the disappearance of GFP-Tlg1 occurs earlier in this strain relative to the wild-type strain.

Statistical tests

For Figures 4.2D-F, 4.3, 4.4, and 4.6G, significance was determined by one-way ANOVA with Tukey's test for multiple comparison. For the data in Figure 4.4A,D,H the variances were not equal among the samples, presumably due to the much faster rates in the Ypt31-stimulated reactions. Therefore, these data were $\log_{10}$ transformed for statistical analysis to equalize the variances prior to performing the ANOVA/Tukey's test. For Figures 4.6F and 4.8D, significance was determined by an unpaired T-test with Welch's correction.

REFERENCES

Abazeed, M.E., and Fuller, R.S. (2008). Yeast Golgi-localized, gamma-Ear-containing, ADP-ribosylation factor-binding proteins are but adaptor protein-1 is not required for cell-free transport of membrane proteins from the trans-Golgi network to the prevacuolar compartment. Mol Biol Cell *19*, 4826-4236.

Bacon, R.A., Salminen, A., Ruohola, H., Novick, P., and Ferro-Novick, S. (1989). The GTP-binding protein Ypt1 is required for transport in vitro: the Golgi apparatus is defective in ypt1 mutants. J Cell Biol *109*, 1015-1022.

Barr, F.A. (2009). Rab GTPase function in Golgi trafficking. Semin Cell Dev Biol *20*, 780-783.

Benli, M., Doring, F., Robinson, D.G., Yang, X., and Gallwitz, D. (1996). Two GTPase isoforms, Ypt31p and Ypt32p, are essential for Golgi function in yeast. EMBO J *15*, 6460-6475.

Brachmann, C.B., Davies, A., Cost, G.J., Caputo, E., Li, J., Hieter, P., and Boeke, J.D. (1998). Designer deletion strains derived from Saccharomyces cerevisiae S288C: a useful set of strains and plasmids for PCR-mediated gene disruption and other applications. Yeast *14*, 115-132.

Buvelot Frei, S., Rahl, P.B., Nussbaum, M., Briggs, B.J., Calero, M., Janeczko, S., Regan, A.D., Chen, C.Z., Barral, Y., Whittaker, G.R., *et al.* (2006). Bioinformatic and comparative localization of Rab proteins reveals functional insights into the uncharacterized GTPases Ypt10p and Ypt11p. Molecular and cellular biology *26*, 7299-7317.

Cao, X., Ballew, N., and Barlowe, C. (1998). Initial docking of ER-derived vesicles requires Uso1p and Ypt1p but is independent of SNARE proteins. EMBO J *17*, 2156-2165.

Casanova, J.E. (2007). Regulation of Arf activation: the Sec7 family of guanine nucleotide exchange factors. Traffic *8*, 1476-1485.

Chen, S., Cai, H., Park, S.K., Menon, S., Jackson, C.L., and Ferro-Novick, S. (2011). Trs65p, a subunit of the Ypt1p GEF TRAPPII, interacts with the Arf1p exchange factor Gea2p to facilitate COPI-mediated vesicle traffic. Mol Biol Cell *22*, 3634-3644.

Chen, S.H., Chen, S., Tokarev, A.A., Liu, F., Jedd, G., and Segev, N. (2005). Ypt31/32 GTPases and their novel F-box effector protein Rcy1 regulate protein recycling. Mol Biol Cell *16*, 178-192.

Chesneau, L., Dambournet, D., Machicoane, M., Kouranti, I., Fukuda, M., Goud, B., and Echard, A. (2012). An ARF6/Rab35 GTPase cascade for endocytic recycling and successful cytokinesis. Curr Biol *22*, 147-153.

Christis, C., and Munro, S. (2012). The small G protein Arl1 directs the trans-Golgi-specific targeting of the Arf1 exchange factors BIG1 and BIG2. J Cell Biol *196*, 327-335.

D'Souza, R.S., Semus, R., Billings, E.A., Meyer, C.B., Conger, K., and Casanova, J.E. (2014). Rab4 Orchestrates a Small GTPase Cascade for Recruitment of Adaptor Proteins to Early Endosomes. Current biology : CB *24*, 1187-1198.

Daboussi, L., Costaguta, G., and Payne, G.S. (2012). Phosphoinositide-mediated clathrin adaptor progression at the trans-Golgi network. Nat Cell Biol *14*, 239-248.

Deitz, S.B., Rambourg, A., Kepes, F., and Franzusoff, A. (2000). Sec7p directs the transitions required for yeast Golgi biogenesis. Traffic *1*, 172-183.

Donaldson, J.G., and Jackson, C.L. (2011). ARF family G proteins and their regulators: roles in membrane transport, development and disease. Nature reviews Molecular cell biology *12*, 362-375.

Duronio, R.J., Jackson-Machelski, E., Heuckeroth, R.O., Olins, P.O., Devine, C.S., Yonemoto, W., Slice, L.W., Taylor, S.S., and Gordon, J.I. (1990). Protein N-myristoylation in Escherichia coli: reconstitution of a eukaryotic protein modification in bacteria. Proc Natl Acad Sci USA *87*, 1506-1510.

Giaever, G., Chu, A.M., Ni, L., Connelly, C., Riles, L., Veronneau, S., Dow, S., Lucau-Danila, A., Anderson, K., Andre, B., *et al.* (2002). Functional profiling of the Saccharomyces cerevisiae genome. Nature *418*, 387-391.

Ha, V.L., Thomas, G.M., Stauffer, S., and Randazzo, P.A. (2005). Preparation of myristoylated Arf1 and Arf6. Methods Enzymol *404*, 164-174.

Ignatev, A., Kravchenko, S., Rak, A., Goody, R.S., and Pylypenko, O. (2008). A structural model of the GDP dissociation inhibitor rab membrane extraction mechanism. J Biol Chem *283*, 18377-18384.

Inoue, H., Ha, V.L., Prekeris, R., and Randazzo, P.A. (2008). Arf GTPase-activating protein ASAP1 interacts with Rab11 effector FIP3 and regulates pericentrosomal localization of transferrin receptor-positive recycling endosome. Mol Biol Cell *19*, 4224-4237.

Jedd, G., Mulholland, J., and Segev, N. (1997). Two new Ypt GTPases are required for exit from the yeast trans-Golgi compartment. J Cell Biol *137*, 563-580.

Jian, X., Cavenagh, M., Gruschus, J.M., Randazzo, P.A., and Kahn, R.A. (2010). Modifications to the C-terminus of Arf1 alter cell functions and protein interactions. Traffic *11*, 732-742.

Jones, S., Jedd, G., Kahn, R.A., Franzusoff, A., Bartolini, F., and Segev, N. (1999). Genetic interactions in yeast between Ypt GTPases and Arf guanine nucleotide exchangers. Genetics *152*, 1543-1556.

Kobayashi, H., and Fukuda, M. (2012). Rab35 regulates Arf6 activity through centaurin-beta2 (ACAP2) during neurite outgrowth. J Cell Sci *125*, 2235-2243.

Lewis, M.J., Nichols, B.J., Prescianotto-Baschong, C., Riezman, H., and Pelham, H.R. (2000). Specific retrieval of the exocytic SNARE Snc1p from early yeast endosomes. Mol Biol Cell *11*, 23-38.

Lipatova, Z., Tokarev, A.A., Jin, Y., Mulholland, J., Weisman, L.S., and Segev, N. (2008). Direct interaction between a myosin V motor and the Rab GTPases Ypt31/32 is required for polarized secretion. Mol Biol Cell *19*, 4177-4187.

Losev, E., Reinke, C.A., Jellen, J., Strongin, D.E., Bevis, B.J., and Glick, B.S. (2006). Golgi maturation visualized in living yeast. Nature *441*, 1002-1006.

Lowery, J., Szul, T., Styers, M., Holloway, Z., Oorschot, V., Klumperman, J., and Sztul, E. (2013). The Sec7 guanine nucleotide exchange factor GBF1 regulates membrane recruitment of BIG1 and BIG2 guanine nucleotide exchange factors to the trans-Golgi network (TGN). The Journal of biological chemistry *288*, 11532-11545.

Matsuura-Tokita, K., Takeuchi, M., Ichihara, A., Mikuriya, K., and Nakano, A. (2006). Live imaging of yeast Golgi cisternal maturation. Nature *441*, 1007-1010.

Miserey-Lenkei, S., Chalancon, G., Bardin, S., Formstecher, E., Goud, B., and Echard, A. (2010). Rab and actomyosin-dependent fission of transport vesicles at the Golgi complex. Nat Cell Biol *12*, 645-654.

Mizuno-Yamasaki, E., Rivera-Molina, F., and Novick, P. (2012). GTPase networks in membrane traffic. Annual review of biochemistry *81*, 637-659.

Novick, P., Field, C., and Schekman, R. (1980). Identification of 23 complementation groups required for post-translational events in the yeast secretory pathway. Cell *21*, 205-215.

Ortiz, D., Medkova, M., Walch-Solimena, C., and Novick, P. (2002). Ypt32 recruits the Sec4p guanine nucleotide exchange factor, Sec2p, to secretory vesicles; evidence for a Rab cascade in yeast. J Cell Biol *157*, 1005-1015.

Panic, B., Whyte, J.R., and Munro, S. (2003). The ARF-like GTPases Arl1p and Arl3p act in a pathway that interacts with vesicle-tethering factors at the Golgi apparatus. Curr Biol *13*, 405-410.

Preuss, D., Mulholland, J., Franzusoff, A., Segev, N., and Botstein, D. (1992). Characterization of the Saccharomyces Golgi complex through the cell cycle by immunoelectron microscopy. Mol Biol Cell *3*, 789-803.

Richardson, B.C., McDonold, C.M., and Fromme, J.C. (2012). The Sec7 Arf-GEF is recruited to the trans-Golgi network by positive feedback Dev Cell *22*, 799-810.

Rivera-Molina, F.E., and Novick, P.J. (2009). A Rab GAP cascade defines the boundary between two Rab GTPases on the secretory pathway. Proceedings of the National Academy of Sciences of the United States of America *106*, 14408-14413.

Robinson, J.S., Klionsky, D.J., Banta, L.M., and Emr, S.D. (1988). Protein sorting in Saccharomyces cerevisiae: isolation of mutants defective in the delivery and processing of multiple vacuolar hydrolases. Mol Cell Biol *8*, 4936-4948.

Sciorra, V.A., Audhya, A., Parsons, A.B., Segev, N., Boone, C., and Emr, S.D. (2005). Synthetic genetic array analysis of the PtdIns 4-kinase Pik1p identifies components in a Golgi-specific Ypt31/rab-GTPase signaling pathway. Mol Biol Cell *16*, 776-793.

Sclafani, A., Chen, S., Rivera-Molina, F., Reinisch, K., Novick, P., and Ferro-Novick, S. (2010). Establishing a role for the GTPase Ypt1p at the late Golgi. Traffic *11*, 520-532.

Segev, N. (1991). Mediation of the attachment or fusion step in vesicular transport by the GTP-binding Ypt1 protein. Science *252*, 1553-1556.

Setty, S.R., Shin, M.E., Yoshino, A., Marks, M.S., and Burd, C.G. (2003). Golgi recruitment of GRIP domain proteins by Arf-like GTPase 1 is regulated by Arf-like GTPase 3. Curr Biol *13*, 401-404.

Sikorski, R.S., and Hieter, P. (1989). A system of shuttle vectors and yeast host strains designed for efficient manipulation of DNA in Saccharomyces cerevisiae. Genetics *122*, 19-27.

Suda, Y., Kurokawa, K., Hirata, R., and Nakano, A. (2013). Rab GAP cascade regulates dynamics of Ypt6 in the Golgi traffic. Proc Natl Acad Sci USA *110*, 18976-18981.

Ullrich, O., Reinsch, S., Urbe, S., Zerial, M., and Parton, R.G. (1996). Rab11 regulates recycling through the pericentriolar recycling endosome. The Journal of cell biology *135*, 913-924.

Wang, W., Sacher, M., and Ferro-Novick, S. (2000). TRAPP stimulates guanine nucleotide exchange on Ypt1p. J Cell Biol *151*, 289-296.

Weiss, O., Holden, J., Rulka, C., and Kahn, R.A. (1989). Nucleotide binding and cofactor activities of purified bovine brain and bacterially expressed ADP-ribosylation factor. J Biol Chem *264*, 21066-21072.

Xu, P., Baldridge, R.D., Chi, R.J., Burd, C.G., and Graham, T.R. (2013). Phosphatidylserine flipping enhances membrane curvature and negative charge required for vesicular transport. J Cell Biol *202*, 875-886.

CHAPTER 5

EXTENSIONS TO GEA1/2: EVIDENCE FOR REGULATION BY RAB GTPASES

Overview

Arf1 controls both retrograde trafficking pathways at the early Golgi and secretory pathways at the late Golgi. My studies have shown that Sec7 acts as a signaling hub at the *trans*-Golgi network by integrating signals from multiple trafficking pathways. However, the mechanisms regulating membrane recruitment and GEF activation of the early Golgi Arf-GEFs, Gea1 and Gea2, remain elusive. I have determined that the HDS2 domain of Gea1 is important for localization to the Golgi. Here I present the results of a targeted screen for Golgi-localized proteins that effect the localization of Gea1 in yeast. Deletion of the Rab GTPase Ypt6 causes Gea1 to lose Golgi localization; however, Ypt6 is unable to recruit Gea1 to membranes *in vitro*. I have also confirmed that Gea1 is an effector of the Rab GTPase Ypt1, and that this interaction is sufficient to recruit Gea1 to membranes. Together, these data hint at links between the early Golgi Arf-GEFs and the Rab pathways, though further studies are needed to investigate the exact nature of these interactions.

Introduction

The Arf-GEFs Gea1 and Gea2 activate Arf1 at the Golgi complex to initiate retrograde trafficking pathways. Both Gea1 and Gea2 are thought to act primarily at the *cis*-Golgi to coordinate retrograde transport between Golgi compartments and from the Golgi to the endoplasmic reticulum (ER) (Peyroche et al., 2001; Zhao et al., 2002). While Gea1 and Gea2 have overlapping functions, they are not completely redundant and only partially colocalize (Spang et al., 2001). Gea2 co-immunoprecipitates with Drs2, a *trans*-Golgi flippase that maintains membrane lipid asymmetry in secretory vesicles, and can be found in late Golgi compartments along with Kex2 and Drs2, which are late Golgi proteins (Chantalat et al., 2004). However, it remains unclear how either recruitment to the Golgi or the GEF activity of Gea1 and Gea2 is regulated.

Although several proteins have been shown to directly interact with either mammalian GBF1 or yeast Gea1/2, few have been shown to regulate membrane recruitment or GEF activity of the Arf-GEFs. Human GBF1 binds to Rab1 via its N-terminus, and TRAPPII binds to Gea2 in yeast (Chen et al., 2011; Monetta et al., 2007). In addition, GBF1/Gea1 interact directly with the γCOP/Sec21 subunit of the COPI coat in humans and yeast (Deng et al., 2009). Both Gea1 and Gea2 interact with Gmh1, a conserved integral membrane protein of unknown function located at the *cis*-Golgi; however, this interaction is not necessary for recruitment of Gea1/2 to the Golgi (Chantalat et al., 2003).

Here I show that the C-terminal HDS2 and HDS3 domains of Gea1 regulate Gea1 localization and that deletion of the Rab GTPase Ypt6 prevents Gea1 from localizing to the Golgi. I also confirm that Gea1 is an effector of the Rab GTPase Ypt1. Taken together, these results provide evidence of potential crosstalk between the Rab GTPases and Gea1.

Results

The HDS2 domain mediates Gea1 localization to the Golgi

I have previously shown that mislocalization of the temperature-sensitive GFP-*sec7-1* mutant can be rescued through dimerization with untagged wild-type Sec7 (Figure 3.1B,C). As the GBF Arf-GEFs have also been shown to homodimerize via the DCB domain, Gea2 could potentially dimerize with the GFP-tagged Gea1 constructs, masking localization defects (Ramaen et al., 2007). I therefore tested whether Gea2 could interact with Gea1 and found that HA-tagged Gea2 co-immunoprecipitates with FLAG-tagged Gea1 (Figure 5.1A). However, the interaction appears to be weak, as only a small fraction of Gea1 interacted with Gea2. Gea2-FLAG also only weakly associated with Gea2-HA, suggesting that the Gea Arf-GEFs may not dimerize *in vivo* or may only interact transiently, in contrast to Sec7 homodimerization (Figure 5.1A). Additionally, Gea1 and Gea2 only partially colocalize *in vivo* (Spang et al., 2001). Therefore, it seems unlikely that wild-type Gea2 would be able to interact with GFP-tagged Gea1 constructs and recruit them to the Golgi.

To investigate the importance of the C-terminal domains of Gea1 for localization, I investigated the localization of four GFP-tagged Gea1 constructs. In addition to full-length Gea1-GFP (residues 1-1408), I created a construct missing the HDS3 domain, Gea1ΔHDS3-GFP (residues 1- 1225), a construct missing the HDS2 and HDS3 domains, Gea1ΔC+HDS1 (residues 1-979), and a construct missing all of the C-terminal HDS domains, Gea1ΔC-GFP (residues 1-760) (Figure 5.1A). Unlike GFP-tagged Sec7, which displays little to no cytoplasmic labeling, full-length Gea1-GFP localizes to the cytoplasm as well as to Golgi punctae (Figure 5.1B). Gea1ΔHDS3-GFP displayed a similar localization pattern as Gea1-GFP, but removal of the HDS2 domain caused Gea1ΔC+HDS1-GFP to become completely cytoplasmic (Figure 5.1B).

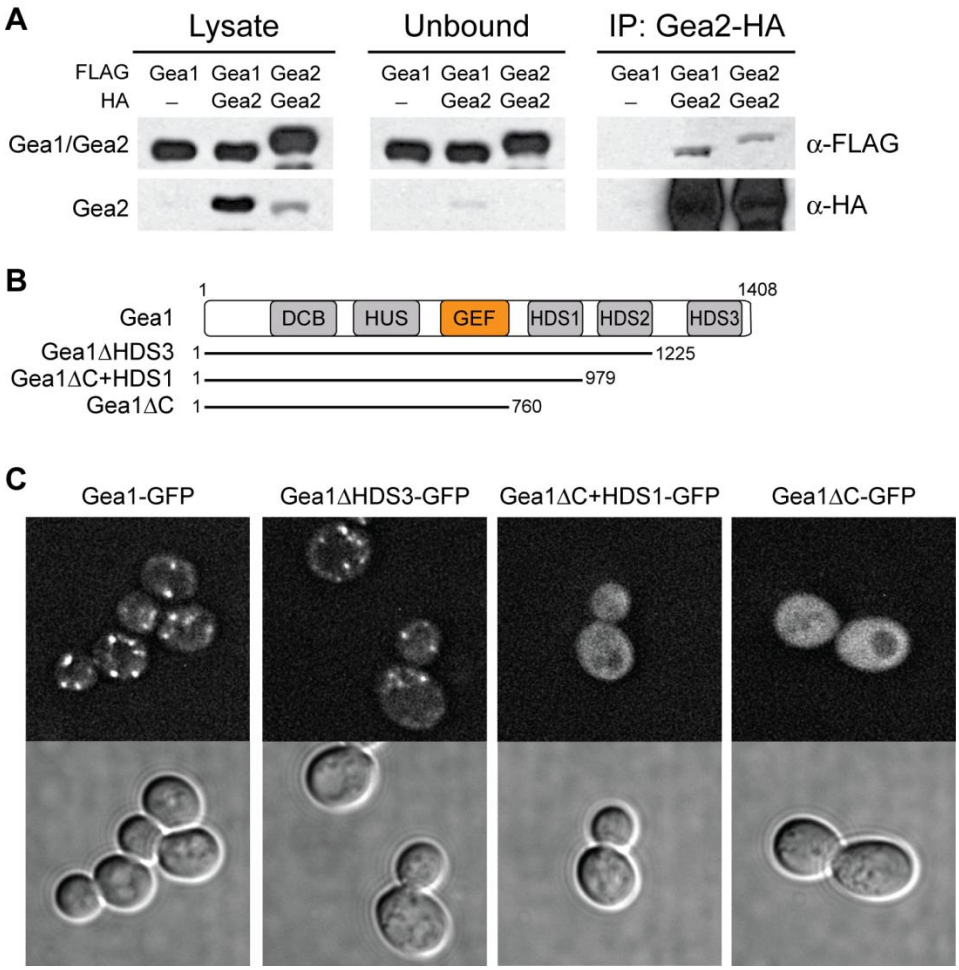

Figure 5.1: Localization of GFP-tagged Gea1 truncation constructs
(A) FLAG-tagged Gea1 and Gea2 weakly co-immunoprecipitate with Gea2-HA. Lane 1: integrated Gea1-FLAG; Lane 2: integrated Gea1-FLAG and Gea2-HA; Lane 3: integrated Gea2-FLAG and Gea2-HA (diploid). **(B)** Schematic diagram of the truncated Gea1 constructs. **(C)** Localization of plasmid-borne GFP-tagged Gea1 truncations in *gea1Δ/GEA2* cells.

This is again in contrast to GFP-Sec7ΔC+HDS1, which retains partial localization to the TGN. These results indicate that the HDS2 domain is necessary to localize Gea1 to Golgi punctae.

Disruption of Ypt6 prevents Gea1 localization to Golgi punctae

An unknown protein might bind to the HDS2 domain to mediate membrane localization *in vivo*. Deletion or disruption of such a factor would result in a cytoplasmic phenotype similar to that of Gea1ΔC+HDS1-GFP. I therefore performed a targeted screen of candidate Golgi-localized proteins, searching for proteins that effected the localization of Gea1ΔHDS3-GFP. I found that deletion of the Rab GTPase Ypt6 causes Gea1ΔHDS3-GFP to lose localization to Golgi punctae and become entirely cytoplasmic (Figure 5.2A). All other deletion strains tested displayed at least a few Golgi punctae labeled with Gea1ΔHDS3-GFP, though the *ypt1-3* temperature-sensitive (ts) strain displayed weaker labeling at Golgi punctae (Fire 5.2B). However, this pattern was observed at both the permissive and restrictive temperatures. To further confirm the role of Ypt6 in recruiting Gea1 to membranes, I examined the localization of Gea1-GFP in a *ypt6*Δ strain. Although occasional punctae were observed, *ypt6*Δ cells displayed more severe cytoplasmic staining of Gea1-GFP than wild-type cells (Figure 5.2C).

Gea1 is an effector of the Ypt1 Rab GTPase

I previously determined that Sec7 is an effector of the Rab GTPases Ypt1 and Ypt31/32 (Chapter 4). I therefore tested whether any of the Golgi-localized small GTPases were able to recruit Gea1 to membranes. Using purified membrane-anchored GTPases, I found that Ypt1 recruited purified Gea1 to liposomes in a nucleotide-dependent manner (Figure 5.3A). Membrane recruitment was only observed with liposomes composed of phosphatidylcholine

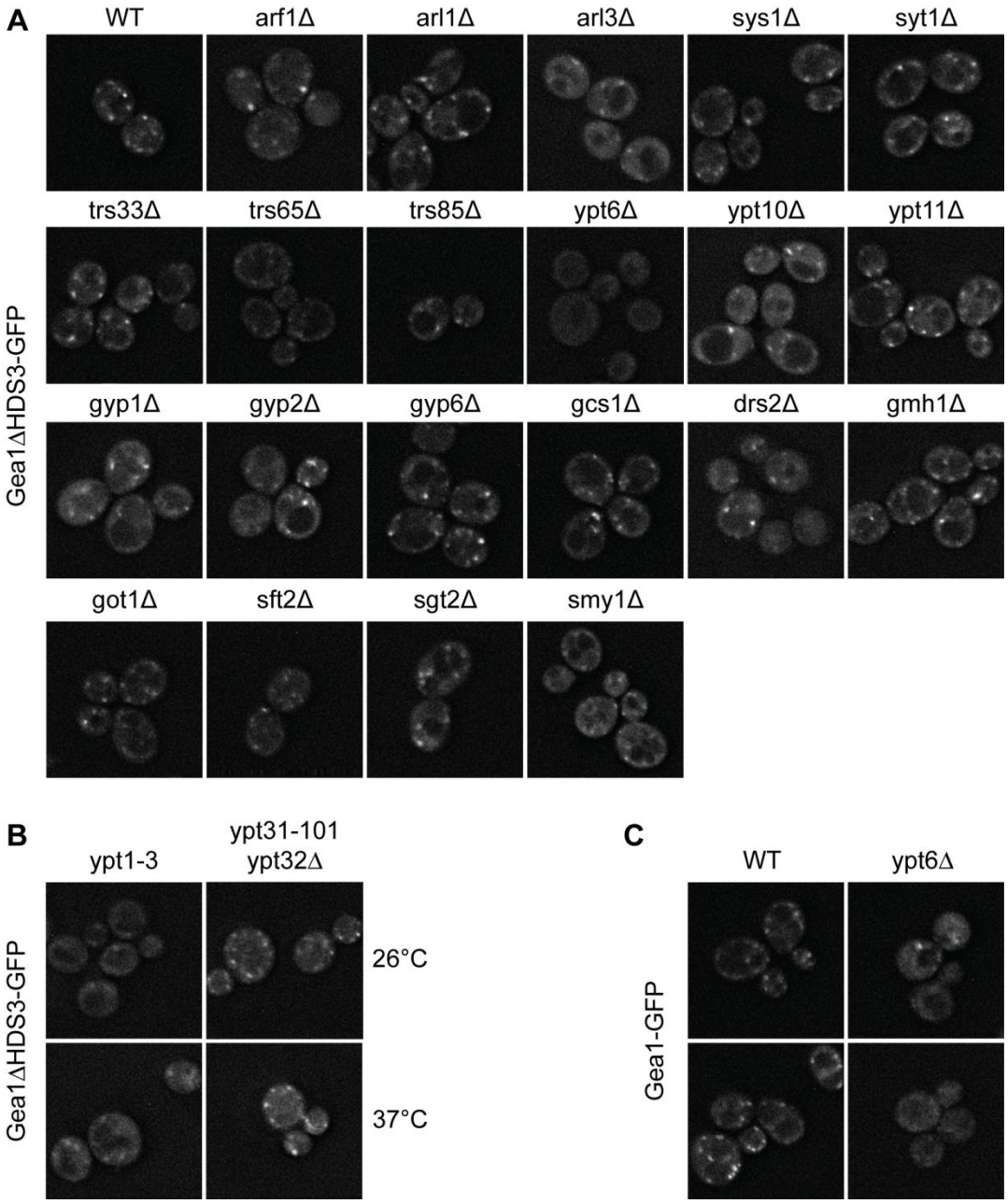

Figure 5.2: Localization of Gea1ΔHDS3-GFP in mutant strains. (A) Localization of plasmid-borne Gea1ΔHDS3-GFP in yeast strains harboring the indicated gene deletion. **(B)** Localization of plasmid-borne Gea1ΔHDS3-GFP in yeast strains harboring *ypt1-3* or *ypt31-101 ypt32*Δ at both permissive (26° C) and restrictive (30 °C) temperatures.**(C)** Localization of plasmid-borne Gea1-GFP in *ypt6*Δ cells.

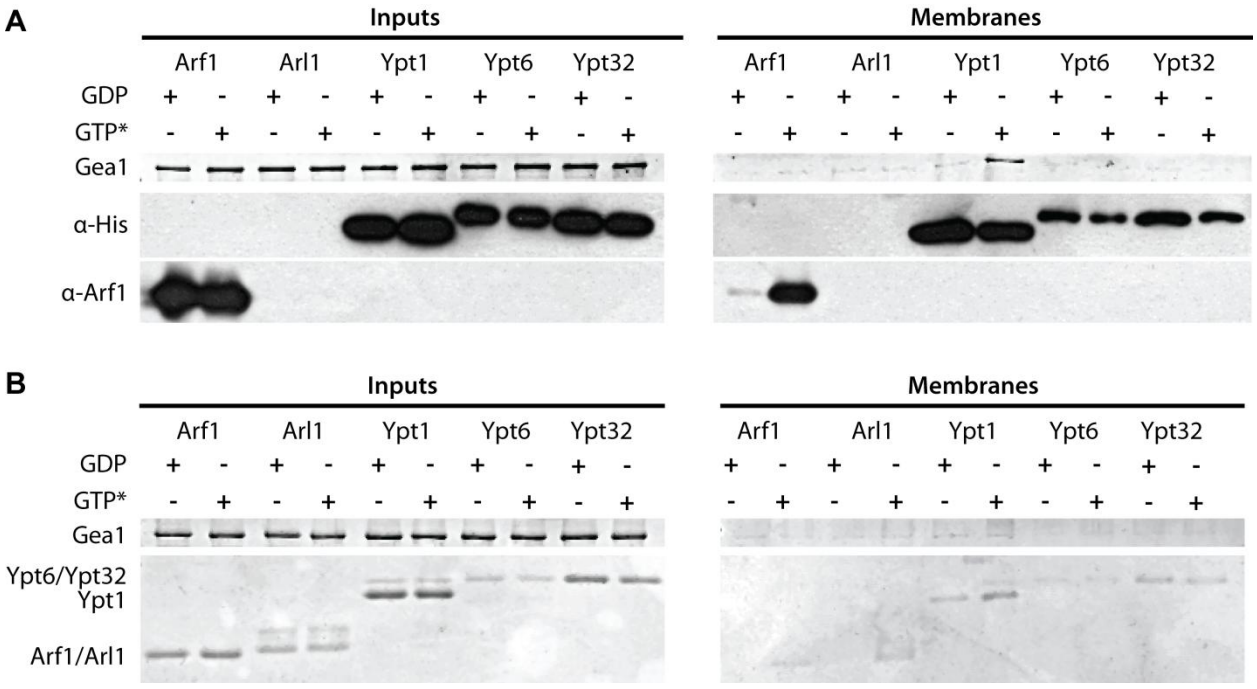

Figure 5.3: Activated Ypt1 recruits Gea1 to membranes. (A) Liposome flotation assays showing activated Ypt1 recruits purified Gea1 to phosphatidylcholine (PC) liposomes. Protein content was determined by total protein staining (Gea1) or Western blot (GTPases).
(B) Activated Ypt1 is unable to recruit Gea1 to TGN-like liposomes. Protein content was determined by total protein staining. GTP* = GMP-PNP (nonhydrolyzable GTP analog). Purified Rabs bind to membranes regardless of their nucleotide state via a 7xHis tag, which is not present on purified Arf1 or Arl1.

(PC) and not with TGN-like liposomes (Figure 5.3B), suggesting that membrane composition also plays a role Gea1 localization. Ypt6 did not recruit Gea1 to liposomes, suggesting that it does not play a direct role in mediating Gea1 localization to the Golgi (Figure 5.3A).

Discussion

My previous studies have demonstrated crosstalk between the Arf and Rab pathways at the TGN via the Arf-GEF Sec7. Here I have investigated the mechanisms of Gea1 membrane localization and presented data suggesting that the early Arf-GEFs may also integrate signals from the Rab pathways.

Ypt6 is a nonessential Rab GTPase that is involved in recycling from endosomes to the Golgi. Deletion of Ypt6 causes localization defects in both Gea1-GFP and Gea1ΔHDS3-GFP. Additionally, I have previously demonstrated that Sec7 partially mislocalizes in *ypt6*Δ cells, and deletion of the HDS4 domain from Sec7 causes complete mislocalization in this background (data not shown). However, Ypt6 is unable to recruit either Sec7 or Gea1 to membranes, nor does it stimulate the GEF activity of Sec7. Therefore, it remains unclear what role Ypt6 may play in maintaining the proper *in vivo* localization patterns of the Golgi Arf-GEFs. Further studies will be necessary to determine whether Ypt6 plays a direct role in regulating the Arf-GEFs or acts upstream of an unidentified factor involved in Arf-GEF regulation. Another possibility is that deletion of *ypt6*Δ destabilizes general Golgi morphology enough to perturb the recruitment of the Arf-GEFs.

I have confirmed that Gea1 is an effector of Ypt1 and can be recruited to membranes by activated Ypt1. Gea1ΔHDS3-GFP also displays decreased localization to Golgi punctae in a *ypt1-3* strain. Several previous studies have also pointed at a role for Ypt1 in regulating Gea1.

Overexpression of Ypt1 suppressed the ts-growth phenotype of the *gea1-6* mutant (Jones et al., 1999). In addition, human GBF1 has been shown to bind to Rab1 via its N-terminus (Monetta et al., 2007). Further studies, including GEF activity assays and overexpression analysis, should provide mechanistic insights into this interaction.

Methods

Plasmids, Strains, and Antibodies

Plasmids and strains were constructed using standard techniques and are described in Table 5.1 and Table 5.2, respectively.

The anti-Arf1 polyclonal antibody was a kind gift from the Schekman lab. The anti-FLAG monoclonal "M2" antibody was purchased from Sigma, and the anti-HA monoclonal antibody "12CA5" was purchased from Roche.

Immunoprecipitations

Cell pellets (25 OD-equivalents of log-phase cells) were resuspended in 1 ml of lysis buffer (50 mM Tris pH 7.5, 150 mM NaCl, 0.2% NP-40, 5 mM EDTA, 1 mM PMSF, 1X Roche protease inhibitor cocktail). The cell suspensions were mechanically disrupted by bead-beating (500 µl glass beads), and the lysates were cleared by centrifugation at 14,000 g for 5 minutes at 4°C. The supernatants were incubated with 10 ul of anti-HA resin (Sigma) overnight at 4ºC. The resin was washed 3 times with lysis buffer before the addition of 15 µl sample buffer. Samples were heated to 55ºC for 15 minutes before separation by SDS-PAGE and immunoblot analysis.

Protein purifications

His-tagged Gea1 was cloned into the pET28 expression vector and purified as previously described (Richardson et al., 2012), with the addition of treatment by TEV-protease to remove the 6xHis-tag prior to the final chromatography step. Myristoylated Arf1 was purified as

Table 5.1: Plasmids used in this study

Name	Description	Vector Backbone	Source
pET28	T7 promoter-driven expression plasmid		Novagen
pRS415	centromeric LEU2 plasmid		(Sikorski and Hieter, 1989)
pCF1163	6xHis-Gea1	pET28	(Richardson et al., 2012)
pNmt1	Nmt1 (S. ce.)	pCYC	(Duronio et al., 1990)
pArf1	Arf1 (S. ce.)	pET3c	(Weiss et al., 1989)
pCF1184	Arl1 (S. ce.)	pET23	Chapter 4
Ypt1-7His	Ypt1 with C-terminal his-tag and cleavable GST-fusion	pGEX-6P	T. Bretscher
pCM14	Ypt6 with C-terminal his-tag and cleavable GST-fusion	pGEX-6P	Chapter 4
Ypt32-7His	Ypt32 with C-terminal his-tag and cleavable GST-fusion	pGEX-6P	T. Bretscher
pCM7	Gea1ΔC-GFP (residues 1-760) driven by P_{GEA1}	pRS415	this study
pCM8	Gea1ΔC+HDS1-GFP (residues 1-979) driven by P_{GEA1}	pRS415	this study
pCM9	Gea1ΔHDS3-GFP (residues 1-1225) driven by P_{GEA1}	pRS415	this study
pCM10	Gea1-GFP (residues 1-1408) driven by P_{GEA1}	pRS415	this study

Table 5.2: Yeast strains used in this study

Name	Genotype	(Strain construction method)	Source
SEY6210	*MATα his3-Δ200 leu2-3,112 lys2-801 trp1-Δ901 ura3-52 suc2-Δ9*		(Robinson et al., 1988)
SEY6210.1	*MATa his3-Δ200 leu2-3,112 lys2-801 trp1-Δ901 ura3-52 suc2-Δ9*		(Robinson et al., 1988)
BY4741	*MATa his3-Δ1 leu2-Δ0 met15-Δ0 ura3-Δ0*		(Brachmann et al., 1998)
BYgeneΔ	*BY4741 geneΔ::KanMX*		(Giaever et al., 2002)
VSY468	*SEY6210 ypt31-101::URA3 ypt32Δ::TRP1*		(Sciorra et al., 2005)
CBY474	*MATa ade2 can1-100 leu2-3,112 trp1-1 ura3-1 ypt1-3*		(Cao et al., 1998)
CFY511	*SEY6210.1 GEA2-HA::HIS3*	(PCR integration into SEY6210.1)	this study
CFY1977	*SEY6210.1 GEA1-3xFLAG-6XHis::TRP1*	(PCR integration into SEY6210.1)	this study
CFY1978	*SEY6210 GEA2-3xFLAG-6XHis::TRP1*	(PCR integration into SEY6210)	this study
CFY1980	*SEY6210.1 GEA1-3xFLAG-6XHis::TRP1 GEA2-3xFLAG-6XHis::TRP1*	(PCR integration into CFY511)	this study
CFY1981	*SEY6210 (diploid) GEA2-3xFLAG-6XHis::TRP1/GEA2-HA::HIS3*	(made by mating CFY511 x CFY1978)	this study

previously reported (Ha et al., 2005). Myristoylated Arl1 and C-terminal 7xHis-tagged Rab GTPases were purified as reported in Chapter 4.

Liposome preparation

TGN-like liposomes were prepared as described (Richardson et al., 2012), except they also contained 5% Ni2+-DOGS for binding His-tagged proteins. PC liposomes were prepared similarly and were composed of 84% DOPC, 10% cholesterol, 5% Ni2+-DOGS, and 1% DiR near-infrared dye (Avanti Polar Lipids). Liposomes were extruded through 100 nm filters.

Liposome floatation (binding) assays

Flotation assays were performed as described (Richardson et al., 2012), using 4 ug of each protein and 0.3 mM of liposomes per 75 ul binding reaction. The His-tags at the C-termini of the Rab proteins allow these proteins to be bound to the liposomes regardless of their activation state. In contrast, the Arf1 and Arl1 proteins only bind to liposomes when activated, due to a conformational change that exposes an N-terminal membrane-inserting helix. 15% SDS-PAGE gels were either stained with IRDye (Li-Cor) and imaged on a Li-Cor Odyssey instrument or assessed by Western blot. Gel images were processed with the ImageJ despeckle filter, and min/max levels were adjusted in ImageJ for clarity.

Microscopy

Cells were grown in synthetic dropout media and imaged in log phase (OD_{600} ~ 0.5) after spotting onto coverslips in growth media. Live cells were imaged at room temperature using a DeltaVision RT wide-field deconvolution microscope (Applied Precision) with a PlanApo 100x objective (1.35 NA; Olympus) and a digital camera (Cool Snap HQ; Photometrics). Acquired

images acquired were deconvolved (“conservative” setting, 6 cycles), and single deconvolved focal planes are shown. Exposure times and image processing were identical for each sample within an experiment, and light levels were scaled equivalently among all samples within an experiment when processed within ImageJ (adjusting only light level min/max settings for clarity).

REFERENCES

Brachmann, C.B., Davies, A., Cost, G.J., Caputo, E., Li, J., Hieter, P., and Boeke, J.D. (1998). Designer deletion strains derived from Saccharomyces cerevisiae S288C: a useful set of strains and plasmids for PCR-mediated gene disruption and other applications. Yeast *14*, 115-132.

Cao, X., Ballew, N., and Barlowe, C. (1998). Initial docking of ER-derived vesicles requires Uso1p and Ypt1p but is independent of SNARE proteins. EMBO J *17*, 2156-2165.

Chantalat, S., Courbeyrette, R., Senic-Matuglia, F., Jackson, C.L., Goud, B., and Peyroche, A. (2003). A novel Golgi membrane protein is a partner of the ARF exchange factors Gea1p and Gea2p. Mol Biol Cell *14*, 2357-2371.

Chantalat, S., Park, S.K., Hua, Z., Liu, K., Gobin, R., Peyroche, A., Rambourg, A., Graham, T.R., and Jackson, C.L. (2004). The Arf activator Gea2p and the P-type ATPase Drs2p interact at the Golgi in Saccharomyces cerevisiae. J Cell Sci *117*, 711-722.

Chen, S., Cai, H., Park, S.K., Menon, S., Jackson, C.L., and Ferro-Novick, S. (2011). Trs65p, a subunit of the Ypt1p GEF TRAPPII, interacts with the Arf1p exchange factor Gea2p to facilitate COPI-mediated vesicle traffic. Mol Biol Cell *22*, 3634-3644.

Deng, Y., Golinelli-Cohen, M.P., Smirnova, E., and Jackson, C.L. (2009). A COPI coat subunit interacts directly with an early-Golgi localized Arf exchange factor. EMBO reports *10*, 58-64.

Duronio, R.J., Jackson-Machelski, E., Heuckeroth, R.O., Olins, P.O., Devine, C.S., Yonemoto, W., Slice, L.W., Taylor, S.S., and Gordon, J.I. (1990). Protein N-myristoylation in Escherichia coli: reconstitution of a eukaryotic protein modification in bacteria. Proc Natl Acad Sci USA *87*, 1506-1510.

Giaever, G., Chu, A.M., Ni, L., Connelly, C., Riles, L., Veronneau, S., Dow, S., Lucau-Danila, A., Anderson, K., Andre, B., *et al.* (2002). Functional profiling of the Saccharomyces cerevisiae genome. Nature *418*, 387-391.

Ha, V.L., Thomas, G.M., Stauffer, S., and Randazzo, P.A. (2005). Preparation of myristoylated Arf1 and Arf6. Methods Enzymol *404*, 164-174.

Jones, S., Jedd, G., Kahn, R.A., Franzusoff, A., Bartolini, F., and Segev, N. (1999). Genetic interactions in yeast between Ypt GTPases and Arf guanine nucleotide exchangers. Genetics *152*, 1543-1556.

Monetta, P., Slavin, I., Romero, N., and Alvarez, C. (2007). Rab1b interacts with GBF1 and modulates both ARF1 dynamics and COPI association. Molecular biology of the cell *18*, 2400-2410.

Peyroche, A., Courbeyrette, R., Rambourg, A., and Jackson, C.L. (2001). The ARF exchange factors Gea1p and Gea2p regulate Golgi structure and function in yeast. J Cell Sci *114*, 2241-2253.

Ramaen, O., Joubert, A., Simister, P., Belgareh-Touze, N., Olivares-Sanchez, M.C., Zeeh, J.C., Chantalat, S., Golinelli-Cohen, M.P., Jackson, C.L., Biou, V., *et al.* (2007). Interactions between conserved domains within homodimers in the BIG1, BIG2, and GBF1 Arf guanine nucleotide exchange factors. The Journal of biological chemistry *282*, 28834-28842.

Richardson, B.C., McDonold, C.M., and Fromme, J.C. (2012). The Sec7 Arf-GEF is recruited to the trans-Golgi network by positive feedback Dev Cell *22*, 799-810.

Robinson, J.S., Klionsky, D.J., Banta, L.M., and Emr, S.D. (1988). Protein sorting in Saccharomyces cerevisiae: isolation of mutants defective in the delivery and processing of multiple vacuolar hydrolases. Mol Cell Biol *8*, 4936-4948.

Sciorra, V.A., Audhya, A., Parsons, A.B., Segev, N., Boone, C., and Emr, S.D. (2005). Synthetic genetic array analysis of the PtdIns 4-kinase Pik1p identifies components in a Golgi-specific Ypt31/rab-GTPase signaling pathway. Mol Biol Cell *16*, 776-793.

Sikorski, R.S., and Hieter, P. (1989). A system of shuttle vectors and yeast host strains designed for efficient manipulation of DNA in Saccharomyces cerevisiae. Genetics *122*, 19-27.

Spang, A., Herrmann, J.M., Hamamoto, S., and Schekman, R. (2001). The ADP ribosylation factor-nucleotide exchange factors Gea1p and Gea2p have overlapping, but not redundant functions in retrograde transport from the Golgi to the endoplasmic reticulum. Mol Biol Cell *12*, 1035-1045.

Weiss, O., Holden, J., Rulka, C., and Kahn, R.A. (1989). Nucleotide binding and cofactor activities of purified bovine brain and bacterially expressed ADP-ribosylation factor. J Biol Chem *264*, 21066-21072.

Zhao, X., Lasell, T.K., and Melancon, P. (2002). Localization of large ADP-ribosylation factor-guanine nucleotide exchange factors to different Golgi compartments: evidence for distinct functions in protein traffic. Molecular biology of the cell *13*, 119-133.

CHAPTER 6

CONCLUSIONS AND FUTURE DIRECTIONS

Conclusions

Prior to my graduate research, very little was known about the regulation of the Sec7 Arf-GEF or the roles of its conserved homology domains. My work in the preceeding chapters has demonstrated that four different GTPases directly bind to Sec7 and regulate both membrane recruitment and GEF activity. I have established Sec7 as a GTPase signaling hub linking the Arf and Rab pathways at the *trans*-Golgi network, allowing me to construct a model in which Sec7 balances the flow of cargo at the TGN by integrating multiple signals from both incoming and outgoing trafficking pathways (Figure 6.1). In this model, Arf1 arriving at the TGN from the *cis*-Golgi is a marker for the load of secretory cargo through the Golgi, while Arl1 and Ypt1 are indicators of the amount of endosomal cargo recycling through the TGN. The arrival of Ypt31 at the TGN drastically stimulates GEF activity, likely resulting in high localized concentrations of Arf1-GTP and subsequent tubulation; this drastic stimulation of GEF activity could potentially drive the fission of secretory vesicles. The different regulatory GTPases all bind to different sites on Sec7, and at least Ypt1 and Ypt31 can act together to further stimulate GEF activity, providing a potentail mechanism for fine-tuning the activation of Arf1 at the TGN. Additionally, tight regulation of Arf1-GTP levels at the TGN appears to be critical for the fidelity of sequential cargo sorting events. My results have established Arf-GEFs as essential regulators of Golgi function and paved the way for future investigations on the roles of both Arf and Rab GEFs in regulating the Golgi complex.

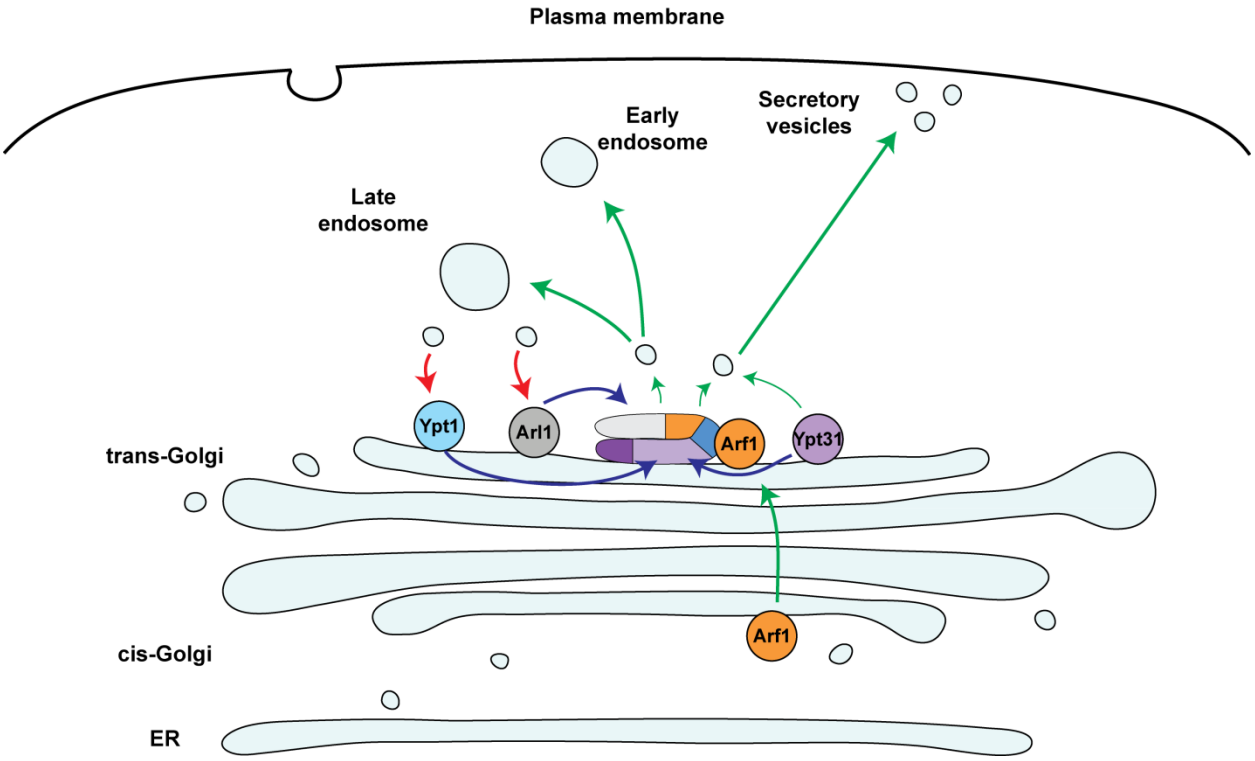

Figure 6.1: Sec7 as a GTPase signalling hub
Sec7 integrates signals from multiple GTPases involved in both incoming and outgoing pathways, providing a potential mechanism for balancing the flow of cargo at the TGN. Arf1 and Ypt31 control the transport of cargo out of the TGN via the secretory pathway, whereas Arl1 and Ypt1 enter the TGN via the endosomal recyclying pathways.

Future Directions

While my studies have established Sec7 as a master regulator of Golgi function, they have also raised many further questions about the roles of Arf and Rab GTPases and their GEFs. As Ypt31 plays such a pivotal role in stimulating GEF activity and driving vesicle biogenesis, determining the Ypt31 GEF will be critical for understanding the regulation of this pathway. As mentioned previously, TRAPPII has been suggested to be the GEF for both Ypt1 and Ypt31, and it remains unclear which GTPase TRAPPII acts on *in vivo*. The number of GTPases inputs controlling Sec7 activity also suggest a potentially regulatory mechanism via signal integration in response to various stimuli. Further studies will be needed to determine the mechanistic details of Sec7 progression from its inactive state to its fully active state. A full understanding of the signals regulating the Golgi complex will also require investigations into each of the Arf and Rab GEFs controlling the flow of cargo through the Golgi.

Additionally, it is still unclear what role Ypt6 may play in Arf-GEF regulation. Deletion of Ypt6 mildly affects the localization of both Sec7 and Gea1, yet Ypt6 does not appear to directly bind to either GEF. Adding to the mystery, Sec7 becomes completely cytoplasmic if both the HDS4 domain and Ypt6 are missing (data not shown). One intriguing possibility is that Ypt6 controls the cycling of another factor that regulates Sec7. Sec7-GFP-labelled punctae appear more fragmented in a *ypt6*Δ strain, suggesting that the integrity of the TGN has been compromised. The removal of HDS4 likely results in enhanced Sec7 GEF activity and increased trafficking out of the TGN via Ypt31. Thus, the mislocalization of Sec7 in this context appears to be a result of increasing secretory trafficking out of the TGN via the hyperactive Sec7ΔHDS4 while simultaneously decreasing endosomal traffic into the TGN via Ypt6. One way to further

investigate this relationship would be to determine the extent of Sec7ΔHDS4 colocalization with wild-type Sec7 and endosomal markers in both a wild type and a *ypt6*Δ background.

Finally, further studies will be needed to determine whether Gea1 and Gea2 are also regulated by GTPases or other proteins. I have already demonstrated that Ypt1 directly binds to Gea1, but further studies are needed to determine the relevance of this interaction. Determining how the regulation of Gea1 and Gea2 differs will also be important in understanding how they perform distinct functions.